Ph.D. Thesis

PARAMETRIC PROCESS DUE TO NONLINEAR INTERACTION OF LASER BEAMS WITH UNIAXIAL CRYSTALS

By

N. K. D. CHOUDHURY

Submitted to the
University of Roorkee
for the award of the Degree of
Doctor of Philosophy
in
ELECTRONICS & COMMUNICATION ENGG.

1968

Dr. Wadhwa

[Ex/66]

UNIVERSITY OF ROORKEE,
ROORKEE (U.P.)

Certified that the attached Thesis/Dissertation on PARAMETRIC PROCESS DUE TO NON-LINEAR INTERACTION OF LASER BEAMS WITH UNIAXIAL CRYSTALS.

was submitted by

Sri N.K.D. Chaudhary.

and accepted for the award of Degree of Doctor of Philosophy/Master of Engineering in

Electronics & Communication Engineering.

vide Notification No. Ex/39/E-191.

dated May 8, 1969.

Assistant Registrar (Exam.)

Dated.....

PSUP (R) 15 Ch. 1969—15 Pads.

CERTIFICATE

Certified that the thesis entitled "PARAMETRIC PROCESS DUE TO NONLINEAR INTERACTION OF LASER BEAMS WITH UNIAXIAL CRYSTALS" which is being submitted by Mr. N.K.D.Choudhury for the award of the degree of Doctor of Philosophy in Electronics and Communication Engineering of the University of Roorkee, is a record of his own work carried out under my supervision and guidance. The matter embodied in this thesis has not been submitted for the award of any other degree of any University.

This is further to certify that he has worked for a period of two years three months from April 20, 1966 to July 20, 1968 at this University to prepare this thesis.

A.K. Kamal

(Dr. A.K. Kamal)
Professor & Head of the
Dept. of Electronics &
Communication Engineering,
University of Roorkee.

Roorkee
Dated 5th August,
1968

Ph.D. THESIS

PARAMETRIC PROCESS DUE TO NONLINEAR INTERACTION OF LASER BEAMS WITH UNIAXIAL CRYSTALS

by

NIRMAL KUMAR DHAR CHOUDHURY

Submitted to the
UNIVERSITY OF ROORKEE
FOR THE AWARD OF THE DEGREE OF
DOCTOR OF PHILOSOPHY
(ELECTRONICS & COMMUNICATION ENGINEERING)
1968

ACKNOWLEDGMENT

The author wishes to record his deep gratitude to Professor Aditya K. Kamal, Head of the Department of Electronics & Communication Engineering, University of Roorkee, for the enthusiasm and encouragement offered not only during the preparation of the thesis but also during the entire Ph.D. curriculum. Thanks are due to all his colleagues who rendered valuable assistance in the preparation of the thesis.

Thanks to the Director, C. B. R. I., Roorkee, for permission to undertake this investigation.

TABLE OF CONTENTS

Page

Page

APPENDIX

NOMENCLATURE

$\bar{a}$ = unit vector of electric field

$a_n(t)$ = time dependent amplitude of wave function

a_o = radius of Bohr orbit

A, A_1 = denote constants in Eq (14.3) and(15.3)

α_{ij} = nonlinear mode coupling coefficient

α_{ii} = loss coefficient

b = confocal parameter of cavity resonator

B = Birefringence of crystal

B = used to denote a constant in Eq (14.3)

$\bar{B}$ = magnetic induction or flux density

β = mismatch gradient

c = velocity of light = 3×10^8 m sec^{-1}

C = Capacitance

C = used to denote a constant in Eq (14.3)

d = spacing between resonator mirrors

d_{ij} = piezo-electric tensor coefficient of third rank

$\bar{D}$ = electric displacement vector

D, D_1 = denote constants in Eq (14.3) and (15.2)

Δ = angle of beam divergence

e = electronic charge = 1.6×10^{19} coulomb

e = a superscript denoting extra-ordinary ray

E = electric field strength (volt/m or cm)

E = used to denote a constant in Eq (14.3)

ϵ_o = permittivity of vacuum = 8.854×10^{12} (rationalized mks unit)

ϵ_s, ϵ_i = relative permittivity or dielectric constant at the signal and idler frequency

ϵ = C/C_o = nonlinear coefficient

F_o = amplitude of the force function

F	= multiplying factor in Fig 19(a)
ϕ	= phase angle in Art 9
ϕ	= complement of angle θ between the wave vector and optic axis
G	= conductance (Art 9)
g	= gain constant (Np/m or cm)
γ	= $\Delta w/w_o$, fractional deviation of frequency
$\hbar$	= Planck's constant (upon 2π)
H	= Hamiltonian
i	= $\sqrt{-1}$
i	= a subscript for idler wave
I	= electric field intensity
i,j,k	= subscripts with a tensor or vector
ξ	= $\Delta n/n_o$, fractional deviation of refractive index
ζ	= a coefficient (vide Eq 3.1)
ξ	= a coefficient (vide Eq 3.1)
$\overline{K}$	= wave vector
K	= a constant in Eq (4.1)
k	= wn/c = wave number
χ	= susceptibility (polarizability)
χ_{ijk}	= susceptibility tensor of third rank
l	= length of the crystal
l_s	= coherence length of signal wave
$l^{(s)}_{coh}$	= coherence length for a pencil of signal rays
L	= loss by reflection in mirror (also δ_r and δ_d are used in Eq 17.11)
λ	= wavelength in free space
λ_o	= wavelength at degenerate frequency
m	= coefficient of dielectric modulation
m,n,p	= subscripts with w and $\overline{P}$ to denote Fourier component

μ = damping rate (Art 10)

n = refractive index

$n_p^e(\theta)$ = refractive index of the extra-ordinary pump wave propagating at an angle θ with the optic axis

N_o = electron density

ν = $1/\lambda$ = waves per meter or centimeter(m^{-1} or cm^{-1})

w (omega) = angular frequency

w_p, w_s, w_i = frequency of pump, signal and idler modes

o = a superscript to denote ordinary ray

o = a subscript to denote degenerate condition

$\bar{P}$ = polarization vector

P = electric power (watts)

P = momentum in Eq (4.1)

Q = electric charge, coulomb (Art 10)

Q_s, Q_i = quality factor of resonator at the signal and idler frequency

Q_o = quality factor at the degenerate frequency

q = an integer denoting the number of nodes(Eq 17.13)

r = radius vector in cartesian coordinate

r_{mi} = electro-optic tensor coefficient (Art 2)

r(w) = ratio of ordinary and extra-ordinary refractive indices at frequency w

R = reflectivity of the dielectric (multilayer) film on mirrors

$R_1(w_i)$ = reflectivity of mirror 1 at frequency w_i

ρ = radial distance from the beam axis

s = increment (or decrement) rate of the field amplitude

ψ = wave function or probability amplitude

σ = normalized frequency deviation (Art 10)

t = time (sec)

τ	= normalized time variable
T	= time period (sec)
θ	= angle between the wave vector and optic axis
θ	= phase angle in Art 10
θ_o	= phase matching angle at the degenerate frequency
θ_M	= phase matching angle for any ratio of w_s/w_i
u	= time (or space) dependent electric field
dV	= element of volume
v	= velocity of propagation
M_p, M_s, M_i	= radius of the pump, signal and idler beams at the waist
M_o	= beam radius at the waist at the degenerate frequency.

ABSTRACT

DHAR CHOUDHURY NIRMAL KUMAR ; Parametric Process due to Nonlinear Interaction of Laser Beams with Uniaxial Crystals. Ph.D. September 1968; Department of Electronics and Communication Engineering, University of Roorkee. Supervisor : Dr. A.K. Kamal

Parametric amplification and oscillation due to nonlinear interaction of laser beams with uniaxial crystals have been known for sometime. Technical data required for the design of these devices are still wanting. The scope of this thesis concerns with the formulation and evaluation of Design Data of Mechanically Tuned Parametric Amplifiers and Optical Generators.

Design data on parametric amplifiers and tunable oscillators using the three types of nonlinear uniaxial crystals, KDP, ADP and $LiNbO_3$, were calculated by digital computer. Five laser frequencies from 3164 Å to 5761 Å are taken for calculation of the phase-matching angles in KDP and ADP crystals, both at the degenerate frequencies and when $\gamma(=\Delta w/w_o)$ changes from 0 to 0.4 . Phase matching angles have also been calculated for $LiNbO_3$ corresponding to four laser pump frequencies from 5300 Å to 11,523 Å. The refractive index data of KDP and ADP used were derived by the computer from the equations by Zernike. These data were then used by the computer to derive the phase match angles from the equation

$$n^e(\theta) = n^o \left[1+(r^2-1)\sin^2\theta\right]^{-\frac{1}{2}}$$

No attempt was made to approximate the equation, which may result in difference between theoretical prediction and experimental results. The curves between θ_o and λ_p are concave in shape showing a minimum at about the middle of the range for λ_p considered. This indicates that employing pump sources of shorter wave-lengths are preferable. Because of larger variation in refractive indices, $LiNbO_3$, especially in shorter wave-lengths show greater angular spread $\Delta\theta$ for a given $\Delta\lambda$.

From the plotted graphs for each of these cases, one can determine the phase matching angles corresponding to any pump frequency and any signal-to-idler frequency ratio. Design Tuning curves are given from which one can readily find the λ_s/λ_i ratio (or γ) as the crystal is rotated away from the degenerate angle θ_o. The mismatch gradients ($dk/d\theta$) are derived wherefrom the power changes caused by divergence of laser beams can be readily estimated.

Laser beams are essentially Gaussian in the transversal direction. The simpler theories of parametric processes originated by plane waves are extended to Gaussian distribution by adopting a simplified concept. Stationary modes of pulsed oscillations are considered in Febry-Perot resonators with plane parallel mirrors having mirror loss-coefficients ranging from 0.01 to 0.1 . The Q-values of resonators with cavity length l=1cm are obtained for different values of λ_p and γ. These Q-values are used to estimate the coefficient of dielectric modulation m and consequently the threshold of pump power required to excite oscillation in these resonators, from Equations

$$m \geq 2/(Q_s Q_i)^{\frac{1}{2}}$$

$$E_p = m n_s^o n_i^o / 2\chi$$

All these are programmed seriatim in digital computer. A set of computed values are given for R=0.99(1 percent loss coefficient) of plane parallel mirrors spaced 1 cm apart. For a KDP crystal at the degenerate wavelength λ_o=1.06 u and beam radius W_o=1 mm of plane waves,

$$Q_o = 4.449 \times 10^6$$

$$m = 4.496 \times 10^7$$

$$E_p = 12.66 \text{ KVcm}^{-1}$$

$$I_p = 0.317 \text{ MWcm}^{-2}$$

$$P_p = 10 \text{ KW}$$

The pump threshold increases as one tunes off the degenerate frequency. Graphical plots are given from which one can readily find out the single-pass parametric gain of amplifiers consisting of KDP, ADP and $LiNbO_3$ for any intensity I_p of the exciting laser pump source and any ratio of the signal and idler frequency. As an illustration, the g values with E_p=100 $KVcm^{-1}$ in $LiNbO_3$ (corresponding to I_p=30 $MWcm^{-2}$) range from 3.46 Np cm^{-1} at λ_o=1.06 u to 1.15 Np cm^{-1} at λ_o=2.3 u. The corresponding signal-power gain are 24 and 4.7 db. The g values reduce with tuning off the degenerate frequency.

CW oscillations caused by well-defined pump beams from CW gas lasers are considered in the lowest modes of confocal type resonators containing $LiNbO_3$ crystals in the focal region. Beam radii at the beam waist are calculated from the equation $W_o^2=b_o\lambda_o/2\pi n_o$ for two typical values of confocal parameter b_o=1 and 5 cm at five laser frequencies. These are then utilized to estimating the power required of

the pump source. At the degenerate frequency

$$P_p = \frac{\epsilon_o c}{8\pi} \mu_o^2 n_o^3 \lambda_o^2 \left(\frac{2l}{\xi_1}\right)^2$$

As an illustration, the pump power required of an Argon-ion (5145 $\mathring{A}$) laser in order to commence parametric oscillation in a confocal resonator with b_o=1 cm and containing $LiNbO_3$ crystal l=1 cm, is 5.27 mW at the degenerate wavelength λ_o=1.03 u. The threshold level rises to 8.87 mW at γ=0.4 .

In CW parametric amplifiers much smaller gains in idler modes are available. If b_o=10 cm, the beam radii are w_s^2=7.33 x 10^5 cm^2 at λ_s=0.936 u and w_p^2=3.66 x 10^5 cm^2 for γ=0.1 and λ_o=1.03 u. With a pump power of 10 mW (λ_p=5145 $\mathring{A}$), the idler-to-signal power ratio $P_i(l)/P_s(o)$ is 2.15 x 10^5 in a l=1 cm long crystal. The corresponding ratio for oscillator is 7.73 x 10^{-3}.

The threshold pump power, power gain and other useful design data for mechanically tuned CW oscillator/ amplifier with $LiNbO_3$ crystal are evaluated by computer at five pump frequencies and given in Tabular form. MKS system of units is used in this Thesis.

INTRODUCTION

Consequent on the development of Lasers the Nonlinear Interaction of light with matter has become an extremely important topic. It is now possible to have monochromatic light of exceedingly high intensity in the order of MW/cm^2. At such high order of intensity, the nonlinear properties of materials make substantial contribution to be useful in the development of optical sources, nonlinear devices and systems.

Nonlinear properties of materials have been known during the last seventy years. The nonlinear permeability of ferromagnetic materials or the familiar BH hysteresis loop leads to considerable heat generation in electrical machinery. Modulation and demodulation of radio waves are obtained from nonlinearity in devices. Parametric amplification of microwaves, although of recent origin, utilizes the basic nonlinearities in certain materials. Nonlinearities in plasma has during the current years offered the scope of gigantic power generation and other applications.

The classical Maxwell's equation

$$\overline{D} = \epsilon(E)\overline{E} \qquad\qquad \overline{B} = \mu(H)\overline{H}$$

were applied to some nonlinear problems in 1900. Optical properties of crystals were explained by Lorentz and Drude by a model in which electrons were assumed to execute harmonic vibrations in an electromagnetic field. But they did not consider the anharmonicity of the electron oscillator caused by the quadratic coulomb forces.

Thomson considered the response of an electron in an electromagnetic wave and obtained the dispersion relation

due to emission of light from the induced dipoles. The Lorentz force on the oscillating electron induces a dipole moment at the second harmonic frequency and is directed along the direction of propagation. The second harmonic intensity is much smaller than the fundamental. For small field intensities this nonlinearity is absolutely negligible at optical frequencies.

The diffused wave by each elementary oscillator interferes in a destructive manner. The coherence and intereference of the scattered radiation are important in nonlinear dispersion. One can describe them by nonlinear polarization and studying its characteristics. The spatial variation of the nonlinear polarization (1) caused by waves w_1 and w_2 is determined by the factor $i(\bar{K}_1 \pm \bar{K}_2)\bar{r}$. When $\bar{K}_3 = \bar{K}_1 \pm \bar{K}_2$, the nonlinear waves at the sum or difference frequency $w_3 = w_1 \pm w_2$ emanating from each element of volume, produce coherence or phase matching.

Power in laser beams has been measured by Kamal and Subramanian (2) by utilizing the dc polarisation in a nonlinear medium owing to the incident beam. The dc polarisation is given by

$$\bar{P} = \epsilon_0 \chi_2 E_0^2 \cos 2\theta$$

where E_0^2 is the intensity to be measured; χ_2 is the polarisation coefficient and θ the angle between the incident polarisation and the crystal x - axis. The power meter developed is based on a cylindrical quartz rod partially enveloped by a pair of concentric electrodes having the shape, $\sigma = F \cos \theta$, and placed perpendicular to the x-axis.

Advantage of the nonlinear polarization at the sum frequency is taken in the generation of second and third harmonic. The parametric process on the other hand uses the nonlinear polarization at the difference frequency. The second and third harmonic generators work at a few spot frequencies whereas optical parametric generators have been tuned continuously through the visible and near infrared frequencies. Excitation of parametric action in uniaxial crystals necessitate in general pump power of the order of megawatts. Such power can only be delivered by solid state pulsed lasers, such as the ruby laser (6940 A) or Nd^{3+} glass laser (1.06 u) Focusing of beams by confocal resonator considerably reduces the power requirement. Confocal resonators containing $LiNbO_3$ crystals have been excited by CW gas lasers such as the Argon-ion (5145 A) laser.

CHAPTER I

REVIEW OF EARLIER WORK

This chapter purports a review of the nonlinear phenomena in dielectric media originated by concentrated high power laser beams. Atomic origin of nonlinear susceptibility due to strong electro-magnetic field is examined both from the classical and the quantum mechanical model. Theoretical calculation is made of the magnitude of nonlinear susceptibility and compared with experimental results. Propagation of waves is described by combining Maxwell's equations with P^{NL}. Coupling of the fundamental mode with its second harmonic or of the signal and idler with the pump mode during their transit through the nonlinear lossless dielectric is examined through two coupled-wave equations.

1. Preview

The original experiments of Franken and his colleagues(3) successfully demonstrated the second harmonic generation (SHG) of coherent light. The electric field from a ruby laser (6940 Å) having an output of one joule in one half millisec was projected on the front surface of a crystalline quartz plate. About 10^{8} of the ruby radiation power was estimated as converted to second harmonic at 3470 Å.

A measure of the further progress in this field is the experiment of Terhune et al (4) with a one MW giant ruby laser. A 15 cm focal length lens was employed to concentrate

the laser radiation in the crystal. Second harmonic conversion efficiency as high as 20 per cent was achieved in ADP crystal.

Parametric amplification and generation of optical frequencies is of comparatively recent origin. Nonlinear uniaxial crystals, the KDP, ADP and $LiNbO_3$ have been utilized for this process. Tuning of the oscillator around the degenerate frequency has been achieved by three different methods

1. rotation of the crystal
2. temperature tuning
3. electro-optic tuning

2. Nonlinear Dielectric Materials

Many crystalline dielectrics exhibit nonlinear phenomena of sufficient magnitude to render them suitable for optical harmonic and parametric generation of coherent light. Amongst these KDP (Potassium dihydrogen phosphate, type $\bar{4}2m$), ADP (Ammonium dihydrogen phosphate, type $\bar{4}2m$) and $LiNbO_3$ (Lithium metaniobate, type 3m) have been widely accepted for SHG and Parametric processes. Materials like GaAs, InSb, etc. are under study.

The material for production of optical harmonic must be relatively transparent to the fundamental and the desired harmonic; besides, the symmetry properties of the crystal also needs consideration. Let us express the optical polarization $\bar{P}$ in the form

$$\bar{P} = 2\epsilon_o(\chi_1\bar{E} + \chi_2\bar{E}^2 + \chi_3\bar{E}^3)$$
$$\bar{E} = \bar{E}_o \cos wt \qquad (2.1)$$

where χ_1, χ_2, χ_3 are the dielectric susceptibility tensor. The nonlinear term $\epsilon_o \chi_2 E^2$ produces the second harmonic and d-c polarization components,

$$\bar{P}(2w) = \epsilon_o \chi_2 E_o^2 \cos 2wt$$

$$\bar{P}_{dc} = \epsilon_o \chi_2 E_o^2$$

Of course, the nonlinear susceptibility χ_2 is a tensor of the third rank.

The general exprèssion for polarization is

$$\bar{P}_i = \epsilon_o \left[\chi_{ij} \bar{E}_j + 2\chi_{ijk} \bar{E}_j \bar{E}_k + 4\chi_{ijkl} \bar{E}_j \bar{E}_k \bar{E}_l \right.$$

$$\left. + \text{their derivatives which are small} \right] \qquad (2.2)$$

The nonlinear second order polarization is thus

$$\bar{P}^{NL}(r,t) = 2\epsilon_o : \chi_{ijk} \bar{E}_j(r,t) \bar{E}_k(r,t) \qquad (2.3)$$

The factor 2 is included so as to conform to common usage.

The electric field and the nonlinear polarization is expandable in Fourier series(5) as

$$\bar{E}(r,t) = \bar{E}_1(o,r) + \tfrac{1}{2} \sum_{p=-N}^{N} \bar{E}_1(w_p, r) \exp\left[i(k_p r - w_p t) \right] \qquad (2.4)$$

$$\bar{P}(r,t) = \bar{P}_1(o,r) + \tfrac{1}{2} \sum_{p=-M}^{M} \bar{P}_1(w_p, r) \exp\ (i w_p t) \qquad (2.5)$$

From (2.3) and (2.4), we get

$$\bar{P}_1^{NL}(2w) = \epsilon_o \chi_{ijk} : \bar{E}_j(w) \bar{E}_k(w) \exp(i 2k_p r) \qquad (2.6)$$

This nonlinear polarization at 2w due to the fundamental w will be responsible for second harmonic generation. At the

difference frequency $w_p = w_m - w_n$,

$$\overline{P}_i^{NL}(w_p) = 2\epsilon_o \chi_{ijk} : \overline{E}_j(w_m)\overline{E}_k^*(w_n)\exp\left[i(k_m - k_n)r\right] \qquad (2.7)$$

If one of these electric field is a d.c. field, one finds the well-known linear electro-optic effect, that is the effect in which the ordinary optical polarizability of a medium is modified by a strong d.c. electric field.

$$\overline{P}_i^{NL}(w_p) = 4\epsilon_o \chi_{ijk} : \overline{E}_j(o)\overline{E}_k(w_p)\exp(ik_p r) \qquad (2.8)$$

The susceptibility tensor χ_{ijk} is found to have an intimate relationship with the electroptic tensor which is denoted here by r_{ij}. Bass (6) has derived the relation for the d.c. susceptibility

$$\chi_{im} = -\frac{n^4}{32\pi} r_{mi}$$

where n is the ordinary index of refraction. The equation provides a method for experimental determination of the second order nonlinear susceptibility.

The third-rank tensor vanishes for any system with centre of inversion. The tensor elements in crystals without inversion symmetry have in general the same form as the nonvanishing elements of the piezo-electric tensor "d". For example in KDP or ADP, the crystal symmetry leaves only three nonvanishing components d_{14}, d_{14} and d_{36} (Appendix 1). Here Voigt notation is used. The measured (approx.) values of the nonlinear susceptibility are $d_{36}=1.26 \times 10^{12}$, $d_{14}=0.6 \times 10^{12}$ M/volt.

Crystals with an inversion symmetry do not generate second harmonic, although generation of third harmonic (THG)

is possible. Non-symmetry may however be induced in these crystals by the application of a strong d.c. electric field. Marker at el (7) have observed production of optical third harmonic in calcite, isotropic liquids and in cubic crystals.

3. Nonlinear susceptibility : Atomic origin

In a classical model for calculating linear polarization of a medium, Drude and Lorentz postulated the electrons as harmonically bound particles. Actually the valence electrons are loosely bound by the Coulomb field and the anharmonicity of the electron oscillator should be taken into account for calculation of nonlinear polarization.

Let us consider the motion of a one-dimensional anharmonic oscillator with damping, and subjected to two fields of frequencies $\pm w_1$, w_2 and wave vectors $\bar{K}_1, \bar{K}_2$ and propagating in the z direction.

$$\ddot{x} + \xi x + w_o^2 x + \zeta x^2 = \frac{e}{m} \mathrm{Re}\left[E_1 \exp i(k_1 z - w_1 t) + E_2 \exp i(k_2 z - w_2 t)\right] \qquad (3.1)$$

First linear approximation gives

$$x(w_j) = \frac{e/m}{D_j} \mathrm{Re}\left[E_j \exp i(k_j z - w_j t)\right]$$

Putting the value of x^2 in Eq (3.1) and equating the coefficients of the Fourier terms, the various dipole moments (e.x) become

$$\bar{P}(w_3 = w_1 + w_2) = \mathrm{Re}\left[\frac{(e^3/m^3)\zeta}{2D_1 D_2 D_3} E_1 E_2 \exp i(k_3 z - w_3 t)\right]$$

$$\bar{P}(w_1 = w_3 - w_2) = \mathrm{Re}\left[\frac{(e^3/m^3)\zeta}{2D_1 D_2^* D_3} E_2^* E_3 \exp i(k_1 z - w_1 t)\right] \qquad (3.2)$$

$$\bar{P}(w_3 = 2w_j) = \mathrm{Re}\left[\frac{(e^3/m^3)\zeta}{2D_j^2 D_3} E_j^2 \exp i(k_3 z - w_3 t)\right]$$

where $D_j = w_o^2 - w_j^2 - i w_j$, $j = 1, 2$

From the last one of these equations, the nonlinear susceptibility causing the second harmonic generation is

$$\epsilon_o \chi(2w) = - \frac{N_o (e^3/m^2) \xi}{2D^2(w) D(2w)} \qquad (3.3)$$

The ratio of the nonlinear polarization at the second harmonic frequency and the linear polarization at the fundamental is

$$\frac{\bar{P}^{NL}(2w)}{\bar{P}^{L}(w)} = \frac{e/m}{2D(w)} \frac{\xi E}{D(2w)} \qquad (3.4)$$

This ratio is of the order of $E/2E_a$, where E_a is the atomic field on an electron (8). Since $E_a = 3 \times 10^8$ volt/cm, we obtain, even for an extreme field intensity $E = 2 \times 10^6$ volt/cm (power-density of 79×10^8 watts/cm^2) at the focus of a Q-switched laser, $E/2E_a \doteq 3 \times 10^{-3}$. Inspite of this small order of the harmonic polarization, experimenters have detected (9) the third harmonic ultraviolet radiation. A typical ruby pulse laser of 1 joule contains 4×10^{18} photons and third harmonic conversion efficiency of $1:10^{15}$ provided about 10^3 photons at $\lambda = 2313$ Å which are readily detectable with optical instruments.

Let us have an estimate of the nonlinear susceptibility from the classical Eq.(3.3)

$$\chi(2w) = \frac{N_o e^3 a_o}{2\epsilon_o (eEa)^2} = \frac{N_o e a_o}{2\epsilon_o E_a^2}$$

For values $N_o = 2.6 \times 10^{28}$ m^{-3}, $e = 1.6 \times 10^{-19}$ Coulomb, $a_o = 10^{-10}$ m, and $E_a = 3 \times 10^{10}$ volt m^{-1}, one obtains

$$\chi(2w) \doteq 26.1 \times 10^{-12} \text{ M/volt}$$

This figure compares favourably with the experimental values of nonlinear susceptibility in the optical region. A similar computation of the linear susceptibility yields,

$$\chi(w) = N_c e a_o / \epsilon_o E_a = 1.57 \text{ M/volt}$$

In these computations we have assumed that none of the fundamental or harmonic frequencies is close to the atomic resonance frequency, in the event of which the ratio in Eq (3.4) increases by a factor w_o/ξ

If the atom is at a centre of symmetry the nonlinearity from the dipole term ξx^2 vanishes, but it may originate in higher order multipole terms like $\xi' x^3$.

4. Quantum Mechanical Treatment

Investigation on the atomic origin of nonlinear polarization from quantum mechanical consideration has been conducted by a few workers in this field. The most intensive and interesting one is the 'Three Field Theory' by Armstrong and Coauthors (10). Here we shall adopt a simplified procedure following Franken and Ward (11).

For an isolated atomic system the Hamiltonian may be written as

$$H_o = \frac{p^2}{2m} + \tfrac{1}{2}Kx^2 \qquad (4.1)$$

Let this be subjected to a perturbing electric field, $E(t) = E \cos wt$. The perturbarbation Hamiltonian in dipole approximation is given by

force-energy dimensions

$$H_{int} = e \times E \cos wt = \frac{H}{2}\left[\exp(iwt)+\exp(-iwt)\right] \qquad (4.2)$$

and the wave function $\Psi_n = a_n \Phi_n \exp(-iw_n t)$

Putting this in the Schrödinger wave equation

$$i\hbar\,\partial\Psi/\partial t = (H_o + H_{int})\Psi \qquad (4.3)$$

The dipole moments at the fundamental and harmonic frequencies become

$$\langle \psi_g^{(o)} | ex | \psi_g^{(1)} \rangle_w = -\frac{e}{\hbar} \sum_n (ex)_{gn} (E.x)_{ng} \left[\frac{1}{w_{ng}+w} + \frac{1}{w_{ng}-w} \right] \cos wt \qquad (4.4)$$

$$\langle \psi_g^{(1)} | ex | \psi_g^{(1)} \rangle_{2\omega} = \sum_{m,n} a_m^{(1)*}(-w)(ex)_{mn} a_n^{(1)}(w) \exp(iw_{mn}t) + c.c.$$

$$= \frac{e^2}{2\hbar^2} \sum_{m,n} (E.x)_{mg} (ex)_{mn} (E.x)_{ng} \left[\frac{1}{(w_{mg}+w)(w_{ng}-w)} \right] \cos 2wt \qquad (4.5)$$

$$\langle \psi_g^{(o)} | ex | \psi_g^{(2)} \rangle_{2\omega} = \frac{e^2}{2\hbar^2} \sum_{m,n} (ex)_{gn} (E.x)_{mn} (E.x)_{mg} \left[\frac{1}{(w_{mg}+w)(w_{ng}+2w)} + \frac{1}{(w_{mg}-w)(w_{ng}-2w)} \right] \cos 2wt \qquad (4.$$

For an approximate comparison of the polarization, we may consider the states m and n very close so that $w_{mo}=w_{no}=w_o$. We may also consider that the matrices (E.x) is simply Ex i.e. a scalar quantity. Then

For $E = 2 \times 10^6$ volt/cm and $x = a_o = 10^{-8}$ cm, $\hbar(2w-w_o) = 5$ evolt, the ratio of the moments at 2w and w is 10^{-3}.

If $w \ll w_o$, we have from Eq (4.4, 4.5, 4.6),

$$\bar{P}(w) = \frac{2e^2x^2E}{\hbar w_o} = \frac{2e^2x^2E}{e^2/4\epsilon_o a_o \pi} = 8\epsilon_o a^3 E \pi$$

$$\bar{P}(2w) = \frac{3}{2}\frac{e^3x^3E^2}{\hbar^2 w_o^2} = \frac{24\pi^2\epsilon_o^2 a_o^5 E^2}{e} \qquad (4.7)$$

$$\frac{\bar{P}(2w)}{\bar{P}(w)} = \frac{3}{4}\frac{exE}{\hbar w_o} = \frac{3\epsilon_o a_o^2 E \pi}{e}$$

This about 10^{-3} for $E = 2 \times 10^8$ volt/m. We may also obtain an

idea of the order of nonlinear susceptibility from the approximation of quantum mechanical derivations. From Eq (4.7)

$$\chi(2w) = \frac{24\pi^2 N_o \epsilon_o a_o^5}{e} = 3.4 \times 10^{-12} \text{ M/volt.}$$

This may be compared with the measured nonlinear susceptibility

$$d_{36}(2w) = 1.2 \times 10^{-12} \text{ M/volt for KDP}$$

5. Interaction of Electromagnetic Radiation with Nonlinear Dielectric Medium

Consider a nonlinear lossless dielectric medium ($\mu = 1$) traversed by two laser-waves with frequencies w_1 and w_2. These two waves will generate nonlinear polarization at sum and difference frequencies ($w_3 = w_1 \pm w_2$). Maxwell's equations in the medium can be written for each frequency as

$$\bar{\nabla} \times \bar{H} = \frac{\partial \bar{D}}{\partial t} + \frac{\partial \bar{P}}{\partial t}$$

$$\bar{\nabla} \times \bar{E} = -\frac{\partial \bar{B}}{\partial t}$$

where $$\bar{D} = \epsilon_o \epsilon_r \bar{E}$$

$$\bar{B} = \mu_o \bar{H} \quad (\because \mu_r = 1)$$

Then $$\bar{\nabla} \times \bar{H} = -c^2 \epsilon_o \bar{\nabla} \times \int (\bar{\nabla} \times \bar{E}) dt \qquad (5.1)$$

The solution of the inhomogeneous equation in an infinite, anisotropic dielectric medium are linearly polarised plane waves, the amplitudes of which are slowly varying functions of distance along the direction of propagation. The nonlinear polarization $\bar{P}^{NL}$ say at (w_3) created by the other two waves at w_1 and w_2 will

interact with the wave at w_3. It will have a component parallel to and in phase and a component parallel to but 90° out of phase with E_3. The component in phase with the field $\bar{E}$ stores an energy.

$$\frac{1}{T}\int_0^T (\bar{E}.\bar{P})dt = \tfrac{1}{2}\mathrm{Re}\left[E_3^*.\bar{P}^{NL}(w_3)\right]$$

per unit volume. The out-of-phase components does work on the wave at a rate

$$\frac{1}{T}\int_0^T (\bar{E}.\frac{\partial \bar{P}}{\partial t})dt = \tfrac{1}{2}w_3\mathrm{Re}\left[\bar{E}_3.\bar{P}^{NL}(w_3)\right]$$

Nonlinear polarization with a 90° lead in phase does work on the wave and hence increases its intensity; if it has a phase retardation of 90°, the work done is negative and the wave at w_3 will decrease in amplitude.

One can restrict himself only to three waves. Although initially several other waves may be created, only those with $\Delta k=0$ will continue to grow. Because of severe mismatch in a dispersive medium, other waves will quickly dissipate their energy.

6. Second Harmonic Generation

Let us consider the simplest case of SHG in an anistropic medium traversed by two waves, that is a second harmonic $w_2=2w$, interacting with the fundamental $w_1=w$.

From Maxwell's equations (5.1) the growth rate of the electric field due to nonlinear polarization $\bar{P}^{NL}$ is described by

$$\frac{d}{dr}\bar{E}_1(w_p,r) = i\frac{k_p}{2\epsilon_0\epsilon_p}\bar{P}(w_p,r)\exp(-ik_p r) \qquad (6.1)$$

Considering only the frequency component w_1 in Eq (2.4) and (2.5), one obtains from (6.1) the coupled wave equations

$$\frac{d}{dr}\bar{E}_i(w) = i\left(\frac{k_1}{2\epsilon_1}\right)2\chi_{ijk}(-w,2w,-w)\bar{E}_j(2w)\bar{E}_k^*(w)\exp(i\Delta kr)$$

$$\frac{d}{dr}\bar{E}_j(2w) = i\left(\frac{k_2}{2\epsilon_2}\right)\chi_{jik}(-2w,w,w)\bar{E}_i(w)\bar{E}_k(w)\exp(-i\Delta kr) \qquad (6.2)$$

where the momentum mismatch $\Delta k = k_2 - 2k_1$. From permutation symmetry relations

$$\chi_{ijk}(-w,2w,-w) = \chi_{jik}(-2w,w,w) \qquad (6.3)$$

Perfect matching : $\Delta k=0$

With exact phase-match between the fundamental and the second harmonic, $k_2=2k_1$, a large second harmonic generation is possible. Assuming that the fundamental intensity remains fairly undepleted, and that the second harmonic grows from zero at r=0, we have from (6.2)

$$E_j(2w) = E_i(w,o)\tanh gr$$
$$E_i(w) = E_i(w,o)\,\mathrm{sech}\, gr \qquad (6.4)$$

where the gain constant

$$g = \left(\frac{k_1}{\epsilon_1}\right)\chi_{ijk}(-w,2w,w)E_i(w,o) \qquad (6.5)$$

The amplitude of the two waves plotted as a function of the distance r is shown in Fig. 6.1. With the growth of the second harmonic the amplitude of the fundamental decreases. The coherent length is defined by

$$l_s = \frac{1}{g} = \frac{n\lambda}{2\pi\chi E_i(w,o)} \qquad (6.6)$$

n is the index of refraction in the medium at λ the free space wavelength of the incident laser beam. After travelling the coherent length l_s the emergent light should contain about 76 per cent of the fundamental power. Although such a large power conversion is predicted by the theory, beam divergence and other factors limit this figure to less than 30 per cent.

Of the various techniques used for increasing the coherence length, the most ingenious one has been the utilization of the birefringence of uniaxial nonlinear crystals. For instance, in KDP crystal the ordinary refractive index n^o at w equals n^e at 2w for the direction of propagation 50° (matching angle) with the crystallographic Z-axis. If we take $n = 1.5$, $\chi = 5 \times 10^{-12}$ M/volt, $E = 10^7$ volt m^{-1} corresponding to a power density of 20 MWcm^{-2} from a ruby laser, $\lambda = 6940$ Å, we calculate $l_s = 0.33$ cm and a gain $g = 3$Np cm^{-1}.

Imperfect Matching : $\Delta k \neq 0$

If the fundamental beam is assumed to remain undepleted, Eq (6.2) may be integrated

$$E_j(2w) = ig\, E_k(w)\left[\frac{1 - \exp(-i\Delta k l)}{\Delta k}\right] \qquad (6.7)$$

This indicates a periodic variation of the amplitude of the second harmonic with crystal length l. Fig. 6.2, due to Marker at al (12) clearly demonstrates this periodic variation in intensity at the exit surface of the crystal.

Kleinman (13) has evaluated the square of the function within the parenthesis of Eq (6.7). The average is

$$\left\langle \frac{\sin^2(\Delta k l/2)}{(\Delta k l/2)^2} \right\rangle = 1 \text{ , for } l \ll l'_{coh}, \text{ thin crystal}$$
$$= l'_{coh}/l, \text{ for } l \gg l'_{coh}, \text{ thick crystal}$$

where the coherent length is defined as

$$l'_{coh} = \frac{2}{\beta \Delta\theta}$$
$$\beta = \frac{2w}{c}\left(\frac{dn}{d\theta}\right)_{\theta_o} \qquad (6.8)$$

$\Delta\theta$ measures the deviation of the beam from the matching direction θ_o. Hence from (6.8) the second harmonic intensity become for a laser intensity I_L,

(a) Thin Crystal

$$P = \frac{2w^2}{\epsilon_o c^3 n^3} \chi^2 l^2 I_L^2 \qquad (6.9)$$

(b) Thick crystal

$$P = \frac{2w^2}{\epsilon_o c^3 n^3} \chi^2 l\, I_L^2\, l'_{coh} \qquad (6.10)$$

The average harmonic power is proportional to I_L^2 and varies as l in thick crystals. In Q-switched laser the conversion efficiency is appreciable, and hence depletion of the fundamental power cannot be neglected. If this is taken into account, the dependence of P is found (14) to be proportional $I_L^{3/2}$. For a laser intensity of 10^3 Mwm^{-2}, Eq (6.10) predicts a conversion efficiency of about 2.5 per cent in a 5 cm long crystal at 0.347 u second harmonic.

The theory of harmonic generation in beams of finite divergence due to Kleinman predicts small conversion efficiency. It was generalized by Akhmanov at el. for large conversion efficiency (15). The dependence of

conversion efficiency on the incident power for different values of mismatch gradient (Fig 6.3) can be calculated. Optical frequency multipliers made on the basis of these studies show large conversion efficiency. For unfocused plane beams with $P_L(w)$ = 100 MW, their experimental results (15) are P(2w) = 25 to 30 MW, P(3w) = 8 to 10 MW and P(4w) = 3 to 4 MW.

In the experiments of Terhune and Coworkers, more than 20 per cent of the fundamental power from a giant ruby laser was converted to second harmonic. The beam was slightly focused and aligned along the phase matched direction (50° with the z-axis) of a KDP crystal. Using this phase matching technique, Akhmanov at el (15) obtained second harmonic conversion efficiency upto 30-35 per cent in ADP and KDP crystals. Saturation in the conversion efficiency may be ascribed to beam divergence, double refraction etc. which cause the power of the laser beam and the second harmonic to propagate along slightly different paths. The effect of double refraction can be reduced by affecting phase-matching at an angle 90° with optic axis.

7. Parametric Amplification and Subharmonic Generation

Coupled growth of two waves in a nonlinear medium in the presence of a strong pump frequency w_p is known as parametric generation. Let us consider the propagation of a signal frequency w_s and an idler frequency $w_i(=w_p-w_s)$ generated in the anisotropic medium through nonlinear interaction. Substitution of $\overline{P}$ from (2.7) in (5.1) leads to coupled wave equations, which under phase-matched

condition become

$$\frac{d}{dr}E_j^*(w_s) = -i\left(\frac{k_s}{2\epsilon_s}\right)2\chi_{jik}(-w_s, w_p, -w_i) : E_i(w_p)E_k(w_i)$$

$$\frac{d}{dr}E_k(w_i) = i\left(\frac{k_i}{2\epsilon_i}\right)2\chi_{kij}(-w_i, w_p, -w_s) : E_i(w_p)E_j^*(w_s) \qquad (7.1)$$

The subscript i with w should not be confused with that with E. When the waves are phase-matched, $\overline{K}_p = \overline{K}_s + \overline{K}_i$. It is essential in optical parametric generators that both the frequency tuning $w_p = w_s + w_i$ and momentum matching (or phase-matching) are simultaneously satisfied. Combining the two equations of (7.1),

$$\frac{d^2}{dr^2}E^*(w_s) = \left(\frac{k_s k_i}{\epsilon_s \epsilon_i}\right)\chi^2 E_p^2 E^*(w_s)$$

If we regard the pump amplitude E_p as constant, we get

$$\frac{d^2}{dr^2}E^*(w_s) = g^2 E^*(w_s)$$

$$\frac{d^2}{dr^2}E(w_i) = g^2 E(w_i) \qquad (7.2)$$

where the gain constant or the coupling parameter g is given by

$$g = \left(\frac{w_s w_i}{n_s n_i}\right)^{\frac{1}{2}} \frac{\chi E_p}{c} \qquad (7.3)$$

Solution of (7.2) is

$$E_s^*(w_s, r) = E_s(w_s, o) \cosh gr$$

$$E_i(w_i, r) = i(w_i/w_s)^{\frac{1}{2}} E_s^*(w_s, o) \sinh gr \qquad (7.4)$$

These equations reveal the growth of the signal and idler frequencies, the pump frequency supplying the

requisite power. It can be shown that Manley-Rowe relations, well known in the theory of microwave parametric amplifiers, are obeyed.

Fig. 7.1 shows the schematic of a travelling wave parametric amplifier where phase matching and consequent tuning off the degenerate frequency may be obtained by rotation of the crystal (16). A lithium metaniobate parametric oscillator has been tuned continuously through the infared by Giordmaine and Miller (17). They have employed variation of crystal temperature to obtain phase matching at 90° with the optic axis for different ratios of w_s and w_i. This parametric oscillator was pumped by a 7 KW, 5290 Å second harmonic radiation from a neodymium-doped $CaWO_4$ laser. Energy conversion efficiencies of the order of 0.2 per cent were obtained.

Parametric amplifiers and oscillators employing KDP and ADP crystals have been worked by Akhmanov and his colleagues (18). Continuous tuning is achieved through rotation of the crystal about the optic axis. At the phase-matched angle the frequency condition is also simultaneously met with. It is to be noted that the optical resonator must be simultaneously resonant to signal and idler frequencies, but relatively transparent to the pump frequency $2w_o$, where w_o is the subharmonic or degenerate frequency.

Recently the method of electro-optic tuning (19) has also been successfully achieved for continuous tuning of $LiNbO_3$ parametric oscillator.

It is evident that parametric oscillation will not be initiated until the gain in the nonlinear medium overcomes the resonator and bulk crystal losses. Thus the pump power must exceed a threshold level, which in pulsed lasers may be several hundred Kwatts. Pump power may be considerably reduced by using confocal resonator. Only a few m-watts of exciting power from CW gas lasers have been found to cause oscillation in $LiNbO_3$ with confocal resonator. The same conditions apply to parametric amplifiers as well, in the sense that there is no amplification of the signal and idler waves until the pump power is above the threshold.

CHAPTER II

SUBHARMONIC GENERATION IN A PARAMETRICALLY EXCITED NONLINEAR CIRCUIT.

This chapter is devoted to the examination of parametric oscillation in two - resonant circuit coupled by a nonlinear capacitance, periodic variation of which is caused by a pump voltage. Such a system bear strong analogy with the parametric oscillation excited in nonlinear crystals by laser field. The three frequencies are related by $w_p = w_1 + w_2$, $w_1 = w_o(1+\gamma)$, $w_2 = w_o(1-\gamma)$, where $w_o = w_p/2$ and γ is a small faction. The conditions of oscillation are derived and the "stability zones" of oscillation calculated by digital computer.

8. Preview of Analogical Treatment

Harmonic Generation in Nonlinear circuits has been known through several decades, but the phenomenon of subharmonic generation is of recent origin, linear differential equations of the form

$$\ddot{x} + \xi \dot{x} + w_o^2 x = F_o \cos wt \qquad (8.1)$$

will have the solution whose period is $T = 2\pi/w$ and is the same as of the forcing function; in other words, if the unforced linear system has no periodic solution, then there can never be an isolated periodic solution of any period

except $2\pi/w$. In nonlinear systems on the other hand, isolated periodic solutions may exist whose least period is an integral multiple $n.2\pi/w$ of the period $2\pi/w$ of the forcing function. For instance nonlinear differential equations of the form

$$\ddot{x} + \xi f(x)\dot{x} + w_o^2 x = F_o \cos wt \qquad (8.2)$$

may have solutions of period nT where the integer n is greater than 1. This phenomenon is known as "Sub-harmonic Resonance" and the solutions describe sub-harmonics of order n.

Little research has thus far been done on the generation of powerful coherent infrared radiation. Giant laser frequencies along with their SHG and THG work mostly in the visible and ultraviolet region. Since molecular vibrational frequencies lie in the infrared, the coherent infrared generators, if developed will exert exceedingly strong resonant interaction on substances. Giordmaine & Miller (17) and Miller & Nordland (21) have utilized the parametric process in Lithium metaniobate $LiNbO_3$, for design of continuously tunable coherent infrared generators/ amplifiers. Akhmanov and Coworkers (22) have employed the same process in KDP and ADP. Sub-harmonic frequency generation may be viewed as a special degenerate parametric process wherein the signal, idler and the pump frequencies are related through the expression $w_s = w_i = w_p/2$. Parametric down conversion and the consequent generation of coherent optical frequencies utilizes the phenomenon of nonlinear coupling in dielectric crystals like KDP, ADP and $LiNbO_3$.

The following embodies an examination and discussion of the phenomenon of subharmonic resonance in a typical lumped nonlinear circuit. The process of subharmonic generation in these parametrically excited systems is more or less identical with those in nonlinear materials containing three colinear phase-matched modes, whose frequencies are related by the equation $w_s+w_i = w_p$. Time variations of the amplitudes in the former is analogous to the amplification of waves in space by nonlinear interaction. As pointed out by Louisell at el (23), the parametric equations in the time domain have the same form as the corresponding spatial equations in the nonlinear dielectric material. Despite these close analogies, however, there is an important difference that optical subharmonic (or parametric) generators require "optical tuning" as well satisfying the requirement $\bar{K}_s+\bar{K}_i = \bar{K}_p$ where K's represent the wave number. A simplified theory of parametric amplification and oscillation in nonlinear material is given in Appendix II.

9. Parametric oscillation in Lumped Nonlinear Circuit

Let us consider two resonant cavities coupled by a nonlinear capacitance of the form

$$C(t) = C_o\left[1 + \epsilon \cos(w_p t+\phi)\right] \qquad (9.1)$$

The time variation in the capacitance is affected by a pump source of frequency $w_p = w_1+w_2$. The phase and amplitude of the pump is such as to cause parametric oscillation/amplification in the circuit. Frequencies of the resonant modes,

w_1 and w_2, are related to the degenerate frequency w_o by

$$w_1 = w_o(1+\gamma) \; ; \; w_2 = w_o(1-\gamma) \qquad (9.2)$$

where γ is a small fraction. Oscillation/amplification in this system is analogous to those in nonlinear crystals to be considered in detail in subsequent chapters. The circuit in Fig.9.1(a) may therefore be considered as an electrical equivalent of the optical parametric generators. Following Louisell (24) the coupled wave equations of this parametrically excited system may be written as

$$\frac{du_1}{dt} = \alpha_{11}u_1 + \alpha_{12}u_2^* \exp(iw_p t)$$
$$\frac{du_2^*}{dt} = \alpha_{22}u_2^* + \alpha_{21}^* u_1 \exp(-iw_p t) \qquad (9.3)$$

where

$$\alpha_{11} = iw_1\left(1 + \frac{i}{2Q_1}\right)$$
$$\alpha_{22} = -iw_2\left(1 - \frac{i}{2Q_2}\right)$$
$$\alpha_{12} = i\frac{w_1 \Delta C}{4(\alpha_{11}\alpha_{22})^{\frac{1}{2}}} \exp(+i\phi) \qquad (9.4)$$
$$\alpha_{21}^* = -i\frac{w_2 \Delta C}{4(\alpha_{11}\alpha_{22})^{\frac{1}{2}}} \exp(-i\phi)$$

To remove the time varying coefficients, let

$$u_1 = U_1(t)\exp(iw_1 t)$$
$$u_2^* = U_2^*(t)\exp(-iw_2 t) \qquad (9.5)$$

The resulting equations for mode amplitudes are

$$\frac{d}{dt}U_1 + (iw_1 - \alpha_{11})U_1 = \alpha_{12}U_2^*$$
$$\frac{d}{dt}U_2^* - (iw_2 + \alpha_{22})U_2^* = \alpha_{21}^* U_1 \qquad (9.6)$$

Solution of (9.6) vary as exp (st) where

$$s = -\tfrac{1}{2}\left[i(w_1-w_2)-(\alpha_{11}+\alpha_{22})\right]$$
$$\pm\tfrac{1}{2}\sqrt{\left\{\left[i(w_1-w_2)-(\alpha_{11}+\alpha_{22})\right]^2 + 4\left[\alpha_{12}\alpha_{21}^{*}+(iw_1-\alpha_{11})(iw_2+\alpha_{22})\right]\right\}} \qquad (9.7)$$

Growing oscillations will only occur, if the square-root-term is larger than the decaying terms, i.e. if

$$\alpha_{12}\alpha_{21}^{*} \geq (\alpha_{11}-iw_1)(\alpha_{22}+iw_2)$$

$$\text{or,} \qquad \alpha_{12}\alpha_{21}^{*} \geq \frac{w_1 w_2}{4Q_1Q_2} \qquad (9.8)$$

In terms of the nonlinear coefficient, $\epsilon = \Delta C/C_o$,

$$\frac{\Delta C}{C_o} \geq \frac{2}{(Q_1Q_2)^{\frac{1}{2}}} \qquad (9.9)$$

At the degenerate frequency $w_1 = w_2 = w_o$ the conductance $G = w_oC_o/Q_o$, should satisfy the relation

$$G \leq \frac{w_o\Delta C}{2} \qquad (9.10)$$

This may be compared with the derivations in Appendix III.

10. Periodic Solution : Degenerate Case

The equivalent lumped circuit is shown in Fig. 9.1(b). The system differential equation is

$$\frac{d^2Q}{dt^2} + \frac{G}{C_o}\frac{dQ}{dt} + w_o^2\left(1+\frac{\Delta C}{C_o}\cos w_p t\right)Q = 0$$

Putting $Q = x(t)\exp(-\xi t/2)$, $\xi = G/C_o$

$$\sigma^2 = \frac{1}{w_p^2}(4w_o^2-\xi^2); \quad \epsilon = \frac{4w_o^2}{w_p^2}\frac{\Delta C}{C_o}$$

and replacing t by the normalized independent variable $\tau = w_p t/2$, one obtains the Mathieu Equation,

$$\frac{d^2x}{d\tau^2} + (\sigma^2 + \epsilon \cos 2\tau)x = 0 \qquad (10.1)$$

In the first unstable zone $w_p = 2w_o$ while in the second $w_p = w_o$.

Following Whittaker, the quasi-periodic solution of (10.1) for small values of ϵ may be written for the first unstable zone as

$$x = (\exp \mu\tau) f(\tau)$$

$$f(\tau) = \sin(\tau-\theta) + a_3 \cos(3\tau-\theta) + b_3 \sin(3\tau-\theta) + \ldots\ldots$$

With the result (25),

$$\mu = \tfrac{1}{2}\epsilon \sin 2\theta - \frac{3}{1024}\epsilon^3 \sin 2\theta + \ldots\ldots\ldots$$

$$\sigma^2 = 1 + \tfrac{1}{2}\epsilon \cos 2\theta + \frac{1}{16}\epsilon^2(-1 + \tfrac{1}{2}\cos 4\theta)$$

$$a_3 = \frac{1}{256}\epsilon^2 \sin 2\theta + \ldots. \qquad (10.2)$$

$$b_3 = \frac{1}{16}\epsilon + \frac{1}{256}\epsilon^2 \cos 2\theta + \ldots.$$

The boundaries of the first unstable region is obtainable from the second of Equation (10.2) by putting $\theta = 0$ and $-\pi/2$. Then, to the first approximation,

$$\sigma^2 = 1 \pm \tfrac{1}{2}\epsilon \qquad (10.3)$$

the nonlinear coefficient $\epsilon < 1$ causing small detuning. These are the transition curves separating the regions of stability and instability in the (σ^2, ϵ) plane. Within the unstable zone, that is the zone of possible parametric oscillation, we have

from the first of equations (10.2)

$$\mu = \tfrac{1}{4} \in \sin 2\theta$$

The charge $$Q = f(\tau)\exp\left[\left(\mu - \frac{\xi}{2w_o}\right)\tau\right]$$

For sustained oscillation of the charge

$$\mu = \xi/2w_o$$

Thus $$\frac{\xi}{2w_o} = \tfrac{1}{4} \in \sin 2\theta$$

or $$\frac{G}{2w_o C_o} = \tfrac{1}{4}\frac{\Delta C}{C_o}\sin 2\theta$$

or $$G = \frac{w_o \Delta C}{2}\sin 2\theta \qquad (10.4)$$

This may be compared with (9.10). Thus in the neighbourhood of parametric resonance $\sigma^2 = 1$, the circuit sees a negative conductance given by the above equation. θ is the phase of the stable oscillation.

With the help of a digital computer, the values of $\cos 2\theta$ (and hence θ) for different values of σ^2 and $\in$ have been computed as shown in Table IV.1 (Appendix IV). These θ values have been used to compute the values of μ and the coefficients a_3, b_3 (Eq.10.2 Higher coefficients a_5, b_5 are comparatively less significant and hence not shown. It is observed that the presence of detuning displaces the phase at the stable point by a small degree. The oscillatory condition is given by Eq (10.4). The values of μ are given in Table IV.1, so that the stability of oscillation and hence the values of G required to substain oscilation may be ascertained.

Results of analysis by analogue computer of subharmonic generation relating to the first unstable region is shown in

Fig. 10.1. Large build up of amplitude at the subharmonic resonance ($w_p/2$) is markedly visible in the trace at the bottom, $\sigma^2 = 0.6, \epsilon = 0.8$ where the nonlinearity is within the unstable zone, vide Eq (10.3).

CHAPTER III

PARAMETRIC AMPLIFICATION AND GENERATION OF NEW OPTICAL FREQUENCIES

Five laser frequencies from 3164 Å to 5761 Å are taken for calculation of the phase matching angles in KDP and ADP crystals, both at the degenerate frequencies and when $\gamma(=\Delta w/w_o)$ changes from 0 to 0.4. Phase matching angles for $LiNbO_3$ are computed at four pump frequencies from 5300 Å to 11,523 Å. The refractive index data of KDP and ADP used are those obtained by computer from the equations by Zernike. Tabular values are given and graphs plotted from which one can readily find the phase matching angles corresponding to any pump frequency and any signal-to-idler frequency ratio in KDP, ADP or $LiNbO_3$. Design Tuning curves given for each case show the values of λ_s and λ_i as one rotates the crystal away from the degenerate angle θ_o.

Mismatch gradients ($dk/d\theta$) are derived wherefrom the power changes caused by divergence of beams can be readily estimated.

11 Preview of the Parametric Process

Although studies have been made on the second and Third Harmonic Generation of optical frequencies, comparatively less investigation seems to have been directed towards resonant nonlinear interactions in the infrared region. The second and third harmonic generators and amplifiers work at a few spot frequencies i.e. the harmonic

frequencies of fixed ultranarrow laser frequencies. The problem of achieving coherent optical oscillators, that could be tuned continuously over the ultraviolet, entire visible and near infrared frequencies pose an exciting proposition.

An effective method of obtaining "Tunable Oscillators at optical frequencies" is to employ the phenomenon of parametric interaction of coherent light waves in a nonlinear transparent dielectric medium. Powerful coherent beam of light from a laser is made to act as the pump wave. Power from the pump wave flow by nonlinear coupling to the signal and idler frequencies, according to Manley-Rowe relationship. The three constituent frequencies are related by

$$\omega_p = \omega_s + \omega_i \tag{11.1}$$

This is the energy conservation equation, as would be clear by multiplying through out by the Planck's constant. The two coupled wave equations at the signal and idler frequencies may be written (vide Eq 7.1) as

$$\frac{dE_s}{dr} = -\frac{imk_s}{2\cos(K_s K_p)} E_i^* \exp\left[i(\bar{K}_p - \bar{K}_s - \bar{K}_i)r\right]$$

$$\frac{dE_i^*}{dr} = +\frac{imk_i}{2\cos(K_i K_p)} E_s \exp\left[-i(\bar{K}_p - \bar{K}_s - \bar{K}_i)r\right] \tag{11.2}$$

where the coefficient of dielectric modulation m is given by

$$m = \frac{2\chi E_p}{\epsilon_{si}} \tag{11.3}$$

It is evident from (11.2) that the interaction is maximum when

$$\bar{K}_p = \bar{K}_s + \bar{K}_i \tag{11.4}$$

This is the condition of phase matching or the law of momentum conservation. Thus for parametric generation of coherent light it is not only necessary to have the "optical tuning" of resonators Eq (11.1), but also to satisfy "wave tuning" or phase matching of the wave vectors (Eq 11.4). The latter condition is also called the "synchronism condition". Combining the two equations of (11.2), we obtain

$$\frac{d^2E_s}{dr^2} = \frac{n_s n_i k_s k_i}{4\cos(K_s K_p)\cos(K_i K_p)} E_s \qquad (11.5)$$

The solutions are

$$E_s(r) = E_s(o)\exp(gr)$$
$$E_i(r) = E_i(o)\exp(gr)$$

where the gain constant or growth rate

$$g = \tfrac{1}{2}\left[\frac{n_s n_i k_s k_i}{\cos(k_s k_p)\cos(k_i k_p)}\right]^{\frac{1}{2}} \qquad (11.6)$$

For oscillation, the gain constant must overcome the losses in the circuit.

Fig.(11.1) shows one scheme of achieving parametric interaction in negative uniaxial crystals. Here the pump wave is extraordinary while the signal and the idler waves are ordinary all coupled together and propagating as one collinear beam through the crystal at an angle θ_M with the optic axis. Rotation of the crystal about the direction of the pump wave will generate new pairs of λ_s and λ_i. Besides mechanical tuning, which is achieved by rotation of the nonlinear crystal, two other types of tuning have been successfully tried.

These are

1. temperature tuning (17), and
2. tuning with electro-optic effect (19).

Because of the superiority of mechanical tuning, elaborate design data for this system have been worked out in this thesis.

12. Negative Uniaxial Crystals : Wave Surfaces

As is known from studies of crystallography, the velocity normal surface in uniaxial negative crystals is an oblate ellipsoid of revolution about the z-axis with an inscribed sphere. Fig. 12.1 shows a section through the principal plane. The vibrations, or the plane of polarization of the ordinary rays are in the equatorial direction (plane) while in the extra-ordinary rays these are in the meridional direction; these directions are shown bydots and dashes in the Figure.

The second order susceptibility tensors, which are the same as the piezo-electric tensor coefficients, are given in Appendix I for three types of crystals, KDP, ADP and $LiNbO_3$. These are the crystals which are todate usable for parametric generation of optical frequencies.

If the pump beam propagates in the zx plane as an extra-ordinary wave at a phase-matched angle θ_M with the optic z-axis, the polarization components of the ordinary waves are

(a) In KDP and ADP

$$P_y^o = 2\epsilon_o d_{14} E_x^e E_z^e$$

(b) In $LiNbO_3$

$$P_y^o = 2\epsilon_o d_{22}\left[(E_y^o)^2 - (E_x^o)^2\right] + 2d_{15} E_y^o E_z^e$$

$$= 2\epsilon_o (2d_{15}) E_y^o E_z^e$$

In order to determine the angle at which phase matching of the three collinear constituent waves occur, it is necessary to determine the angular variation of refractive index of the extra-ordinary rays.

In uniaxial crystals, the wave normal surface for the ordinary rays is a sphere

$$n^o(\theta) = n^o(o)$$

For the extra-ordinary rays the surface is an oblate ellipsoid of revolution about the optic axis. The Fresnel equation for this extra-ordinary wave normal surface in anisotropic crystals is

$$\frac{1}{[n^e(\theta)]^2} = \frac{1}{[n^e(0)]^2}\cos^2\theta + \frac{1}{[n^e(90^o)]^2}\sin^2\theta \qquad (12.1)$$

where θ is the angle of the wave vector $\overline{K}$ with respect to the optic axis. Note from Fig. 12.1 that

$$n^o = n^e(o)$$

From Eq (12.1),

$$n^e(\theta) = n^o\left[1+(r^2-1)\sin^2\theta\right]^{-\frac{1}{2}} \qquad (12.2)$$

where the ratio $$r(w) = \frac{n^o}{n^e(90)}$$

Further simplification of Eq (12.1) is possible. If the complement $\phi = \frac{\pi}{2}-\theta$ of the angle θ is taken

$$\frac{1}{[n^e(\phi)]^2} = \frac{1}{[n^o]^2}\sin^2\phi + \frac{1}{[n^e(0)]^2}\cos^2\phi \qquad (12.3)$$

$$\text{or,}\quad \frac{n^e(\phi)}{n^e(0)} = \left[1+\left\{\frac{[n^e(0)]^2}{[n^o]^2}-1\right\}\sin^2\phi\right]^{-\frac{1}{2}}$$

$$= 1-\frac{1}{2}\left\{\frac{[n^e(0)]^2}{[n^o]^2}-1\right\}\sin^2\phi$$

$$= 1-\frac{(n^e(0)-n^o)(n^e(0)+n^o)}{2(n^o)^2}\sin^2\phi \qquad (12.4)$$

Here the zero within parentheses means $\phi=0$. Putting birefringence $B=n^e(0)-n^o$, the resultant equation is

$$\frac{n^e(\phi)}{n^e(0)} = 1-\frac{B[n^e(0)-n^o+2n^o]}{2(n^o)^2}\sin^2\phi$$

$$= 1-\left[\frac{B}{n^o}+\frac{B^2}{2(n^o)^2}\right]\sin^2\phi$$

$$\text{or}\qquad n^e(\phi) = \frac{n^e(0)}{2n^o}\left[2n^o-B\left(2+\frac{B}{n^o}\right)\sin^2\phi\right]$$

$$= \frac{1}{2r}\left[2n^o-B\left(2+\frac{B}{n^o}\right)\sin^2\phi\right] \qquad (12.5)$$

Either the exact equation (12.2) could be used to compute the extra-ordinary refractive index at an angle θ from the z-axis, or the approximate equation (12.5) where ϕ is the complement of the angle θ. It may be noted that the approximate equation (12.5) should be used only when sin ϕ are small, i.e., when the propagation is nearly at right angles to the optic axis.

13. Phase-matching angle at the Subharmonic Frequency

Subharmonic generation is a special degenerate case of the general parametric process where $w_o=w_s=w_i=w_p/2$. The phase matching angle at the subharmonic frequency $\nu_o=1/\lambda_o$ will be designated by θ_o, measured from the optic axis. Usually

for parametric generation of optical frequencies, the monochromatic coherent light beam from a laser is used to function as the pump energy and is made to propagate through the crystal as extra-ordinary waves. The generated subharmonics are ordinary rays. At the degenerate frequency, we have from (11.1) and (11.4)

$$\lambda_o = 2\lambda_p \ , \ n^e(\theta_o) = n^o$$

Here n^e is at w_p and n^o is for w_o

This equation may be satisfied in negative uniaxial crystals where the refractive index surface is a prolate ellipsoid of revolution inscribed in a sphere Fig. 13.1. For calculation of θ_o, we need determining the direction of the ellipse at which the extra-ordinary refractive index $n^e(2w_o)$ equals the ordinary refractive index $n^o(w_o)$. This is done with the help of Eq (12.2).

Phase matching angles θ_o at the degenerate frequency have been calculated for a few laser pump frequencies in the three types of crystals. These are tabulated in Table 13.1. As subharmonic generation is a special degenerate case of general parametric process, these values will be again seen in the general Tables for phase matching angles. The first row for each pump frequency in the general Tables show the value of θ_o. These values are also plotted and shown in Fig. 13.2 (a) to (c) for the three types of crystals, KDP, ADP and $LiNbO_3$. Any slight deviation in the values in the Table and the Fig. are due to the small, but negligible, difference between the measured and computed values of refractive indices of the nonlinear crystals.

TABLE 13.1 PHASE MATCHING ANGLES AT THE SUBHARMONIC OPTICAL FREQUENCY

	λ_p^e(Å)	λ_o^o(Å)	ν_o(cm^{-1})	θ_o(deg)		
				KDP	ADP	$LiNbO_3$
(a)	3,164	6,328	15,802	56.12	57.77	-
(b)	3,472	6,943	14,401	51.04	52.18	-
(c)	4,332	8,664	11,542	42.78	43.38	-
(d)	5,300	10,600	9,434	41.37	41.57	83.91
(e)	5,761	11,522	8,679	41.97	42.29	66.51
(f)	6,943	13,886	7,201	46.66	47.12	52.27
(g)	11,523	23,046	4,339	-	-	44.56

PUMP SIGNAL (a) He - Ne gas laser, second harmonic ; (b) Ruby laser second harmonic ; (c) A difference frequency ; (d) Nd^{3+} glass laser, second harmonic ; (e) He - Ne gas laser, second harmonic ; (f) Ruby laser R_1 radiation ; (g) He - Ne gas laser.

Pattern of the curves between λ_p and θ_o is similar, although in $LiNbO_3$, it is more shallow and spread out. Because of its larger refractive index values, $LiNbO_3$ covers an extended range of wavelengths. These curves also indicate that mechanical tuning of this type of parametric oscillators will be easier at (shorter) pump wave-lengths where the gradient $\Delta\theta_o/\Delta\lambda$ is steep; in other words, employing pump sources having frequencies around the cusp of the curve may better be avoided.

14. Phase-matching Angle for Optical Parametric Generators and Amplifiers

In order to obtain parametric oscillations at optical frequencies, it is essential to have not only "Optical tuning" of the resonators, but also to satisfy matching between the wave vectors. Optical and wave tuning must be simultaneously satisfied in order to design coherent light generators that are continuously tunable over a band of optical frequencies. The energy conservation equation (11.1) may be written as

$$\frac{\lambda_p^e}{\lambda_s^o} = 1 - \frac{\lambda_p^e}{\lambda_i^o} \qquad (14.1)$$

From the momentum conservation equation (11.4),

$$n_p^e(\theta) = n_i^o + \frac{\lambda_p}{\lambda_s}(n_s^o - n_i^o) \qquad (14.2)$$

Equations (14.1) and (14.2) are used to compute the extra-ordinary refractive index $n^e(\theta)$, that will satisfy the two matching conditions. These values are then used in the

following equation to calculate $\sin\theta_M$ and consequently θ_M, the phase matching angle for different pairs of λ_s and λ_i or ratios λ_s/λ_i.

$$n_p^e(\theta) = n_p^o\left[1+(r^2-1)\sin^2\theta\right]^{-\frac{1}{2}} \qquad (12.2)$$

Here the superscripts e and o refer to extra-ordinary and ordinary waves. The subscripts p, s and i refer to the pump, signal and idler waves respectively. Computations of $n^e(\theta)$ and $\sin\theta$ were entirely programmed on and executed in digital computer.

Refractive index data of Lithium metaniobate used are those measured by Boyd at el (26). The values of refractive index vary to some extent depending on the preparation. In addition to variation with temperature, it has been observed in phase-matched nonlinear optical measurements that the refractive index varies from sample to sample. These variations are related to the increasing purity of $LiNbO_3$ crystals since the original measurement in multidomain material (27). Indices of refraction for the ordinary rays at the signal and idler frequencies in KDP and ADP were computed by Digital Computer from the following empirical equation (28)

$$n^2 = A+\frac{B\nu^2}{1-\frac{\nu^2}{C}}+\frac{D}{E-\nu^2} \qquad (14.3)$$

where frequency $\nu=1/\lambda(cm^{-1})$. Values of the constants A, B, C, D, and E as given in ref (28) for the ordinary and extra-ordinary rays in KDP and ADP, were used in computation.

TABLE 14.1 PHASE MATCHING ANGLES FOR OPTICAL PARAMETRIC ACTION IN KDP AND ADP

λ_p^o(Å)	γ	λ_s^o(Å)	λ_i^o(Å)	ν_s (cm^{-1})	θ_M(deg) KDP	θ_M(deg) ADP
3164	0	6328	6328	15,802	56.12	57.77
	.1	5753	7031	17,383	55.80	57.45
	.2	5273	7910	18,963	54.87	56.49
	.3	4868	9040	20,543	53.36	54.95
	.4	4520	10,546	22,123	51.34	52.91
3472	0	6943	6943	14,401	51.04	52.18
	.1	6313	7715	15,841	50.82	51.95
	.2	5786	8680	17,281	50.15	51.29
	.3	5341	9920	18,721	49.12	50.22
	.4	4960	11,573	20,161	47.65	48.80
4332	0	8664	8664	11,542	42.78	43.38
	.1	7876	9626	12,695	42.71	43.24
	.2	7220	10,830	13,850	42.50	43.05
	.3	6664	12,377	15,004	42.20	42.78
	.4	6188	14,440	16,158	41.90	42.54
5300	0	10,600	10,600	9434	41.37	41.57
	.1	9636	11,777	10,377	41.42	41.62
	.2	8833	13,250	11,321	41.59	41.82
	.3	8154	15,143	12,263	41.95	42.24
	.4	7571	17,666	13,208	42.67	43.05
5761	0	11,522	11,522	8679	41.97	42.29
	.1	10,474	12,802	9547	42.08	42.40
	.2	9602	14,401	10,414	42.41	42.77
	.3	8863	16,460	11,282	43.07	43.50
	.4	8230	19,203	12,151	44.27	44.80

TABLE 14.2 PHASE MATCHING ANGLES FOR OPTICAL PARAMETRIC ACTION IN $LiNbO_3$

λ_p^o(Å)	γ	λ_s^o(Å)	λ_i^o(Å)	ν_s (cm^{-1})	θ_M(deg)
5300	0	10,600	10,600	9434	83.91
	.1	9636	11,777	10,377	80.25
	.2	8833	13,250	11,321	76.62
	.3	8154	15,143	12,263	71.41
	.4	7571	17,666	13,208	66.45
5761	0	11,522	11,522	8679	66.51
	.1	10,474	12,802	9547	65.90
	.2	9602	14,401	10,414	64.98
	.3	8863	16,460	11,282	62.32
	.4	8230	19,203	12,151	59.12
6943	0	13,886	13,886	7201	52.27
	.1	12,620	15,430	7924	52.00
	.2	11,571	17,357	8642	51.50
	.3	10,681	19,837	9362	50.97
	.4	9918	23,143	10,082	49.71
11,523	0	23,046	23,046	4339	44.56
	.1	20,950	25,606	4773	44.85
	.2	29,205	28,807	5206	45.27
	.3	17,727	32,922	5641	45.85
	.4	16,461	38,410	6075	47.33

The phase matching angles θ_M thus computed are given in Tables 14.1 and 14.2 for KDP, ADP and $LiNbO_3$ respectively. All the computed matching angles are not given in these Tables. For this, graphs are plotted for different pump wavelengths and materials in Fig. 14.1 to 14.7. From these curves, one may determine the matching angles for any pair of values of ν_s and ν_i.

It may be observed from these figures for matching angles that while the general pattern is the same, the slope of the ν_s/ν_o and $\sin^2\theta$ (or $\sin^2\phi$) is higher in KDP and ADP for a given pump wave-length. At λ_p=0.53 u, the average slope is 2.8 in $LiNbO_3$ and 180 in ADP. Hence the matching angles are limited within a small region in KDP and ADP. Shorter pump wavelengths reduces the slope in a given material. In KDP the average slope is 4.6 for λ_p=0.316 u and 20 for λ_p=0.433 u. In $LiNbO_3$ especially for shorter pump wavelengths phase matching over a large deviation angle from θ_o is possible. For instance, with a pump wavelength of 0.53 u, matching in $LiNbO_3$ is possible from 84 to 60 deg, an angular spread of 24 deg, whereas the corresponding angles in KDP are 41.37 to 42 deg, a spread of hardly 0.6 deg. If a pump source of the shortest possible wavelength of 0.316 u is used in KDP the angles range from 56.12 to about 51 deg.

It is interesting to note that the matching angle θ_o is 84 deg for λ_p=0.53 u in $LiNbO_3$. This has a definite advantage.

15 Design Tuning Curves

The design tuning curves for parametric oscillations utilizing the three nonlinear dielectric crystals, KDP, ADP and $LiNbO_3$ are contained in Fig. 15.1 to 15.7. These have been plotted from the values obtained with the help of digital computer. It is observed that for shorter pump wavelengths, the traces are practically straight lines in all the three crystals; that is $(\Delta\nu)^2$ bears a linear relationship with $\sin^2\phi$, as is predicted by the approximate equation (15.3) given later. It may also be noted that with a pump wavelength λ_p=3164 Å, the whole range of visible wavelengths may be covered by parametric tuning of KDP or ADP. Using a pump source λ_p=5300 Å, a portion of near infrared may be covered by tuning of $LiNbO_3$. Because of large negative birefringence of $LiNbO_3$, phase matching over a wide range of optical wavelengths is possible. For this crystal the matching angle θ_o=84 deg at the degenerate frequency ν_o=9434 cm^{-1}. Since it is almost at right angles to the optic axis, the pump and the signal waves closely interact.

It may be observed that the Figures 15.1 - 15.7 contain signal wavelengths (λ_s) which lie between the pump and the corresponding degenerate frequency. In fact the signal and idler waves are interchangeable and either ν_s or ν_i frequencies could be picked up as both are tuned in the optical resonator. In other words, the region of wavelengths between the subharmonic and the upper limit where idler absorption commences could also be covered provided the crystal is transparent in this region and the resonators are of adequate size and reflectivity to contain them. For example when λ_p=0.53 u, the oscillator

could be tuned at least theoretically over the entire band of wavelengths from 0.53 - 5 u. Miller and Nordland (21) tuned it from 0.68 to 2.34 u, i.e. 70% of the theoretical range.

It may be noted that because of the larger variation of refractive indices in $LiNbO_3$, the angular spread is higher for a given change in wavelength. The following comparison would illustrate :

	λ_p(A)	$\Delta\lambda$(A)	θ(deg)
KDP	3164	1808	4.78
ADP	3164	1808	4.86
$LiNbO_3$	5300	1767	7.28

Furthermore, the nonlinear susceptibility of $LiNbO_3$ is at least an order of magnitude larger than those of KDP or ADP. For instance,

$LiNbO_3$, $d_{31} = 14.9 \times 10^{-12}$ M/volt
KDP , $d_{36} = 1.257 \times 10^{-12}$ M/volt (λ=6328 Å)
ADP , $d_{36} = 0.57 \times 10^{-12}$ M/volt

As will be shown later, this results in a large reduction in the threshold pump power in $LiNbO_3$ parametric amplifiers or oscillators.

An analytic expression for the frequency changes obtainable in parametric process may be deduced as follows. For small deviations from the subharmonic (degenerate) frequency, the signal and idler frequencies may be expressed by

$$w_s = w_o + \delta w$$
$$w_i = w_o - \delta w \qquad (15.1)$$

Hence $w_s+w_i = 2w_o$ (as before at the degenerate stage)

From Eq (11.4) one obtains

$$\frac{w_p n_p^e(\phi)}{c} = \frac{w_s n_s^o}{c} + \frac{w_i n_i^o}{c}$$

Expressing the refractive indices of the signal and idler waves by the Taylor expansion series, and retaining only three terms, we have,

$$\frac{w_p}{c} n_p^e(\phi) = \frac{w_s}{c}\left[n_o^o + \left(\frac{\partial n^o}{\partial w}\right)_o \delta w + \tfrac{1}{2}\left(\frac{\partial^2 n^o}{\partial w^2}\right)(\delta w)^2\right]$$

$$+\frac{w_i}{c}\left[n_o^o - \left(\frac{\partial n^o}{\partial w}\right)_o \delta w + \tfrac{1}{2}\left(\frac{\partial^2 n^o}{\partial w^2}\right)(\delta w)^2\right]$$

Here n_o^o is the ordinary index of refraction at w_o, and the derivatives give dispersion of this index at the degenerate frequency w_o. Since $w_s+w_i = w_p$ and $w_s-w_i = 2\delta w$

$$w_p\left[n_p^e(\phi)-n_o^o\right] = 2\left(\frac{\partial n^o}{\partial w}\right)_o (\delta w)^2 + \tfrac{1}{2} w_p \left(\frac{\partial^2 n^o}{\partial w^2}\right)(\delta w)^2$$

or,
$$(\delta w)^2 = \frac{w_o\left[n_p^e(\phi)-n_o^o\right]}{\left(\frac{\partial n^o}{\partial w}\right)_o + \frac{1}{2} w_o \left(\frac{\partial^2 n^o}{\partial w^2}\right)}$$

or,
$$(\delta \nu)^2 = \frac{\nu_o\left[n_p^e(\phi)-n_o^o\right]}{\left(\frac{\partial n^o}{\partial \nu}\right)_o + \frac{1}{2}\,{}_o\left(\frac{\partial^2 n^o}{\partial \nu^2}\right)}$$

$$= D_1\left[n_p^e(\phi)-n_o^o\right] \qquad (15.2)$$

where
$$D_1 = \nu_o\left[\left(\frac{\partial n^o}{\partial \nu}\right)_o + \frac{1}{2}\nu_o\left(\frac{\partial^2 n^o}{\partial \nu^2}\right)\right]^{-1}$$

Eq (15.2) shows that there will be two frequencies, one above and another below the degenerate frequency ν_o. These obviously correspond to the signal and idler frequencies. Substituting

the approximate expression for $n^e(\phi)$ from Eq (12.5).

$$[\delta\nu(\phi)]^2 = D_1\left[\Delta n - \frac{B}{2r}\left(2+\frac{B}{n_p^o}\right)\sin^2\phi\right]$$

where $\Delta n = n_p^e(0) - n_o^o$. Usually Δn will be found negative.

Putting another constant

$$A_1 = \frac{B}{2r}\left(2+\frac{B}{n_p^o}\right)$$

$$[\delta\nu(\phi)]^2 = D_1[\Delta n - A_1\sin^2\phi] \qquad (15.3)$$

Thus $(\delta\nu)^2$ varies linearly with $\sin^2\phi$, provided $\sin\phi$ is small. $\delta\nu$ has been computed for one such case and compared with the accurate values calculated from (12.2). This is done in order to examplify the magnitude of error in Eq (15.3) and also to assess the regime of its application for calculation of the frequency deviation $\delta\nu$.

For $LiNbO_3$ at λ_p=0.53 u, n_p^o=2.325 and $n_p^e(0)$=2.232. At the degenerate frequency ν_o=9434 cm^{-1} (λ_o=1.06 u) n_o^o=2.233. Therefore

$$\Delta n = n_p^e(0) - n_o^o = -0.001$$

$$r(w) = n_p^o/n_p^e(o) = 1.04166$$

$$B = n_p^e(o) - n_p^o = -0.093$$

Hence $A_1 = -0.08749$

$\delta\nu$ will be zero when $A_1\sin^2\phi_M = \Delta n$

or $$\sin^2\phi_M = \frac{\Delta n}{A_1} = 0.011429$$

or $$\phi_M = 83.87 \text{ deg}$$

This is slightly lower than the value in Table 14.2, because of the approximation in A_1. For a graphical plot of n^o versus ν around the degenerate frequency $\nu_o = 9434\ cm^{-1}$, we compute

$$\left(\frac{\partial n^o}{\partial \nu}\right)_{\nu_o} = 6 \times 10^{-6}\ cm$$

$$\left(\frac{\partial^2 n^o}{\partial \nu^2}\right) = 2 \times 10^{-10}\ cm^2$$

$$\therefore \quad D_1 = 1.36 \times 10^9 \qquad (cm^{-2})$$

$$\therefore \quad (\delta\nu)^2 = 1.36 \times 10^7 (8.749 \sin^2\phi - 0.1) \qquad (15.4)$$

The results are plotted in Fig. 15.4(c) beside the more accurate values from (12.2). In the figure $(\Delta\nu)^2$ instead of $(\delta\nu)^2$ are written. The linear relationship between $(\Delta\nu)^2$ and $\sin^2\phi$ may be noted. The slope of the straight line (full line) between $(\Delta\nu)^2$ and $\sin^2\phi$ obtained from (15.4) is $1.178 \times 10^8 cm^{-1}$. This may be compared with the slope $(1.03 \pm 0.02) \times 10^8 cm^{-2}$ of the experimental and 1.17×10^8 of the theoretically computed plots obtained by Miller and Nordland (21). The slope of the dotted line computed by (12.2) is 1.02×10^8 and agrees excellently well with the figure $(1.03 \pm 0.02) \times 10^8 cm^{-2}$ in the experiment of the above authors. The differences between the theoretical values from Eq (12.2) and (15.4) are due to the approximations involved in the latter, and also due to the inaccuracy in the calculation of the derivatives in the denominator of D_1.

Equation (15.3) when applied to calculate $(\delta\nu)^2$ for fairly large values of $\sin\phi$ yeilded enormously large errors and hence were not used in other cases. The design curves in Fig. 14.1 to 14.7 and 15.1 to 15.7 are those computed from Eq (12.2) with digital computer.

TABLE 15.1 Gradient $(\partial\nu/\partial\theta)$ in $LiNbO_3$ for λ_p=0.53 u, ν_o=9434 cm^{-1}

λ_s^o(Å)	λ_i^o(Å)	$\Delta\nu$ cm^{-1}	$-(\partial\nu/\partial\theta)$	
			cm^{-1} deg^{-1}	cm^{-1} rad^{-1}
9636	11,777	943	366	2.10×10^4
8833	13,250	1887	246	1.41
8231	14,722	2641	225	1.29
7910	16,060	3298	211	1.21
7571	17,666	3774	201	1.15

Curves have also been plotted between $\Delta\nu - \Delta\theta$ and between $\Delta\lambda - \Delta\theta$ so as to directly obtain the frequency or wave-length deviations Fig. 15.8 and 15.9 . An approximate equation for the slope of the $\Delta\nu - \Delta\theta$ curve may be derived. From Eq (15.3)

$$\frac{\partial\nu}{\partial\phi} = -\frac{D_1 A_1}{2\delta\nu}\sin 2\phi$$

or

$$\frac{\partial\nu}{\partial\theta} = +\frac{D_1 A_1}{2\delta\nu}\sin 2\phi \qquad (15.5)$$

Table 15.1 shows the gradient of the $\Delta\nu - \Delta\theta$ curve calculated for the parametric action in $LiNbO_3$ for a pump wavelength $\lambda_p = 0.53$ u. In this case $D_1 = 1.36 \times 10^9 cm^{-2}$, $A_1 = -8.749 \times 10^2$.

Comparison of these slopes with the slope of the trace for $\lambda_p = 5300$ ($\mathring{A}$) in Fig.15.8(c), will reveal that these values are higher. This is because of the approximations contained in Eq (15.5). Nevertheless, the general trend is the same. The approximate curve takes off with an infinite slope at $\Delta\nu = 0$ and then gradually stoops downwards.

It would be apparent from Fig. 15.8 and 15.9 that larger angular spread and consequently superior mechanical tuning is achieveable by using pump sources having shorter wavelengths. Threshold of pump power required will also be reduced, which is a distinct advantage.

16. Mismatch Gradient

It will be shown subsequently that the average signal power in a parametric process is, among other things, proportional to l_{coh}, the average coherence length for the pencil of signal rays.

$$\langle P_s \rangle \propto l_{coh}^{(s)}$$

Here it is assumed that the crystal is thick, $l \gg l_{coh}$, and that the anisotropy in the crystal is of a small order of magnitude. Kleinman (13) has evaluated the effective coherence length for the pencil of rays having an angular spread as

$$l_{coh}^{(s)} = 2/\,{}^{(s)} \qquad (16.1)$$

where $${}^{(s)} = \frac{(w_s w_i)^{\frac{1}{2}}}{c}\left(\frac{dn^e}{d\theta}\right)_{\theta_M}$$

Since, $dk^e/d\theta = w_p c^{-1}(dn^e/d\theta)$, we have

$${}^{(s)} = \frac{(w_s w_i)^{\frac{1}{2}}}{w_p}\left(\frac{dk^e}{d\theta}\right)_{\theta_M} \qquad (16.2)$$

At the degenerate frequency w_o,

$${}_o^{(s)} = \tfrac{1}{2}\left(\frac{dk^e}{d\theta}\right)_{\theta_o} \qquad (16.3)$$

Thus the signal power is inversely proportional to the mismatch gradient $(dk^e/d\theta)_{\theta_M}$. These have been calculated for the crystals KDP, ADP and $LiNbO_3$. Tabular values may be seen in the last columns of Table 16.1 - 16.3 . The $(dn^e/d\theta)_{\theta_M}$ values from which the mismatch gradient have been evaluated are shown in the fourth columns of these Tables.

It will be observed from these Tables that variations in the mismatch gradient with λ_s are small. In KDP and ADP the gradient reach constant values at higher signal frequencies; this is especially noticeable at longer pump wavelengths that occur near the cusps of the θ_o-λ_p curves in Fig. 13.2 . Because of their comparatively larger refractive indices, variations in the mismatch gradient are higher in $LiNbO_3$. Since these changes are clearly discernable in $LiNbO_3$, more

TABLE 16.1 Mismatch gradient for optical parametric oscillations in KDP

λ_p^e(Å) / ν_o(cm^{-1})	λ_s^o(Å)	$\gamma = \Delta\nu/\nu_o$	$(\frac{dn}{d\theta})_{\theta_M} \times 10^{-4}$ deg^{-1}	$(\frac{dk}{d\theta})_{\theta_M} \times 10^{2}$ cm^{-1} deg^{-1}	$(\frac{dk}{d\theta})_{\theta_M} \times 10^{2}$ cm^{-1} rad^{-1}
3164 Å	6328	0	7.37	1.463	83.8
	5753	.1	7.40	1.469	84.2
	5273	.2	7.44	1.477	84.6
15,802 cm^{-1}	4868	.3	7.66	1.521	87.1
	4520	.4	8.00	1.588	91.0
3472 Å	6943	0	7.58	1.371	78.6
	6313	.1	7.69	1.391	79.7
	5786	.2	7.8	1.411	80.8
14,401 cm^{-1}	5341	.3	7.83	1.417	81.2
	4960	.4	7.9	1.[illegible]	81.9
4332 Å	8664	0	8.05	1.167	66.9
	7876	.1	7.90	1.145	65.6
	7220	.2	7.78	1.128	64.6
11,542 cm^{-1}	6664	.3	7.65	1.109	63.5
	6188	.4	7.50	1.087	62.3
5300 Å	10600	0	7.35	.871	49.9
9434 cm^{-1}	7571	.4	7.35*	.871*	49.9
5761 Å	11,522	0	7.2	.785	45.0
8679 cm^{-1}	8230	.4	7.2*	.785*	45.0*

* The values are same for all the ratios of $\Delta\nu/\nu_o$ between 0 and 0.4 and thereafter.

TABLE 16.2 Mismatch gradient for optical parametric oscillations in ADP

λ_p^o(Å) / ν_o(cm^{-1})	λ_s^o(Å)	$\gamma = \Delta\nu/\nu_o$	$(\frac{dn}{d\theta})$ x 10^4 deg^{-1}	$(\frac{dk}{d\theta_M})$ x 10^2 cm^{-1} deg^{-1}	$(\frac{dk}{d\theta_M})$ x 10^2 cm^{-1} rad^{-1}
	6328	0	7.85	1.559	89.3
3164 Å	5753	.1	7.93	1.575	90.2
	5273	.2	8.00	1.588	91.0
15,802 cm^{-1}	4868	.3	8.15	1.618	92.7
	4520	.4	8.65	1.718	98.4
	6943	0	8.2	1.484	85.0
3472 Å	6313	.1	8.26	1.495	85.6
	5786	.2	8.35	1.511	86.6
14,401 cm^{-1}	5341	.3	8.41	1.522	87.2
	4960	.4	8.5	1.538	88.1
	8664	0	8.96	1.30	74.5
4332 Å	7876	.1	8.73	1.266	72.5
	7220	.2	8.49	1.231	70.5
11,542 cm^{-1}	6664	.3	8.24	1.195	68.5
	6188	.4	8.0	1.160	66.5
5300 Å	10,600	0	8.10	.960	55.0
	9636	.1	8.05	.955	54.7
9434 cm^{-1}	8833	.2	8.00*	.954*	54.6*
5761 Å	11,522	0	8.01	.873	50.0
	10,474	.1	7.99	.871	49.9
8679	9602	.2	7.96*	.868*	49.7*

* The values are the same for all the ratios of $\Delta\nu/\nu_o$ between 0.2 and 0.4 and thereafter.

TABLE 16.3 Mismatch gradient for optical parametric oscillations in $LiNbO_3$.

λ_p^e(Å) ν_o (cm^{-1})	λ_s(Å)	$\gamma = \Delta\nu/\nu_o$	$\left(\frac{dn}{d\theta}\right)_{\theta_M} \times 10^4$ deg^{-1}	$\left(\frac{dk}{d\theta}\right)_{\theta_M} \times 10^2$	
				$cm^{-1}\ deg^{-1}$	$cm^{-1}\ rad^{-1}$
	10,600	0.0	3.95	.468	26.8
5300 Å	9636	0.1	4.9	.581	33.3
	8833	0.2	6.95	.824	47.2
9434 cm^{-1}	8154	0.3	9.20	1.090	62.4
	7571	0.4	11.47	1.360	77.9
	11,522	0.0	10.95	1.194	68.4
5761 Å	10,474	0.1	11.12	1.212	69.4
	9602	0.2	11.62	1.267	72.6
8679 cm^{-1}	8863	0.3	12.47	1.360	77.9
	8230	0.4	13.50	1.472	84.3
	13,886	0.0	13.70	1.240	71.0
6943 Å	12,620	0.1	13.90	1.258	72.1
	11,571	0.2	14.10	1.276	73.1
7201 cm^{-1}	10,681	0.3	14.28	1.292	74.0
	9918	0.4	14.45	1.307	74.9
11,523 Å	23,046	0.0	14.1	.769	44.06
4339 cm^{-1}	16,461	0.4	14.1*	.769*	44.06*

* The values are the same for all the ratios of $\Delta\nu/\nu_o$ in between and thereafter.

so at shorter pump wave-lengths, the mismatch gradient as a function of $\Delta\nu/\nu_o$ have been plotted in Fig. 16.1 . Notice from the trace for λ_p = 0.53 u that if the decrease in the signal power was solely due to the increase in the mismatch gradient, we could define a bandwidth for the parametric oscillator. The 3 db power reduction occurs at $\Delta\nu/\nu_o$ = 0.2 or at λ_s = 0.88 u for λ_p = 0.53 u in $LiNbO_3$.

Coherence length l_{coh} have also been computed. These are shown in Table 16.4 .

TABLE 16.4 Coherence length, l_{coh} in KDP, ADP and $LiNbO_3$ crystals for beam divergence angle $\Delta = 0.25$ deg $= 4.36 \times 10^{-3}$ rad.

λ_p^o(Å)	λ_s^o(Å)	λ_i^o(Å)	l_{coh} (cm)		
			KDP	ADP	$LiNbO_3$
3164	6328	6328	0.109	0.103	
	5273	7910	0.111	0.103	
	4520	10,546	0.110	0.102	
3472	6943	6943	0.117	0.108	
	5786	8680	0.116	0.108	
	4960	11,573	0.112	0.113	
4332	8664	8664	0.137	0.123	
	7220	10,830	0.145	0.133	
	6188	14,440	0.161	0.150	
5300	10,600	10,600	0.184	0.167	0.342
	9636	11,777	0.185	0.168	0.278
	8833	13,250	0.188	0.172	0.198
	8154	15,143	0.193	0.176	0.154
	7571	17,666	0.201	0.183	0.128
5761	11,522	11,522	0.204	0.183	0.134
	10,474	12,802	0.205	0.185	0.133
	9602	14,401	0.208	0.189	0.129
	8863	16,460	0.214	0.193	0.124
	8230	19,203	0.222	0.201	0.119
6943	13,886	13,886	-	-	0.129
	11,571	17,357	-	-	0.128
	9918	23,143	-	-	0.134
11,523	23,046	23,046	-	-	0.208
	19,205	28,807	-	-	0.212
	16,461	38,410	-	-	0.227

CHAPTER IV
OPTICAL CAVITY RESONATOR

This chapter is devoted to obtaining a relation between the resonator losses and the gain in the nonlinear medium. Consequently an expression is derived relating the coefficient of dielectric modulation m with the resonator Q. By digital computer Q values are computed for different mirror reflectivity. Three types of media, the KDP, ADP and $LiNbO_3$ are covered. Threshold values of m required to overcome the resonator losses are computed therefrom. Beam widths of the resonant fundamental mode at the focal region of confocal resonator are computed for two values of confocal parameter.

17.1 Cavity Resonator of the Febry-Perot type

As stated in Article 11, nonlinear parametric oscillation will occur when the growth rate g, Eq (11.6) is greater than zero; that is when $\exp(gl) > 1$. The distance d between the mirrors of the resonator is related to the optical length of the cavity by the expression

$$d_i' = \frac{d}{\cos(K_i K_p)} \qquad (17.1)$$

when reflection losses on the surface of the two mirrors are taken into account, the modified condition for the growth rate g evidently is

for the signal, $R_1(w_s)R_2(w_s)\exp(gl) \geq 1$

for the idler , $R_1(w_i)R_2(w_i)\exp(gl) \geq 1$

where l is the length of the crystal. Since g is small, gl is a small quantity. The two inequalities above may be simplified and written as

$$R_1(w_s)R_2(w_s)(1+gl) \geq 1$$

$$R_1(w_i)R_2(w_i)(1+gl) \geq 1$$

The quality factor Q of the optical cavity resonator with plane parallel mirrors having coefficient of reflection $R_1(w_1)$ at w_1(Fig.17.1) is defined by

$$Q_i = \frac{k_i d_i'}{1 - R_1(w_i)R_2(w_i)} \tag{17.2}$$

Thus

$$\begin{aligned} R_1(w_s)R_2(w_s)gl &\geq \frac{k_s d_s'}{Q_s} \\ R_1(w_i)R_2(w_i)gl &\geq \frac{k_i d_i'}{Q_i} \end{aligned} \tag{17.3}$$

In many practical situation, $R_1(w_i) = R_2(w_i) \doteq 1$. Therefore, the condition of oscillation may be simply expressed as

$$(gl)^2 \geq \frac{k_s k_i d_s' d_i'}{Q_s Q_i} \tag{17.4}$$

or $$gl \geq 2L$$

where the round-trip power loss $2L = 1-R^2 \doteq 2(1-R)$.
At the degenerate frequency, one finds from (17.4)

$$\frac{w_o \mathcal{F} E_p l}{cnd} \geq \frac{2L}{d} \tag{17.5}$$

When the space between the mirrors is filled with the dielectric material, i.e. if we assume $l = d$, we obtain

from Eq (11.6), (17.1) and (17.4),

$$\frac{m_s m_1}{4} \geq \frac{1}{Q_s Q_1}$$

$$\text{or} \quad \frac{m}{2} \geq \left(\frac{1}{Q_s Q_1}\right)^{\frac{1}{2}} \tag{17.6}$$

At the degenerate frequency w_o,

$$\frac{m}{2} \geq \frac{1}{Q_o} \tag{17.7}$$

The condition $m = 2/Q_o$ specifies the minimum values of m_o needed for commencement of parametric oscillation. The analysis follows the derivation by Akhmanov and Khokhlov (22) and (29). A complete theory of the parametric process is given in Appendix II.

It may be worthwhile digressing for a while and compare some of the above results with those obtained in Chapter II for subharmonic generation in parametrically excited nonlinear systems. The condition of self oscillation in the neighbourhood of the subharmonic frequency in a resonant circuit with a time-dependent capacitance of the form

$$C = C_o\left[1 + \frac{\Delta C}{C_o}\cos w_p t\right] \tag{9.1}$$

was found to be

$$\frac{\Delta C}{2C_o} \geq \frac{1}{Q}$$

$$\text{or} \quad \frac{\epsilon}{2} \geq \frac{1}{Q} \tag{9.9}$$

where $\epsilon = \Delta C/C_o$ is the nonlinear coefficient. This coefficient is analogous to the coefficient of dielectric modulation in

nonlinear material given by

$$\epsilon = \epsilon_o \left[1 + m \cos(w_p t - \bar{k}_p r)\right] \qquad (17.8)$$

The two equations (17.7) and (9.9) are identical. They differ in that while ϵ is in the time domain, m is in the space of the nonlinear material. This is another instance proving the equivalence of the coupled wave equations (9.3) in the time domain and (11.2) in space. In fact one is convertible to the other by interchanging t with r/c.

The stability analysis of the exponential growth of the signal and idler amplitudes need not be separately carried out "in space". By an analytical treatment similar to that for the Mathieu equation in Art 9 (CH II), it is possible to determine the regions in the analogous $E_p - \Delta k$ plane where parametric oscillation will occur. In fact the curve separating the unstable from the stable regions in the $E_p - \Delta k$ plane is identical with that in the analogous $\epsilon - \sigma^2$ plane (CH.II). It is observed that for the same detuning in a lossy medium larger pump power is needed. Again, for greater mismatch, evidently, higher pump excitation is called for parametric oscillation.

Reverting to the original discussion, the minimum values of m required to induce parametric oscillation in KDP, ADP and $LiNbO_3$, may be calculated from Eq (17.6). From these threshold values of the dielectric modulation, we may compute the smallest growth rate possible in parametric oscillation in nonlinear material.

Assuming that $\cos(k_i k_p) = 1$, we obtain from (17.4) & (17.6)

$$g = \left(\frac{k_s k_i}{Q_s Q_i}\right)^{\frac{1}{2}} = \left(\frac{4\pi^2 n_s n_i}{\lambda_s \lambda_i Q_s Q_i}\right)^{\frac{1}{2}} \qquad (17.9)$$

At the degenerate frequency

$$g = \frac{k_o}{Q_o} = \frac{2\pi n_o^o}{\lambda_o Q_o}$$

If in Eq (17.4) the value of Q is substituted from Eq (17.2) the resultant equation is

$$g^2 l^2 \geq \left[1-R^2(w_s)\right]\left[1-R^2(w_i)\right] \qquad (17.10)$$

This expression obviously equates the gain in field strength with the round trip reflection losses in the dielectric layers of the mirror. Bulk losses in the crystal are neglected(30).

By digital computer the quality factor Q of cavity resonators containing nonlinear crystals KDP, ADP and $LiNbO_3$ have been calculated. Values for a few typical combinations of λ_s and λ_i and at different pump wave-lengths are given in Table 17.1 and 17.3. It may be noticed that there is a substantial rise in Q values in resonators having mirrors of higher reflectivity. As one tunes off the degenerate frequencies Q_s and Q_i changes are relatively small. If the variations in refractive index with frequency could be ignored, the quality factor of a resonator of a given reflectivity and having the same material would be inversely proportional to the pump wavelength; i.e. would be larger at shorter pump wave-lengths. This is another advantage of using high frequency pump source. Of course attaining high coefficient of reflection and simultaneous resonance at the signal and idler frequencies with a given γ is more difficult at shorter pump wave lengths.

Table 17.1 Q values for different reflectivity of mirrors in plane parallel Febry-Perot resonator filled with KDP, d =1 cm

λ_o( )	γ	R = 0.90		R = 0.95		R = 0.98		R = 0.99	
		$Q_s x10^5$	$Q_i x10^5$	$Q_s x10^6$	$Q_i x10^6$	$Q_s x10^6$	$Q_i x10^6$	$Q_s x10^6$	$Q_i x10^6$
0.633	0	7.875	7.875	1.535	1.535	3.779	3.779	7.519	7.519
	.1	8.679	7.075	1.691	1.379	4.164	3.395	8.286	6.755
	.2	9.484	6.277	1.848	1.223	4.550	3.012	9.055	5.993
	.3	10.29	5.480	2.006	1.068	4.939	2.629	9.827	5.232
	.4	11.11	4.684	2.164	.913	5.329	2.247	10.60	4.472
0.694	0	7.166	7.166	1.396	1.396	3.438	3.438	6.841	6.841
	.1	7.898	6.438	1.539	1.255	3.790	3.089	7. 541	6.147
	.2	8.627	5.712	1.681	1.113	4.139	2.741	8.236	5.454
	.3	9.360	4.985	1.824	.971	4.491	2.392	8.937	4.759
	.4	10.10	4.260	1.968	.830	4.844	2.044	9.640	4.067
0.866	0	5.722	5.722	1.115	1.115	2.745	2.745	5.463	5.463
	.1	66.304	5.140	1.228	1.002	3.025	2.466	6.019	4.908
	.2	6.887	4.558	1.342	.888	3.305	2.187	6.576	4.352
	.3	7.471	3.976	1.456	.775	3.585	1.908	7.133	3.796
	.4	8.056	3.393	1.570	.661	3.865	1.628	7.691	3.239
1.06	0	4.660	4.660	.908	.9080	2.236	2.236	4.449	4.449
	.1	5.135	4.184	1.001	.8153	2.464	2.007	4.903	3.995
	.2	5.611	3.708	1.093	.723	2.692	1.779	5.357	3.540
	.3	6.086	3.230	1.186	.630	2.920	1.550	5.810	3.084
	.4	6.563	2.750	1.279	.5360	3.149	1.320	6.266	2.626
1.15	0	4.279	4.279	.834	.834	2.053	2.053	4.085	4.085
	.1	4.717	3.841	.919	.749	2.263	1.843	4.503	3.667
	.2	5.154	3.402	1.004	.663	2.473	1.632	4.920	3.248
	.3	5.591	2.962	1.090	.577	2.682	1.421	5.338	2.828
	.4	6.029	2.519	1.175	.491	2.893	1.209	5.756	2.405

TABLE 17.2 Q values for different reflectivity of mirrors in plane parallel Febry-Perot resonator filled with ADP. d =1 cm

λ_o(u)	γ	R = 0.90		R = 0.95		R = 0.98		R = 0.99	
		$Q_s x10^5$	$Q_i x10^5$	$Q_s x10^6$	$Q_i x10^6$	$Q_s x10^6$	$Q_i x10^6$	$Q_s x10^6$	$Q_s x10^6$
0.633	0	7.951	7.951	1.550	1.550	3.815	3.815	7.592	7.592
	.1	8.764	7.142	1.708	1.392	4.205	3.427	8.367	6.819
	.2	9.579	6.335	1.867	1.235	4.596	3.040	9.146	6.049
	.3	10.40	5.529	2.026	1.077	4.989	2.653	9.927	5.279
	.4	11.22	4.724	2.187	.921	5.384	2.267	10.71	4.510
0.694	0	7.234	7.234	1.410	1.410	3.471	3.471	6.906	6.906
	.1	7.972	6.498	1.553	1.266	3.825	3.118	7.611	6.204
	.2	8.711	5.763	1.698	1.123	4.180	2.765	8.317	5.503
	.3	9.454	5.029	1.842	.980	4.536	2.413	9.026	4.801
	.4	10.20	4.295	1.988	.837	4.894	2.061	9.738	4.101
0.866	0	5.774	5.774	1.125	1.125	2.770	2.770	5.513	5.513
	.1	6.362	5.186	1.240	1.011	3.052	2.488	6.074	4.951
	.2	6.952	4.597	1.355	.896	3.335	2.206	6.637	4.389
	.3	7.542	4.008	1.470	.781	3.619	1.923	7.201	3.827
	.4	8.134	3.418	1.585	.666	3.903	1.640	7.766	3.264
1.06	0	4.700	4.700	.916	.916	2.255	2.255	4.487	4.487
	.1	5.180	4.219	1.009	.822	2.485	2.024	4.946	4.028
	.2	5.661	3.737	1.103	.728	2.716	1.793	5.405	3.568
	.3	6.142	3.254	1.197	.634	2.947	1.561	5.864	3.107
	.4	6.624	2.768	1.291	.539	3.178	1.328	6.324	2.643
1.15	0	4.315	4.315	.841	.841	2.070	2.070	4.120	4.120
	.1	4.757	3.872	.927	.754	2.283	1.858	4.542	3.696
	.2	5.199	3.428	1.013	.668	2.494	1.645	4.964	3.273
	.3	5.642	2.982	1.099	.581	2.707	1.431	5.386	2.847
	.4	6.085	2.533	1.186	.494	2.919	1.215	5.809	2.419

TABLE 17.3 Q values for different reflectivity of mirrors in plane parallel Febry-Perot resonator filled up with $LiNbO_3$, d=1cm

λ_o(u)	γ	R = 0.90		R = 0.95		R = 0.98		R = 0.99	
		$Q_s x10^5$	$Q_i x10^5$	$Q_s x10^6$	$Q_i x10^6$	$Q_s x10^6$	$Q_i x10^6$	$Q_s x10^6$	$Q_i x10^6$
1.06	0	6.963	6.963	1.357	1.357	3.341	3.341	6.648	6.648
	.1	7.682	6.253	1.497	1.219	3.686	3.000	7.335	5.970
	.2	8.407	5.542	1.638	1.080	4.034	2.659	8.027	5.291
	.3	9.437	4.550	1.839	.887	4.528	2.183	9.010	4.345
	.4	9.881	4.127	1.925	.804	4.741	1.980	9.434	3.940
1.15	0	6.393	6.393	1.246	1.246	3.067	3.067	6.104	6.104
	.1	7.049	5.741	1.374	1.119	3.382	2.754	6.731	5.481
	.2	7.710	5.086	1.502	.991	3.699	2.440	7.361	4.856
	.3	8.376	4.437	1.632	.865	4.019	2.129	7.998	4.236
	.4	9.051	3.787	1.764	.738	4.343	1.817	8.642	3.616
1.39	0	5.281	5.281	1.029	1.029	2.534	2.534	5.042	5.042
	.1	5.825	4.742	1.135	.924	2.795	2.275	5.561	4.527
	.2	6.366	4.202	1.241	.819	3.055	2.016	6.078	4.012
	.3	6.909	3.663	1.346	.714	3.315	1.757	6.597	3.497
	.4	7.456	3.124	1.453	.609	3.577	1.499	7.119	2.983
2.3	0	3.138	3.138	.611	.611	1.506	1.506	2.996	2.996
	.1	3.462	2.813	.675	.548	1.661	1.350	3.305	2.686
	.2	3.786	2.487	.738	.485	1.816	1.193	3.614	2.375
	.3	4.112	2.158	.801	.421	1.973	1.036	3.926	2.061
	.4	4.437	1.827	.865	.356	2.129	.877	4.236	1.745

TABLE 17.4 Threshold values of m for different reflectivity of mirrors in plane parallel Febry-Perot resonator filled with KDP, d=1 cm

λ_o(u)	γ	R = 0.90 m x 10^6	R = 0.95 m x 10^6	R = 0.98 m x 10^7	R = 0.99 m x 10^7
0.633	0	2.540	1.303	5.293	2.660
	.1	2.552	1.310	5.320	2.673
	.2	2.592	1.330	5.403	2.715
	.3	2.663	1.367	5.550	2.789
	.4	2.773	1.423	5.780	2.904
0.694	0	2.791	1.432	5.817	2.923
	.1	2.805	1.439	5.846	2.938
	.2	2.849	1.462	5.938	2.984
	.3	2.928	1.502	6.102	3.067
	.4	3.050	1.565	6.356	3.194
0.866	0	3.495	1.794	7.285	3.661
	.1	3.513	1.803	7.323	3.680
	.2	3.570	1.832	7.440	3.739
	.3	3.670	1.883	7.648	3.843
	.4	3.826	1.963	7.973	4.007
1.06	0	4.292	2.203	8.946	4.496
	.1	4.315	2.214	8.993	4.519
	.2	4.385	2.250	9.140	4.593
	.3	4.511	2.315	9.402	4.725
	.4	4.707	2.416	9.811	4.930
1.15	0	4.674	2.399	9.742	4.896
	.1	4.699	2.411	9.794	4.922
	.2	4.777	2.451	9.955	5.003
	.3	4.915	2.522	10.24	5.148
	.4	5.132	2.634	10.70	5.375

TABLE 17.5 Threshold values of m for different reflectivity of mirrors in plane parallel Febry-Perot Resonator filled with ADP, d = 1 cm.

λ_o(u)	γ	R = 0.90 m x 10^{-6}	R = 0.95 m x 10^{-6}	R = 0.98 m x 10^{-7}	R = 0.99 m x 10^{-7}
0.633	0	2.515	1.291	5.242	2.634
	.1	2.528	1.297	5.269	2.648
	.2	2.567	1.317	5.351	2.689
	.3	2.638	1.354	5.498	2.763
	.4	2.747	1.410	5.725	2.877
0.694	0	2.765	1.419	5.763	2.896
	.1	2.779	1.426	5.792	2.911
	.2	2.823	1.448	5.883	2.956
	.3	2.901	1.488	6.046	3.038
	.4	3.022	1.551	6.298	3.165
0.866	0	3.464	1.778	7.219	3.628
	.1	3.482	1.787	7.257	3.647
	.2	3.538	1.815	7.374	3.705
	.3	3.637	1.867	7.581	3.810
	.4	3.793	1.946	7.905	3.973
1.06	0	4.256	2.184	8.869	4.457
	.1	4.278	2.195	8.917	4.481
	.2	4.348	2.231	9.063	4.554
	.3	4.474	2.296	9.325	4.686
	.4	4.671	2.397	9.735	4.892
1.15	0	4.635	2.379	9.661	4.855
	.1	4.660	2.391	9.713	4.881
	.2	4.738	2.431	9.875	4.962
	.3	4.876	2.502	10.16	5.107
	.4	5.094	2.614	10.62	5.336

TABLE 17.6 Threshold values of m for different reflectivity of mirrors in plane parallel Febry-Perot resonator filled with $LiNbO_3$, d=1cm.

λ_o(u)	γ	R = 0.90 m x 10^{-6}	R = 0.95 m x 10^{-6}	R = 0.98 m x 10^{-7}	R = 0.99 m x 10^{-7}
1.06	0	2.872	1.474	5.987	3.008
	.1	2.886	1.481	6.014	3.022
	.2	2.930	1.504	6.107	3.069
	.3	3.052	1.566	6.361	3.197
	.4	3.132	1.607	6.528	3.280
1.15	0	3.128	1.605	6.520	3.277
	.1	3.144	1.613	6.553	3.293
	.2	3.194	1.639	6.657	3.345
	.3	3.281	1.683	6.837	3.436
	.4	3.416	1.753	7.120	3.578
1.39	0	3.787	1.943	7.893	3.966
	.1	3.806	1.953	7.932	3.986
	.2	3.867	1.984	8.059	4.050
	.3	3.976	2.040	8.286	4.164
	.4	4.144	2.126	8.636	4.340
2.3	0	6.374	3.271	13.28	6.676
	.1	6.409	3.289	13.36	6.713
	.2	6.518	3.345	13.58	6.826
	.3	6.713	3.445	13.99	7.031
	.4	7.023	3.604	14.64	7.356

The threshold values of the coefficient of modulation m for the different values of Q in Table 17.1 to 17.3 are given in tabular form in Table 17.4 to 17.6. Since m is inversely proportional to Q, reduction in m occur in high Q resonators or mirrors having high reflectivity. Because of comparatively greater Q-values in resonators using $LiNbO_3$, the m values for a given pump wavelength are lower. In addition χ in $LiNbO_3$ is about ten times higher. It would therefore be desirable to use $LiNbO_3$ for the design of a parametric oscillator pumped preferably by a shorter wavelength source. It is further interesting to note that, as one tunes the oscillator off the degenerate frequency, the value of m rises, calling thereby larger pump power.

17.2 Confocal Resonator

The merits inherent in confocal resonator offer the possibility of CW parametric action when excited by CW gas lasers. In a confocal spherical system the diffraction losses δ_d are orders of magnitude less than for plane parallel mirrors. This is because of greater concentration of the field along the mirror axis (31). For a given reflector loss δ_r and reflector radius a, Q is maximum as a function of the confocal spacing b when δ_d is a definite fraction (32) of δ_r. If $a^2/b\lambda = 1$, $\delta_d/\delta_r \doteq 0.1$. This ratio decreases with increasing $a^2/b\lambda$. The optimization, however, requires values of b that are impracticably large. Since for the dominant TEM_{oo} mode δ_d is of the order of 10^{-5} for $a^2/b\lambda = 1$, we may ignore the diffraction loss in comparison with δ_r which

be of the order of 10^{-2}. Consequently we may write

$$Q = \frac{kb}{\delta_r + \delta_d} \doteq \frac{kb}{\delta_r} \qquad (17.11)$$

The confocal parameter b is equal to the spacing d between the mirrors. It is defined by

$$w_o^2 = \frac{b}{k} \qquad (17.12)$$

where w_o is the beam radius at the waist which in a confocal system occurs in the focal region (33). The multiple layers of the dielectric coating on the mirror surfaces are coincident with the phase fronts of the resonator modes, both the signal and the idler waves being simultaneously resonant in the lowest mode.

The resonant mode frequencies are given by

$$\frac{4nb}{\lambda} = 2q + (m+n+1) \qquad (17.13)$$

where q is an integer denoting the number of nodes of the axial standing-wave pattern (q+1 is the number of half wave lengths). m and n are the mode numbers. For the TEM_{oo} mode (i.e. m=0, n=0) Eq (17.13) yields

$$\begin{aligned} n_s b_s &= q_s \lambda_s/2 \\ n_i b_i &= q_i \lambda_i/2 \end{aligned} \qquad (17.14)$$

the subscripts refer to the signal and idler modes.

By digital computer beam widths have been calculated for two values of confocal parameter. These are given in Table 17.7 for a $LiNbO_3$ filled confocal cavity. As is clear from (17.12) the beam diameter shrinks with shorter spacing of the spherical mirrors.

of confocal cavity resonator filled with $LiNbO_3$

$\lambda_o(u)$	γ	b_o=1 cm			b_o=5 cm*		
		$w_s^2 \times 10^5$ (cm^2)	$w_1^2 \times 10^5$ (cm^2)	$w_p^2 \times 10^5$ (cm^2)	$w_s^2 \times 10^4$ (cm^2)	$w_1^2 \times 10^4$ (cm^2)	$w_p^2 \times 10^4$ (cm^2)
1.03	0	.7335	.7335	.3667	.3667	.3667	.1833
	.1	.6647	.8168	.3665	.3324	.4084	.1833
	.2	.6074	.9218	.3661	.3037	.4609	.1831
	.3	.5585	1.058	.3655	.2792	.5289	.1827
	.4	.5168	1.237	.3645	.2584	.6187	.1823
1.06	0	.7552	.7552	.3776	.3776	.3776	.1888
	.1	.6847	.8413	.3775	.3424	.4206	.1887
	.2	.6257	.9492	.3771	.3128	.4746	.1885
	.3	.5746	1.090	.3763	.2873	.5449	.1881
	.4	.5324	1.274	.3755	.2662	.6372	.1878
1.15	0	.8228	.8228	.4114	.4114	.4114	.2057
	.1	.7462	.9163	.4113	.3731	.4582	.2056
	.2	.6823	1.034	.4111	.3411	.5172	.2055
	.3	.6280	1.185	.4105	.3140	.5927	.2052
	.4	.5812	1.389	.4098	.2906	.6945	.2048
1.39	0	.9960	.9960	.4980	.4980	.4980	.2490
	.1	.9034	1.109	.4979	.4517	.5547	.2489
	.2	.8263	1.252	.4978	.4132	.6259	.2489
	.3	.7614	1.436	.4976	.3807	.7182	.2488
	.4	.7055	1.684	.4972	.3528	.8419	.2486
2.3	0	1.676	1.676	.8380	.8382	.8382	.4191
	.1	1.520	1.870	.8384	.7598	.9350	.4191
	.2	1.389	2.115	.8384	.6947	1.058	.4193
	.3	1.279	2.437	.8388	.6396	1.218	.4193
	.4	1.186	2.878	.8398	.5928	1.439	.4199

* The values for b_o=5 cm are simply five times the values for b_o=1 cm.

CHAPTER V

POWER CONSIDERATION

From the results on Q and m values in Chapter IV, we calculate by digital computer the threshold levels of the pump field E_p and the pump intensity I_p for plane waves. As the power involved are enormous, these are strictly applicable to the design of pulsed parametric oscillators and amplifiers. Use of focused beams considerably reduces the power. Beam widths of the lowest resonant TEM_{oo} modes as calculated in Chapter IV are employed to compute the threshold level. With $LiNbO_3$ the pump power P_p is several mW from 1.03 u to 2.3 u and hence within the range of CW gas lasers.

Single-pass parametric amplifier gain is calculated and graphical plots given from which one can readily find out the gain of amplifiers consisting of KDP, ADP or $LiNbO_3$ for any pump intensity at any frequency. Power ratio $P_i(l)/P_s(o)$ is calculated both for plane waves and for focused Gaussian beams.

18 ### Threshold Pump Power in Pulsed Parametric Oscillator with Plane Parallel Resonator

In Article 17 we had considered a cavity resonator and derived the condition of oscillation by equating the round-trip loss of the signal and idler to the one-way gain assuming that the pump signal traverses the resonator only once. The cavity is resonant simultaneously to the signal and idler modes, but transparent to the pump mode.

Transverse intensity distributions of laser beams are essentially Gaussian. The beam contracts to a minimum diameter $2w_o$ at the beam waist where the phase front is plane. This aspect will be considered in later sections.

Initially, we imagine the nonlinear uniaxial crystal of length l to be located in a small region along the axis of the mirrors where the wave-fronts are effectively parallel and planer (Fig. 17.1). We consider only the lowest order or the fundamental TEM_{oo} modes of the signal and idler, as higher order modes will not be phase-matched with the pump mode. The fundamental mode frequencies are $\nu = qc/2d_i$, where d_i is the distance between the plane mirrors and q an integer. In the following, we derive in a very simplified manner, an expression for the pump power required to induce parametric oscillation in a resonant cavity. We assume plane waves of uniform cross section over the interacting region and that the beam radii are related by $w_s^2 = w_i^2 = 2w_p^2$ although the latter stipulation may appear redundant.

The minimum pump power needed to excite oscillation in a plane parallel Febry-Perot Cavity resonator may be estimated from the condition

$$m = 2/(Q_s Q_i)^{\frac{1}{2}} \qquad (17.6)$$

Here m means the minimum quantity of modulation that must be caused by the pump intensity in the nonlinear material. Since $m = 2\chi E_p/\epsilon$, we obtain for the pump field

$$E_p = \frac{m n_s^o n_i^o}{2\chi} \qquad (18.1)$$

Taking the appropriate coefficients of susceptibility tensor χ from Art 12, we obtain

(a) For <u>KDP & ADP</u>

$$E_p = \frac{m n_s^o n_i^o}{2 d_{14} \sin \theta_M} \qquad (18.2)$$

(b) <u>For $LiNbO_3$</u>

$$E_p = \frac{m n_s^o n_i^o}{4 d_{15} \sin \theta_M} \qquad (18.3)$$

Because of the absence of any exact value of these tensor coefficients, only approximate values have been taken as used in computation of E_p. The values (MKS units/volt) are

(a) For KDP , $d_{14} = 6.0 \times 10^{-13}$

(b) For ADP , $d_{14} = 5.6 \times 10^{-13}$

(c) For $LiNbO_3$, $d_{15} = 6.6 \times 10^{-12}$

The values of E_p for different values of Q, and hence reflectivity of the plane parallel Febry-Perot cavity resonator using the three uniaxial crystals have been computed by the help of digital computer. The values of R chosen for computation are the same as in Tables 17. The computed values of Q and m at different frequencies in the three types of crystals are given in Table 17.1 - 17.6 . The corresponding values of E_p are shown for each values of R in Tables 18.1 - 18.3 .

The threshold pump intensity I_p may now be easily obtained from the equation

$$I_p = \tfrac{1}{2} \epsilon_o c n E^2$$

For the parametric process under consideration

$$I_p = \tfrac{1}{2}\epsilon_o c n_p^e(\theta) E_p^2 \qquad (18.4)$$

$$= 1.326 \times 10^3 n_p^e(\theta) E_p^2 \quad \text{watts m}^{-2}$$

$$P_p = \frac{\pi}{2}\epsilon_o c n_p^e(\theta) w_p^2 E_p^2$$

$$= 4.16 \times 10^3 n_p^e(\theta) w_p^2 E_p^2 \quad \text{watts}$$

The E_p values calculated above together with the appropriate values $n_p^e(\theta)$ at different phase matching angles of the three types of crystals were fed to the digital computer. The threshold pump power, thus computed, are shown in Table 18.1 - 18.3. Eq (18.4) may be expressed more conveniently in terms of the loss coefficients. From Eq (III.1), the pump field

$$E_p = \frac{gc}{\mathcal{L}}\left(\frac{n_s n_i}{w_s w_i}\right)^{\frac{1}{2}} \qquad (18.5)$$

Substituting this in (18.4) and writing n_p for $n_p^e(\theta)$, we have for the pump intensity

$$I_p = \tfrac{1}{2}\epsilon_o c n_p E_p^2$$

$$= \frac{\epsilon_o c}{8\pi^2}\left(\frac{g}{\mathcal{L}}\right)^2 (n_p n_s n_i \lambda_s \lambda_i) \qquad (18.6)$$

$$= 3.36 \times 10^5 \left(\frac{g}{\mathcal{L}}\right)^2 (n_p n_s n_i \lambda_s \lambda_i) \quad \text{watts m}^{-2}$$

λ's are the free space wavelength of the oscillating modes. Substituting for g from Eq (17.4), the power required in the exciting laser beam with radius w_p is

$$P_p \geq \frac{\epsilon_o c w_p^2}{8\pi}(n_p n_s n_i \lambda_s \lambda_i)\left(\frac{2L}{\mathcal{L}_1}\right)^2 \qquad (18.7)$$

$$\geq 4.23 \times 10^4 w_p^2 (n_p n_s n_i \lambda_s \lambda_i)\left(\frac{2L}{\mathcal{L}_1}\right)^2 \quad \text{watts}$$

TABLE 18.1 Threshold pump field E_p(volt cm^{-1}) and pump intensity I_p(watts cm^{-2}) for Parametric Oscillation in a cavity Resonator with KDP. Mirror spacing d = 1 cm; $R_1(w) = R_2(w) = R$

$\lambda_o(\mu)$	R = 0.90		R = 0.95		R = 0.98		R = 0.99	
	$E_p \times 10^4$	$I_p \times 10^6$	$E_p \times 10^4$	$I_p \times 10^6$	$E_p \times 10^3$	$I_p \times 10^5$	$E_p \times 10^3$	$I_p \times 10^4$
0.633	5.797	6.720	2.975	1.770	12.08	2.919	6.072	7.372
	5.849	6.842	3.001	1.801	12.19	2.973	6.126	7.505
	6.004	7.215	3.081	1.900	12.51	3.134	6.288	7.915
	6.286	7.915	3.226	2.084	13.10	3.438	6.585	8.682
	6.720	9.053	3.449	2.384	14.00	3.932	7.039	9.930
0.694	6.783	9.188	3.481	2.420	14.14	3.992	7.105	10.08
	6.836	9.333	3.508	2.458	14.25	4.053	7.16	10.24
	7.010	9.813	3.597	2.583	14.61	4.263	7.341	10.76
	7.312	10.69	3.752	2.814	15.25	4.643	7.659	11.72
	7.775	12.09	3.990	3.185	16.21	5.253	8.143	13.26
0.866	9.65	18.54	4.954	4.881	20.12	8.053	10.11	20.34
	9.71	18.77	4.985	4.944	20.24	8.155	10.17	20.59
	9.90	19.49	4.980	5.133	20.63	8.467	10.37	21.38
	10.22	20.77	5.243	5.470	21.29	9.022	10.70	22.78
	10.68	22.69	5.480	5.977	22.23	9.859	11.18	24.90
1.06	12.09	28.95	6.203	7.625	25.18	12.58	12.66	31.76
	12.14	29.19	6.229	7.688	25.03	12.68	12.71	32.03
	12.27	29.84	6.297	7.856	25.58	12.96	12.85	32.73
	12.50	30.94	6.413	8.145	26.04	13.44	13.09	33.94
	12.80	32.44	6.568	8.543	26.66	14.09	13.40	35.59
1.15	12.97	33.25	6.654	8.756	27.03	14.44	13.58	36.48
	13.00	33.44	6.672	8.807	27.10	14.53	13.62	36.69
	13.11	33.98	6.726	8.951	26.93	14.76	13.73	37.29
	13.27	34.80	6.808	9.163	27.65	15.11	13.89	38.16
	13.47	35.84	6.910	9.436	28.06	15.57	14.10	39.31

TABLE 18.2 Threshold pump field E_p(volt cm^{-1}) and pump intensity I_p(watts cm^{-2}) for Parametric oscillation in a cavity Resonator with ADP.
Mirror spacing d = 1 cm ; $R_1(w) = R_2(w) = R$

λ_o (u)	R = 0.90		R = 0.95		R = 0.98		R = 0.99	
	$E_p \times 10^4$	$I_p \times 10^6$	$E_p \times 10^4$	$I_p \times 10^6$	$E_p \times 10^3$	$I_p \times 10^5$	$E_p \times 10^3$	$I_p \times 10^4$
0.633	6.156	7.651	3.159	2.015	12.83	3.324	6.447	8.397
	6.209	7.786	3.186	2.051	12.94	3.382	6.503	8.544
	6.372	8.207	3.270	2.161	13.28	3.564	6.674	9.003
	6.665	8.980	3.421	2.365	13.89	3.902	6.981	9.857
	7.114	10.25	3.651	2.699	14.82	4.452	7.452	11.24
0.694	7.220	10.51	3.705	2.767	15.04	4.564	7.562	11.53
	7.279	10.68	3.735	2.813	15.17	4.640	7.624	11.72
	7.458	11.22	3.827	2.954	15.54	4.873	7.812	12.30
	7.776	12.20	3.989	3.218	16.20	5.299	8.144	13.38
	8.256	13.76	4.237	3.624	17.20	5.979	8.647	15.10
0.866	10.33	21.44	5.303	5.644	21.53	9.310	10.82	23.51
	10.40	21.71	5.335	5.714	21.67	9.426	10.89	23.80
	10.59	22.51	5.435	5.927	22.27	9.777	11.09	24.70
	10.92	23.94	5.604	6.304	22.76	10.40	11.44	26.26
	11.39	26.09	5.849	6.871	23.75	11.33	11.93	28.63
1.06	13.02	33.86	6.677	8.916	27.12	14.70	13.63	37.14
	13.06	34.08	6.702	8.974	27.22	14.80	13.68	37.38
	13.20	34.83	6.775	9.172	27.51	15.13	13.83	38.20
	13.43	36.02	6.891	9.488	27.98	15.65	14.06	39.53
	13.85	37.58	7.107	9.898	28.87	16.33	14.51	41.23
1.15	13.91	38.65	7.144	10.18	29.01	16.79	14.58	42.40
	13.95	38.84	7.162	10.23	29.08	16.87	14.62	42.61
	14.05	39.42	7.213	10.38	29.29	17.13	14.72	43.24
	14.21	40.27	7.295	10.60	29.63	17.49	14.88	44.18
	14.40	41.33	7.390	10.88	30.02	17.95	15.08	45.33

TABLE 18.3 Threshold pump field E_p(volt cm^{-1}) and pump intensity I_p(watts cm^{-2}) for parametric oscillation in a cavity Resonator with $LiNbO_3$
Mirror spacing d = 1 cm ; $R_1(w) = R_2(w) = R$

λ_o(u)	R = 90		R = 0.95		R = 0.98		R = 0.99	
	$E_p \times 10^3$	$I_p \times 10^5$	$E_p \times 10^3$	$I_p \times 10^4$	$E_p \times 10^3$	$I_p \times 10^3$	$E_p \times 10^3$	$I_p \times 10^3$
1.06	5.459	.8824	2.801	2.324	1.138	3.834	.5717	.9682
	5.537	.9087	2.841	2.392	1.154	3.946	.5801	.9966
	5.697	.9627	2.924	2.536	1.187	4.181	.5965	1.056
	6.165	1.131	3.164	2.978	1.285	4.911	.6458	1.241
	6.461	1.243	3.314	3.272	1.346	5.398	.6766	1.363
1.15	6.421	1.218	3.295	3.208	1.338	5.294	.6726	1.337
	6.482	1.243	3.327	3.272	1.351	5.399	.6789	1.363
	6.631	1.300	3.402	3.424	1.382	5.650	.6946	1.427
	6.965	1.438	3.575	3.787	1.452	6.247	.7300	1.577
	7.480	1.660	3.839	4.373	1.559	7.215	.7833	1.822
1.39	8.933	2.349	4.584	6.185	1.862	10.20	.9159	2.577
	9.008	2.388	4.622	6.292	1.878	10.38	.9435	2.620
	9.210	2.497	4.725	6.577	1.919	10.85	.9648	2.739
	9.522	2.669	4.885	7.028	1.984	11.59	.9971	2.928
	10.08	2.993	5.171	7.883	2.100	13.00	1.055	3.284
2.3	16.48	7.880	8.458	20.75	3.435	34.24	1.726	8.649
	16.47	7.871	8.455	20.72	3.432	34.18	1.725	8.632
	16.58	7.970	8.506	20.99	3.455	34.63	1.737	8.746
	16.81	8.199	8.629	21.59	3.504	35.61	1.761	8.991
	16.99	8.363	8.716	22.02	3.541	36.32	1.780	9.171

where 2L = 1-R is the loss in the resonator during "a round trip" of the signal and idler modes.

An alternative approach leading to the estimation of the threshold pump intensity required for exciting oscillation in a cavity resonator with plane parallel mirrors is given in Appendix III.

It is observed from the Table 18.1-3 that the minimum pump power required decreases with increasing Q or reflectivity of the resonator. Furthermore, the pump power required is about two orders of magnitude lower in $LiNbO_3$ for the same mirror reflectivity. This is evident from Eq (18.7) where it is shown that the minimum pump power is inversely proportional to χ^2. Thus considerable advantage may be derived by using high Q resonator with $LiNbO_3$ crystals.

It may also be observed that the threshold power for sustaining the oscillation increases as one tunes the oscillator off the subharmonic frequency. Again, the use of higher frequency pump source yields an advantage.

It is evident from Table 18.1 - 18.3 that the pump power is significantly high and beyond the limits of CW power from gas lasers. Only pulsed solid state lasers can meet such power requirement. Furthermore, beams from these pulsed lasers diffuse enough to elevate the threshold.

18.1 Divergent Beams

Parametric oscillation in a Febry-Perot cavity considered above requires a pump intensity significantly higher than the minimum values shown in Tables 18.1 - 18.3

This higher threshold occurs because of slight mismatch introduced by beam divergence.

The frequency offset due to mismatch of the oscillating modes in the resonator is

$$\Delta w = w_p - (w_{so}+w_{io})$$

where w_{so} and w_{io} are the resonant frequencies of the unperturbed modes and $w_{so}+\Delta w/2$ and $w_{io}+\Delta w/2$ are the oscillation frequencies (30). The modified phase mismatch is

$$\Delta k' = \bar{K}_p - (\bar{K}_{so}+\bar{K}_{io})$$

$$k_{io} = q\pi/d_i \qquad (17.14)$$

For the optimum case of exact phase matching, $\Delta k'=0$, of the two modes, $\Delta w=0$ and the threshold is, as stated before, identical with the minimum value predicted by Eq (18.7). Then it can be shown that the pump intensity when $\Delta k' \neq 0$ increases by the factor

$$\frac{(\Delta k' l/2)^2}{\sin^2(\Delta k' l/2)}$$

The maximum possible mismatch is $(\Delta k')_{max}=\pi/2l$, and hence the threshold level of pump power increases by a factor of 1.24 maximum.

It may be interesting to compare this derivation with those derived by Kleinman for second harmonic generation with slightly divergent beams(13). The threshold pump power in Table 18.1 - 18.3 should therefore be increased by a factor of 1.24 in order to estimate the minimum requirement.

18.2 CW Parametric Oscillator with Confocal Resonator: Threshold Power

With a Febry-Perot type of cavity resonator with plane parallel mirrors, the pump power required to excite oscillatory modes with common radius W_o is given by Eq (18.7). As an illustration (34), consider a cavity of length l = 1 mm with loss 2L = 0.01 (1 percent) and containing modes of radius W_o=1 mm at λ_o=1 u. Using KDP crystal (χ= 0.85 x 10^{12} M/volt) the threshold pump power predicted by (18.7) is about 200 KW. This power is immensely high for a CW oscillator. We, therefore, consider confocal type of cavity containing focused beams interacting with a thin slab of uniaxial nonlinear material inside the cavity. The oscillating modes w_s and w_i (note that the subscript o has been dropped) are simultaneously resonant and are phase matched, such that the dielectric planes on mirror surface are coincident with the spherical phase planes of the resonator modes. The pump, as before, is assumed to traverse the resonator only once and emerge undepleted. The focused beams are matched in the optimum condition such that their widths conform (34),(35) to the relation,

$$\frac{1}{W_p^2} = \frac{1}{W_s^2} + \frac{1}{W_i^2} \qquad (18.8)$$

The threshold pump power for parametric oscillation in this optimum situation is from Eq (II.7)

$$P_p = \frac{\epsilon_o c}{16\pi}(n_p n_s n_i \lambda_s \lambda_i)\left(\frac{2L}{\chi l}\right)^2 (W_s^2 + W_i^2) \qquad (18.9)$$

where the beam widths y's are determined by the confocal parameter b_o according to the equations (see Eq 17.12)

$$y_s^2 = \frac{b_o \lambda_s}{2\pi n_s}, \quad y_i^2 = \frac{b_o \lambda_i}{2\pi n_i} \tag{18.10}$$

and $y_o^2 = \frac{b_o \lambda_o}{2\pi n_o}$ (all at the beam waist)

Further,

$$\lambda_s = \frac{\lambda_o}{1+\gamma}, \quad \lambda_i = \frac{\lambda_o}{1-\gamma}$$

$$n_s = n_o(1-\zeta), \quad n_i = n_o(1+\zeta)$$

and from (Eq (11.4) for phase matching $n_p \doteq n_o(1+\gamma\zeta)$

Hence $$y_s^2+y_i^2 = 2y_o^2 \frac{1+\gamma\zeta}{(1-\zeta^2)(1-\gamma^2)}$$

Substitution of this in (18.9) yields

$$P_p = \frac{\epsilon_o c}{8\pi}(n_p n_s n_i \lambda_s \lambda_i)\left(\frac{2l}{\pi l}\right)^2 y_o^2 \frac{1+\gamma\zeta}{(1-\zeta^2)(1-\gamma^2)} \tag{18.11}$$

We may write (18.9) in the form

$$P_p = \frac{4l^2}{K} \frac{2}{1-\gamma^2} \frac{y_s^2+y_i^2}{l^2} \tag{18.12}$$

where $$K = \frac{32\pi}{\epsilon_o c} \frac{\chi^2}{n_p n_s n_i \lambda_o^2} \tag{18.13}$$

At the degenerate frequency

$$P_p = \frac{\epsilon_o c}{8\pi} y_o^2 n_o^3 \lambda_o^2 \left(\frac{2l}{\pi l}\right)^2$$

$$= \frac{4l^2}{K}\left(\frac{2y_o}{l}\right)^2$$

Let us estimate the pump power requirement of a CW oscillator using a KDP crystal. The confocal parameter approximately is equal to the radius of curvature of the mirrors; thus let $b_o = l = 1$ cm. Then with KDP crystal $y_o^2 = 10^{-9} m^2$ at $\lambda_o = 1$ u.

TABLE 18.4 Threshold Pump Power (Eq 18.12) in $LiNbO_3$ Parametric Oscillator with confocal resonator. $b_o=1=1$ cm. $2L=10^2$ mks/volt, for values of M_s, M_1, in Table 17.7

$\lambda_o(u)$	γ	$K \times 10^7$ (MKS/watt)	P_p(mw)*
1.03	0	5.567	5.271
	.1	5.464	5.478
	.2	5.321	5.987
	.3	5.089	6.981
	.4	4.709	8.870
1.06	0	5.208	5.801
	.1	5.112	6.030
	.2	4.975	6.594
	.3	4.709	7.769
	.4	4.398	9.782
1.15	0	3.775	8.718
	.1	3.738	8.986
	.2	3.685	9.705
	.3	3.514	11.34
	.4	3.297	14.22
1.39	0	1.958	20.35
	.1	1.944	20.91
	.2	1.918	22.58
	.3	1.893	25.51
	.4	1.829	31.10
2.3	0	.583	114.9
	.1	.590	116.0
	.2	.600	121.5
	.3	.616	132.4
	.4	.655	147.7

* The threshold power will increase by a factor of 2 if χ is reduced by $1/\sqrt{2}$ to account for the longitudinal modes.

From (18.12) the threshold pump power for $2L=10^{-2}$ is computed as 2.5 watts. Although this is within the range of a CO_2-N_2-He type CW laser, (λ_p=10.6 u) it is rather high for a Argon-ion laser at λ_p=0.5145 u. If a $LiNbO_3$ crystal is used instead, the pump power exciting oscillation in an identical resonator would be 7.7 mW ($2d_{15}=13.2 \times 10^{-12}$ M/volt). CW power upto 1 watt is available from argon-ion CW laser.

Threshold pump power of the exciting CW laser beam using confocal resonator with $LiNbO_3$ crystal is shown in Table 18.4 .

19 Power Gain in Optical Parametric Amplifier

To date no systematic theory seem to have emerged with which one can reasonably estimate the power of the signal or idler wave in an optical parametric process. The beam used as pump source is not a ray of light without divergence. Within the narrow pencil of rays the phase Δk is not zero through the cross-section of the beam. As a result the signal power is lower than the value of $\Delta k=0$ along the beam axis. We shall derive expressions for the power gain in an optical parametric amplifier in an ideal condition ($\Delta k=0$) and in a practical situation where due to beam divergence $\Delta k \neq 0$.

The coupled wave equations describing the growth of the signal and idler waves in a nonlinear medium pumped by a strong laser source are from (11.2)

$$\frac{dE_s}{dr} = -\frac{im_s k_s}{2\cos(k_s k_p)} E_i^* e^{i\Delta k r}$$

$$\frac{dE_i^*}{dr} = \frac{im_i k_i}{2\cos(k_i k_p)} E_s e^{-i\Delta k r} \qquad (19.1)$$

where $\Delta k = \bar{K}_p - \bar{K}_s - \bar{K}_i$, is the phase mismatch. Combining the two equations,

$$\frac{d^2E_s}{dr^2} = \frac{m_s m_i k_s k_i}{\cos(k_s k_p)\cos(k_i k_p)} E_s + i\Delta k \frac{dE_s}{dr}$$

$$\text{or } \frac{d^2E_s}{dr^2} - i\Delta k \frac{dE_s}{dr} - g^2 E_s = 0 \qquad (19.2)$$

where g is the gain constant given in Eq (11.6)

Assuming that $(k_i k_p)$ is a small quantity

$$g = \tfrac{1}{2}(m_s m_i k_s k_i)^{\frac{1}{2}} \qquad (11.6)$$

The roots of the differential operator in (19.2) are

$$i\frac{\Delta k}{2} \pm \left[g^2 - \left(\frac{k}{2}\right)^2\right]^{\frac{1}{2}}$$

$$\text{writing } g' = \left[g^2 - \left(\frac{\Delta k}{2}\right)^2\right]^{\frac{1}{2}} \qquad (19.3)$$

the solution of (19.2) is

$$E_s(r) = (A_1 e^{g'r} + A_2 e^{-g'r}) e^{i\Delta k r/2} \qquad (19.4)$$

Here g' is the growth rate modified by the beam divergence. To determine the constants, we put the boundary conditions

at r=0. This leads to

$$A_1 = \tfrac{1}{2}\left[E_s(o) - \frac{i}{2g'}m_s k_s E_i^*(o)\right] - \frac{i\Delta k}{4g'}E_s(o)$$

and $$A_2 = \tfrac{1}{2}\left[E_s(o) + \frac{i}{2g'}m_s k_s E_i^*(o)\right] + \frac{i\Delta k}{4g'}E_s(o)$$

Hence

$$E_s(r) = \left\{E_s(o)\cosh g'r - \left[\frac{i}{2g'}m_s k_s E_i^*(o) + \frac{i\Delta k}{2g'}E_s(o)\right]\sinh g'r\right\} e^{i\Delta kr/2}$$

$$E_i^*(r) = \left\{E_i^*(o)\cosh g'r + \left[\frac{i}{2g'}m_i k_i E_s(o) + \frac{i\Delta k}{2g'}E_i^*(o)\right]\sinh g'r\right\} e^{-i\Delta kr/2}$$

(19.5)

The influence of the beam divergence and the consequent phase mismatch are contained in the exponential factor $\exp(i\Delta kr/2)$ and in g'. It would be exceedingly difficult to find an exact analytic expression for the average of the terms involving Δk so as to account for the variation of Δk across the beam section.

The growth rate g' in divergent beams is lower than the unmodified g. Equation (19.3) suggests that there will be no parametric amplification until the pump intensity is sufficiently high such that $g > \Delta k/2$. In the ideal case ($\Delta k=0$) g is only required to be greater than zero for amplification.

19.1 Perfect matching $\Delta k=0$

When the three waves are perfectly matched Eq (19.5) becomes

$$E_s(r) = E_s(o)\cosh gr - \frac{i}{2g}m_s k_s E_i^*(o)\sinh gr$$

$$E_i^*(r) = E_i^*(o)\cosh gr + \frac{i}{2g}m_i k_i E_s(o)\sinh gr \qquad (19.6)$$

With a signal input $E_s(o)$ at r=0, the idler field grows from zero, so that $E_s(o) \neq 0$, but $E_i^*(0) = 0$. Then

$$E_s(r) = E_s(o)\cosh gr$$

$$E_i^*(r) = \frac{i}{2g} m_i k_i E_s(o)\sinh gr \qquad (19.7)$$

or $$E_i(r) = -i\left(\frac{w_i n_s}{w_s n_i}\right)^{\frac{1}{2}} E_s(o)\sinh gr$$

Power in the travelling signal and idler waves are given by

$$P_s(l) = P_s(o)\cosh^2 gl$$

$$P_i(l) = \left(\frac{w_i n_s}{w_s n_i}\right) P_s(o)\sinh^2 gl \qquad (19.8)$$

where l is the length of the crystal, and $P_s(o)$ is the initial signal power at r=0. The coherence length for the waves is defined by

$$l_s^{-1} = g = \chi \frac{E_p}{c}\left(\frac{w_s w_i}{n_s n_i}\right)^{\frac{1}{2}} \qquad (19.9)$$

At the degenerate frequency

$$g = 172\chi I_p^{\frac{1}{2}}/\lambda_o n_o^{3/2}$$

Here χ is the tensor $\bar{a}_1 . d : \bar{\bar{a}}_2 \bar{\bar{a}}_3$, see Eq (II.3) in Appendix II. "d" is the piezoelectric tensor coefficient. Thus Eq (19.8) become

$$P_s(l) = P_s(o)\cosh^2(l/l_s)$$

$$P_i(l) = (w_i n_s / w_s n_i) P_s(o)\sinh^2(l/l_s) \qquad (19.10)$$

The values of the gain constant g or the reciprocal of the coherence length, are computed from Eq (19.9) at a few subharmonic frequencies These are given in the first three columns of Table 19.1, for the

TABLE 19.1 Single-Pass Parametric gain Eq (19.9) and (19.10) at the subharmonic frequency for a 1 cm long crystal. E_p = 100 kv cm^{-1}.

$\lambda_o(u)$	$g(N_p\ cm^{-1})^*$ $\Gamma_s^1(cm^{-1})$			$P_1(l)/P_s(o)$			$P_s(l)/P_s(o)$ (db)		
	KDP	ADP	$LiNbO_3$	KDP	ADP	$LiNbO_3$	KDP	ADP	$LiNbO_3$
.6328	.33	.308	-	.113	.097		.41	.41	
.6943	.28	.263	-	.081	.071		.33	.33	
.8664	.196	.184	-	.039	.034		.17	.17	
1.06	.156	.146	3.46	.025	.022	252	.08	.08	24
1.1522	.146	.136	2.94	.022	.018	88.9	.04	.04	19.5
1.3886	-	-	2.12	-	-	17.0	-	-	12.5
2.3046	-	-	1.15	-	-	2.02	-	-	4.7

* KDP $d_{14} = 0.6 \times 10^{-12}$ MKS unit/volt

ADP $d_{14} = 0.56 \times 10^{-12}$ MKS unit/volt

$LiNbO_3$ $2d_{15} \times 13.2 \times 10^{-12}$ MKS unit/volt

three crystals pumped by a laser field E_p=100 kv cm^{-1} (about 20 MW cm^{-2} in KDP and ADP, and 30 MW cm^{-2} in $LiNbO_3$). Eq (19.10) indicates that under perfect phase matched condition the signal intensity grows exponentially with crystal length. Furthermore, larger growth rate and hence larger power gain for a given length of crystal and pump power are obtainable from $LiNbO_3$. For instance, with E_p=100 kv cm^{-1} the power gain in a 2 mm thick $LiNbO_3$ crystal is 1.6 db at λ_o=1.06 u the corresponding coherence length l_s is 2.9 mm. In KDP the power gain, with E_p=100 kv cm^{-1} and l = 1 cm, is 0.41 db and l_s = 3 cm at λ_o = 6328 Å. In order to facilitate design work, the g values are plotted as a function of pump intensity in Fig. 19.1. From these curves, the gain constant may be found for any material at any laser frequency by simply multiplying the values in Fig. 19.1 (a) by the factor F.

19.2 Imperfect matching $\Delta k \neq 0$

Due to finite width of the beam, $\Delta k \neq 0$, except along the axial line of the beam. We envision that the laser beam has a small but definite angular width . Then from Eq (19.5)

$$E_s(r) = \left[\cosh g'r - \frac{i\Delta k}{2g'}\sinh g'r\right] E_s(o)e^{i\Delta kr/2} \qquad (19.11)$$

$$E_i^*(r) = i\left(\frac{w_i n_s}{w_s n_i}\right)^{\frac{1}{2}}\sinh g'r \cdot E_s(o)e^{-i\Delta kr/2}$$

The second term inside the paranthesis of the first equation may be treated as negligible. Further the gain constant g' may

also be assumed constant. For small values of phase mismatch

$$g' \doteq g\left[1-\tfrac{1}{2}\left(\frac{k}{2g}\right)^2\right] = g\left[1-\tfrac{1}{2}\left(l_s/l^\circ_{coh}\right)^2\right]$$

where l°_{coh} is the coherent length at the degenerate frequency according to the definition adopted in Eq (16.1). For numerical values of l_{coh}, reference may be made to Table 16.4 . Thus for $l_s \ll l_{coh}$, we may find an expression for the average field as follows :

$$\begin{aligned}\left\langle e^{i\Delta k l/2}\right\rangle &= \frac{1}{\Delta}\int_{-\Delta/2}^{\Delta/2} \exp\left[il(dk/d\theta)_o\theta/2\right]\,d\theta \\ &= \frac{2}{il(dk/d\theta)_o\Delta}\left[\exp(il(dk/d\theta)_o\theta/2)\right]_{-\Delta/2}^{\Delta/2} \\ &= \frac{\sin l(dk/d\theta)_o\Delta/4}{l(dk/d\theta)_o\Delta/4} \\ &= \frac{\sin(l/l^\circ_{coh})}{l/l^\circ_{coh}}\end{aligned}$$

Here $(dk/d\theta)_o = (dk/d\theta)_{\theta_M}$ as per definition (ref.13) adopted in Eq (16.3). Thus Eq (19.11) yield

$$E_s(l) = E_s(o)\cosh g'l \cdot \frac{\sin(l/l^\circ_{coh})}{l/l^\circ_{coh}}$$

$$E_i(l) = -i\left(\frac{1-\gamma}{1+\gamma}\frac{n_s}{n_i}\right)^{\frac{1}{2}} E_s(o)\sinh g'l \,\frac{\sin(l/l^\circ_{coh})}{l/l^\circ_{coh}}$$

The expressions for power are

$$\begin{aligned}P_s(l) &= P_s(o)\cosh^2 g'l \,\frac{\sin^2(l/l^\circ_{coh})}{(l/l^\circ_{coh})^2} \\ P_i(l) &= \left(\frac{1-\gamma}{1+\gamma}\frac{n_s}{n_i}\right)P_s(o)\sinh^2 g'l \,\frac{\sin^2(l/l^\circ_{coh})}{(l/l^\circ_{coh})^2}\end{aligned} \qquad (19.12)$$

According to this equation the power gain is reduced by the factor $\sin^2(l/l^\circ_{coh})/(l/l^\circ_{coh})^2$. Beams from solid state lasers exhibit substantial divergence and hence account for low parametric gain.

19.3 Low Gain Parametric Amplifier : Plane Waves

For small gain in single-pass parametric amplifier Eq (19.10) for plane waves may be approximated by

$$P_s(l)-P_s(o) = P_s(o)(l/l_s)^2$$
$$P_i(l) = \frac{1-\gamma}{1+\gamma}\frac{n_s}{n_i}P_s(o)(l/l_s)^2 \qquad (19.13)$$

As an illustration, let us take the experiment by Wang and Rachetti (14). They used second harmonic (λ_p=3470 Å) of a ruby laser, P_p=2 MW, and an input signal λ_s=6328 Å $P_s(o)$=8.2 mW. With an ADP crystal l=8 cm they obtained $P_i(l)$ = 1.2 mW. From Fig. 19.1, we observe for I_p=2 MW cm^{-2} and λ_o=6940 Å that g/F = 0.095 Np cm^{-1}, and F = 0.713, for ADP at γ=0.096 . (λ_i = 7660 Å). Consequently gl = 0.542. Hence from (19.8) we calculate a signal power gain of 1.2 db and an idler power of 2.6 mW. The agreement between the theoretical predication and experimental result is good, considering especially the inaccuracy involved in the value of χ used.

In the above treatment we have assumed plane waves, the field amplitude is uniform along the beam the widths of the three beams as the same.

20 Low Gain Parametric Amplifier : Gaussian beam

The radial variation in the transverse electric field of a Gaussian beam in the near field of the TEM_{oo} mode is represented by

$$E_i(\rho,r) = E_{io}(r)e^{-\rho^2/w_i^2} \qquad (20.1)$$

where E_{io} is the amplitude at and ρ is the radial distance from the centre of the beam. Consequently, the gain along the transverse direction will be also of the form

$$g = g_o e^{-\rho^2/W_p^2} \qquad (20.2)$$

From Eq (19.13)

$$E_{io}^2(l)\int e^{-2\rho^2/W_i^2} 2\pi\rho d\rho = \left(\frac{n_s}{n_i}\frac{1-\gamma}{1+\gamma}\right) g_o^2 l^2 E_{so}^2(o)\int e^{-2\rho^2\left(\frac{1}{W_s^2}+\frac{1}{W_p^2}\right)} \times 2\pi\rho d\rho$$

or, $$E_{io}^2(l)W_i^2 = \left(\frac{n_s}{n_i}\frac{1-\gamma}{1+\gamma}\right) g_o^2 l^2 E_{so}^2(o)\frac{W_s^2 W_p^2}{W_s^2+W_p^2}$$

Writing $g_o^2 = K(1-\gamma^2)P_p/2W_p^2$ (see Eq II.11), and substituting for P from equation

$$P = \tfrac{1}{2}\epsilon_o c n \pi W^2 E^2,$$

one obtains

$$\frac{P_i(l)}{n_i} = \left(\frac{n_s}{n_i}\frac{1-\gamma}{1+\gamma}\right) K(1-\gamma^2)\frac{P_p}{2}\frac{P_s(o)}{n_s}\frac{l^2}{(W_s^2+W_p^2)}$$

The constant

$$K = \frac{32\pi}{\epsilon_o c}\frac{\chi^2}{\lambda_o^2 n_p n_s n_i} \qquad (18.13)$$

After simplification,

$$P_i(l) = K(1-\gamma)^2 P_p P_s(o)\frac{l^2}{2(W_s^2+W_p^2)}$$

$$P_s(l)-P_s(o) = K(1+\gamma)^2 P_p P_s(o)\frac{l^2}{2(W_s^2+W_p^2)} \qquad (20.3)$$

The K values are computed at different frequencies for the three types of crystals and given in Table 20.1. The power ratio

TABLE 20.1 Computed values of K(MKS/watt) Eq (18.13) for different materials and at different frequencies

λ_o(u)	γ	K x 10^9 KDP	K x 10^9 ADP	K x 10^7 $LiNbO_3$
.6328	0	6.8416	6.0089	
	.1	6.7896	5.9674	
	.2	6.6372	5.8369	
	.3	6.3864	5.6268	
	.4	5.9518	5.3409	
.6943	0	5.005	4.3774	
	.1	4.9776	4.3489	
	.2	4.8834	4.276	
	.3	4.7304	4.1433	
	.4	4.5294	3.977	
.8664	0	2.4828	2.1454	
	.1	2.4756	2.1409	
	.2	2.457	2.1268	
	.3	2.4324	2.1098	
	.4	2.4132	2.0981	
1.03	0			5.567
	.1			5.464
	.2			5.321
	.3			5.089
	.4			4.709
1.06	0	1.5876	1.3576	5.208
	.1	1.5918	1.3621	5.112
	.2	1.6051	1.3746	4.975
	.3	1.6326	1.4025	4.709
	.4	1.6884	1.4555	4.398
1.15	0	1.3872	1.194	3.775
	.1	1.3939	1.1998	3.738
	.2	1.4157	1.2198	3.685
	.3	1.4579	1.2591	3.514
	.4	1.5329	1.3299	3.297

KDP, $d_{14} = 0.6 \times 10^{12}$ M/volt

ADP, $d_{14} = 0.56 \times 10^{12}$ M/volt

$LiNbO_3 2d_{15} = 13.2 \times 10^{12}$ M/volt

$P_i(l)/P_s(o)$ for $LiNbO_3$ amplifier are given in Table 20.2 .

As an example, let us take the case of CW parametric amplification in a $LiNbO_3$ crystal l = 1 cm, excited from a argon-ion gas laser P_p = 10 mW. The input signal is $P_s(o)$ = 1 mW, λ_o = 1.03 u, γ = 0.1. The beam radii for b_o = 10 cm are $w_s^2 = 6.65 \times 10^{-5}$ cm^2, $w_p^2 = 3.66 \times 10^{-5}$ cm^2. From Table 18.4, $K = 5.56 \times 10^{7}$ M/watts. Thus the idler power for γ = 0.1 is according to Eq(20.3), $P_i = 2.15 \times 10^{-8}$ watts (see Table 20.2).

The above description pertains to travelling wave parametric amplification. If a resonant cavity containing nonlinear material is employed, parametric oscillation may occur when the minimum gain exceeds the reflection and propagation losses. A cavity resonator will also cause a much lower threshold for gain.

1 Gain of Parametric Oscillator with Resonant Confocal Cavity

A parametric oscillator with a confocal resonant cavity will have better gain. Inside the cavity the signal and idler electric fields are in the lowest modes with beam radii w_s and w_i. These will mix with the pump field in a mode of radius w_p to cause increments in the signal and idler fields through the nonlinear coupling coefficient. With this mode coupling taken into account, the spatial rate of growth of the signal and idler frequencies become (see Eq II.12)

$$\frac{dE_s(\rho)}{dr} = g_o \frac{w_i^2}{w_s^2+w_i^2}\left(\frac{1+\gamma}{1-\gamma}\frac{n_i}{n_s}\right)^{\frac{1}{2}} E_{io}\, e^{-\rho^2/w_s^2}$$

$$\frac{dE_i(\rho)}{dr} = g_o \frac{w_s^2}{w_s^2+w_i^2}\left(\frac{1-\gamma}{1+\gamma}\frac{n_s}{n_i}\right)^{\frac{1}{2}} E_{so}\, e^{-\rho^2/w_i^2} \qquad (21.1)$$

TABLE 20.2 Single-pass parametric gain of $LiNbO_3$ amplifier, Eq (20.3), for confocal parameters b_o = 1 cm, crystal length l = 1 cm; pump power P_p = 10 mW.

$\lambda_o(u)$	γ	$P_1(l)/P_s(o)$
1.03	0	2.530×10^4
	.1	2.146
	.2	1.749
	.3	1.349
	.4	0.962
1.06	0	2.299×10^4
	.1	1.948
	.2	1.573
	.3	1.206
	.4	0.872
1.15	0	1.527×10^4
	.1	1.308
	.2	1.0777
	.3	0.828
	.4	0.599
1.39	0	6.559×10^3
	.1	5.607
	.2	4.640
	.3	3.678
	.4	2.739
2.3	0	1.16×10^5
	.1	1.014
	.2	0.862
	.3	0.712
	.4	0.582

We assume that the field is independent of r. For small gain the incremental power gain in the idler mode can be written as

$$\frac{dP_i}{dr} = \tfrac{1}{2}\epsilon_o c n_i \int_o^\infty 2E_i(\rho)\frac{dE_i}{dr}2\pi\rho\,d\rho$$

$$= 2\pi\epsilon_o c n_i g_o \frac{W_s^2}{W_s^2+W_i^2}\left(\frac{1-\gamma}{1+\gamma}\frac{n_s}{n_i}\right)^{\frac{1}{2}} E_{io}E_{so}\int_o^\infty e^{-2\rho^2/W_i^2}\rho\,d\rho$$

Now $$g_o^2 = K(1-\gamma^2)\frac{P_p}{2W_p^2}$$

and $$\int_o^\infty e^{-2\rho^2/W_i^2}\rho\,d\rho = \frac{W_i^2}{4}$$

$$\therefore \quad \frac{dP_i}{dr} = 2\pi\epsilon_o c\left[K(1-\gamma^2)\frac{P_p}{2W_p^2}\right]^{\frac{1}{2}} \frac{W_s^2}{W_s^2+W_i^2}\left(\frac{1-\gamma}{1+\gamma}n_s n_i\right)^{\frac{1}{2}} \times$$

$$\frac{2}{W_s}\left(\frac{P_s}{\pi\epsilon_o c n_s}\right)^{\frac{1}{2}}\frac{2}{W_i}\left(\frac{P_i}{\pi\epsilon_o c n_i}\right)^{\frac{1}{2}}\frac{W_i^2}{4}$$

$$= (KP_pP_sP_i)^{\frac{1}{2}}(1-\gamma)\frac{\sqrt{2}W_iW_s}{W_p(W_s^2+W_i^2)}$$

or, $$\frac{dP_i}{dr} = (KP_sP_iP_p)^{\frac{1}{2}}(1-\gamma)\left(\frac{2}{W_s^2+W_i^2}\right)^{\frac{1}{2}}$$

$$\frac{dP_s}{dr} = (KP_sP_iP_p)^{\frac{1}{2}}(1+\gamma)\left(\frac{2}{W_s^2+W_i^2}\right)^{\frac{1}{2}} \qquad (21.2)$$

Integration of which will yield, with $P_s = P_i$, and when P_s, P_i within the braces are regarded as constant,

$$\frac{\Delta P_i}{P_s} = (KP_p)^{\frac{1}{2}}(1-\gamma)\left(\frac{2}{W_s^2+W_i^2}\right)^{\frac{1}{2}}l \qquad (21.3)$$

Power gain P_i/P_s calculated from this equation for $LiNbO_3$ parametric oscillator are shown in Table 21.1. Comparison of the figures in this Table with the corresponding values in Table 20.2

TABLE 21.1 Power Gain $\Delta P_i/P_s$ of $LiNbO_3$ Parametric Oscillator Eq (21.3) with different confocal parameter b_o. Crystal length l = 1 cm ; Pump power 10 mW.

$\lambda_o(u)$	γ	$(\Delta P_i/P_s) \times 10^2$		
		b_o = 1 cm	b_o = 5 cm	b_o = 10 cm
1.03	0	2.755	1.232	.871
	.1	2.444	1.093	.773
	.2	2.110	.944	.667
	.3	1.757	.785	.555
	.4	1.390	.622	.440
1.06	0	2.626	1.174	.830
	.1	2.330	1.042	.737
	.2	2.011	.899	.636
	.3	1.665	.745	.526
	.4	1.324	.592	.419
1.15	0	2.142	.958	.677
	.1	1.908	.853	.603
	.2	1.658	.741	.524
	.3	1.378	.616	.436
	.4	1.098	.491	.347
1.39	0	1.402	.627	.443
	.1	1.251	.559	.395
	.2	1.087	.486	.344
	.3	.919	.411	.290
	.4	.742	.332	.235
2.3	0	.590	.264	.187
	.1	.531	.237	.168
	.2	.468	.209	.148
	.3	.403	.180	.127
	.4	.341	.152	.108

and also comparison of (21.3) with (20.3) will reveal that the amplifier gain is approximately square of that of oscillator. Hence for small gains ($o < \underline{gl} < 1$), an oscillator (with cavity resonator) offer higher gain for the same pump power. In other words, threshold of pump power is attained at a lower level in oscillators.

CHAPTER VI

SUMMARY OF RESULTS AND CONCLUSIONS

1. The calculated values of phase matching angles are in excellent agreement with the experimental results. The factors that contribute to the prediction accuracy are
   (a) the use of exact equation (12.2)
   (b) and putting the calculation on the digital computer

2. The $\lambda_p - \theta_o$ curves are concave in shape, suggesting the merits of pump sources with shorter wavelengths. The curve for $LiNbO_3$ is more spread out; consequently mechanical tuning by rotation of the crystal is more convenient with this type of crystal.

   The phase match angle is about 90^o at the degenerate wavelength λ_o = 1.03 u. Propagation at right angles to the optic axis minimizes the disadvantages of double refraction and beam divergence.

3. The design tuning curves for shorter pump wavelengths are straight lines; that is $(\Delta\nu)^2$ bear linear relationship with $\sin^2\phi$. A pump wavelength λ_p = 3472 Å may initiate parametric gain in KDP or ADP in the wavelength range of 0.45 to 1.5 u. In $LiNbO_3$ with λ_p = 5300 Å mechanical tuning may cover the range 0.65 to 2.5 u.

4. The Q-values of optical resonators (d = 1 cm, R = 0.95) is about 10^6 at 1 u. As Q is inversely proportional to the mirror losses, reduction of the losses from 5 to 1 percent raises the Q-values 5 times. The corresponding threshold

values of m are about 2×10^6 and 4×10^7. The m values show slight rise with increase in γ. Consequently the threshold level of pump increases as one tunes away from the degenerate position.

5 Pump power required in exciting parametric oscillation in resonators with plane parallel mirrors is enormous. Pulsed solid state or glass lasers, having a few hundred KW of power are capable of such action. Use of focused beams reduces the power considerably. The pump power for a confocal resonator $b_o = d = 1$ cm, and containing $LiNbO_3$ is only 5.8 mW at $\lambda_o = 1.03$ u. Although the saving in pump power is enormous, the resulting power gain $P_i(\underline{l})/P_s(o)$ is also proportionately depleted. This is because the power gain is proportional to P_p. The single-pass parametric gain in $LiNbO_3$ amplifier at 1.06 u are

	Resonator	P_p	$P_i(\underline{l})/P_s(o)$
1.	Plane parallel $d = 1$ cm $\quad \underline{l} = 1$ cm	30 KW	252
2.	Confocal $b_o = d = 1$ cm, $\underline{l} = 1$ cm	10 mW	2.3×10^4

6 The simplified theory and its extension to the travelling wave mode form the basis of calculation of power by the digital computer.

7. The subject of parametric amplification and generation of optical frequencies is replete with potentiality and more research need be done on :

a) covering wider bandwidth with fewer resonators.

b) combining the three methods of optical tuning, viz. the mechanical tuning, temperature tuning, electro-optic tuning, and

c) improving the power conversion efficiency.

APPENDIX I

Piezoelectric Tensor Coefficients and Polarization of KDP, ADP and $LiNbO_3$ crystals

KDP and ADP : (Class $\bar{4}2m$)

$$\chi_{ij} = d_{ij} = \begin{matrix} 0 & 0 & 0 & d_{14} & 0 & 0 \\ 0 & 0 & 0 & 0 & d_{14} & 0 \\ 0 & 0 & 0 & 0 & 0 & d_{36} \end{matrix}$$

$$P_x = 2\epsilon_o d_{14} E_y E_z$$

$$P_y = 2\epsilon_o d_{14} E_z E_x$$

$$P_z = 2\epsilon_o d_{36} E_x E_y$$

$LiNbO_3$: (Class 3 m)

$$\chi_{ij} = d_{ij} = \begin{matrix} 0 & 0 & 0 & 0 & 2d_{15} & -2d_{22} \\ -d_{22} & d_{22} & 0 & 2d_{15} & 0 & 0 \\ d_{31} & d_{31} & d_{33} & 0 & 0 & 0 \end{matrix}$$

$$P_x = 2\epsilon_o \left[2d_{15} E_z E_x - 2d_{22} E_x E_y \right]$$

$$P_y = 2\epsilon_o \left[-d_{22} E_x^2 + d_{22} E_y^2 + 2d_{15} E_y E_z \right]$$

$$P_z = 2\epsilon_o \left[d_{31} E_x^2 + d_{31} E_y^2 + d_{33} E_z^2 \right]$$

Appendix II

Theory of Parametric Amplification and Oscillation in a Cavity Resonator containing Nonlinear Material.

Let us consider a cavity resonator containing a thin slab of uniaxial crystal of length l. We consider the fundamental TEM_{oo} modes. The cavity is resonant simultaneously at the mode frequencies ν_s and ν_i, but is transparent to the pump mode ν_p. The stationary field inside the cavity may be expressed by

$$\begin{aligned} \bar{E}_p &= \bar{a}_p E_{po} \bar{e}^{\rho^2/W_p^2} \\ \bar{E}_s &= \bar{a}_s u_s(t) \bar{e}^{\rho^2/W_s^2} \\ \bar{E}_i &= \bar{a}_i u_i(t) \bar{e}^{\rho^2/W_i^2} \end{aligned} \qquad \text{(II.1)}$$

where the subscript o denotes field amplitude at the axis of the Gaussian beam, and $\bar{a}$ are unit vectors. In the above we have omitted the terms like $\exp(-ik_p r)$ because of the assumption of perfect phase matching. Owing to nonlinear coupling the field amplitude varies slowly at a rate described by $u_s(t)$ and $u_i(t)$.

Extending Eq (9.6) for lumped circuit to the present problem, the coupled mode amplitude equations may be written as

$$\begin{aligned} \frac{du_s}{dt} &= \alpha_{si} u_i^* - \alpha_{ss} u_s \\ \frac{du_i^*}{dt} &= \alpha_{is}^* u_s - \alpha_{ii} u_i^* \end{aligned} \qquad \text{(II.2)}$$

If we envision that perturbation of the cavity field is caused by modulation of the dielectric constant i.e. by m which is varied harmonically in time (Eq. 17.8),

we find

$$\alpha_{si} = -iw_s \frac{\int_{V_m} \frac{m_s}{2} E_s^* E_i^* \, dV}{\int_{V_c} E_s E_s^* \, dV} = -i \frac{w_s}{\epsilon_s} \frac{\int_{V_m} E_p \cdot \chi : E_s^* E_i^* \, dV}{\int_{V_c} E_s E_s^* \, dV} \qquad \text{(II.3)}$$

Here the integration in the numerator is over the volume V_m of the material, while in the denominator it is over the cavity volume V_c. Writing $dV = r \cdot 2\pi\rho d\rho$, and considering only the situation of small gain i.e., E_s and E_i approximately independent of r, one obtains from (II.1) and (II.3)

$$\alpha_{si} = -i \frac{w_s}{\epsilon_s} \frac{\chi E_{po} l}{d} \frac{\int_0^\infty \exp\left[-\rho^2\left(\frac{1}{W_p^2}+\frac{1}{W_s^2}+\frac{1}{W_i^2}\right)\right] 2\pi\rho d\rho}{\int_0^\infty \exp\left(-2\rho^2/W_s^2\right) 2\pi\rho d\rho}$$

d is the spacing between the cavity mirrors, and l is the length of the crystal. Performing the integration and assuming the optimum value for W_p (18.8), one finds

$$\alpha_{si} = -i \frac{w_s}{\epsilon_s} \frac{\chi E_{po} l}{d} \frac{W_i^2}{W_s^2 + W_i^2} \qquad \text{(II.4)}$$

We also note that the cavity loss coefficient

$$\alpha_{ss} = \frac{w_s}{Q_s} \quad , \quad \alpha_{ii} = \frac{w_i}{Q_i} \qquad \text{(II.5)}$$

and $$Q_s = \frac{k_s d}{2L} \quad , \quad Q_i = \frac{k_i d}{2L}$$

The condition for oscillation is from (II.2)

$$\alpha_{si} \alpha_{is}^* \geq \alpha_{ss} \alpha_{ii} \qquad \text{(II.6)}$$

Therefore

$$\frac{\chi E_{po} l}{(\epsilon_s \epsilon_i)^{\frac{1}{2}} d} \frac{W_s W_i}{W_s^2 + W_i^2} \geq \frac{1}{(Q_s Q_i)^{\frac{1}{2}}} \qquad \text{(II.7)}$$

At the degenerate frequency of the cavity modes with Gaussian distribution, $\bar{w}_s = \bar{w}_i$. Hence

$$\frac{\chi E_{po} l}{n_o^2 d} \geq \frac{2}{Q_o} \qquad \text{(II.8)}$$

This expression is valid for plane waves as well.

Travelling-Wave Mode

As pointed out by Louisell et al. the parametric equations in the time domain have the same form as the corresponding spatial equations. Hence, the spatial equivalents of (II.2) are (36)

$$\frac{du_s}{dr} = \alpha_{si} u_i^* - \alpha_{ss} u_s$$

$$\frac{du_i^*}{dr} = \alpha_{is}^* u_s - \alpha_{ii} u_i^* \qquad \text{(II.9)}$$

where the coefficients α are 1/c times the coefficients in Equation (II.3) in the time domain and the integration is over the sectional area of the beams. Hence for the propagating mode the gain coefficient is

$$g'' = (\alpha_{si} \alpha_{is}^*)^{\frac{1}{2}}$$

or

$$g'' = \left(\frac{k_s k_i}{\epsilon_s \epsilon_i}\right)^{\frac{1}{2}} \chi E_{po} \frac{W_s W_i}{W_s^2 + W_i^2} \qquad \text{(II.10)}$$

or

$$g'' = g_o \frac{W_s W_i}{W_s^2 + W_i^2}$$

where

$$g_o = \left(\frac{k_s k_i}{\epsilon_s \epsilon_i}\right)^{\frac{1}{2}} \chi E_{po} \qquad \text{(II.11)}$$

From (II.9) the travelling-wave parametric equations for a single pass through the nonlinear material inside the resonant cavity may be written as

$$\frac{du_i^*(r)}{dr} = -ig_o \frac{w_s^2}{w_s^2+w_i^2}\left(\frac{1-\gamma}{1+\gamma}\frac{n_s}{n_i}\right)^{\frac{1}{2}} u_s \qquad \text{(II.12)}$$

Power in a mode is given by

$$P_i = \tfrac{1}{2}\epsilon_o c n_i \frac{\pi w_i^2}{2}|u_i|^2$$

or

$$\frac{dP_i}{dr} = \tfrac{1}{2}\epsilon_o c n_i \pi w_i^2 \, u_i \frac{du_i}{dr}$$

Substituting for du_i/dr from (II.12)

$$\frac{dP_i}{dr} = \frac{\pi\epsilon_o c}{2} w_i^2 \left[K(1-\gamma^2)\frac{P_p}{2w_p^2}\right]^{\frac{1}{2}} \frac{w_s^2}{w_s^2+w_i^2}\left(\frac{1-\gamma}{1+\gamma}n_s n_i\right)^{\frac{1}{2}} u_i u_s$$

or

$$\frac{dP_i}{dr} = (KP_pP_sP_i)^{\frac{1}{2}}(1-\gamma)\frac{\sqrt{2}\, w_s w_i}{w_p(w_s^2+w_i^2)} \qquad \text{(II.13)}$$

This gives the spatial rate of growth of the idler mode as it propagates during one travel through the nonlinear material inside the resonant cavity. A similar equation exists for the signal mode. Since the gain coefficient is assumed small Eq (II.13) may be integrated by regarding P_s and P_i on the right side as substantially constant.

APPENDIX III

Threshold Pump Intensity in Parametric Oscillation : Plane Waves.

The minimum growth rate when equated to the losses by reflection on the surfaces of the two mirrors of a Febry-Perot Cavity resonator containing the nonlinear material is given by

$$g \geq \frac{2(1-R)}{l} \qquad (17.4)$$

From Art 11,

$$g = \frac{1}{2}\left[\frac{m_s m_i k_s k_i}{\cos(k_s k_p)\cos(k_i k_p)}\right]^{\frac{1}{2}} \qquad (11.6)$$

$$= \frac{1}{2}\left[\left(\frac{2\chi E_p}{\epsilon_{1,2}}\right)^2 \cdot \frac{w_s w_i n_s n_i}{c^2}\right]^{\frac{1}{2}}$$

or,
$$g = \frac{\chi E_p}{c}\left(\frac{w_s w_i}{n_s n_i}\right)^{\frac{1}{2}} \qquad (III.1)$$

If we assume that the field amplitude is constant along the radial direction, we have for the pump intensity

$$I_p = 1.326 \times 10^3 \, n_p E_p^2 \quad \text{watts } m^{-2} \qquad (III.2)$$

$$\therefore \quad g = 172.5 \left(\frac{1}{n_p n_s n_i \lambda_s \lambda_i}\right)^{\frac{1}{2}} I_p^{\frac{1}{2}} \qquad (III.3)$$

Substituting from (17.4)

$$I_p = 1.344 \times 10^4 (n_s n_i n_p \lambda_s \lambda_i)\left(\frac{1-R}{\chi l}\right)^2 \qquad (III.4)$$

All the parameters are in MKS units. Thus, for a given material, the threshold pump power is inversely proportional to the square of the susceptibility coefficient and to Q of the resonator. Considerable advantage is thus derived by using $LiNbO_3$ crystal in high Q resonator.

Appendix IV

SUBHARMONIC GENERATION - SOLUTION OF MATHIEU EQUATION IN THE FIRST UNSTABLE REGION.

1	2	3	4	5	6	7
σ^2-1	ϵ	cos 2θ	θ	$-\mu$	a_3	b_3
.8	1.9	.9732	6.65	.1092	.0097	.1325
.8	2.0	.9494	9.15	.1570	.0147	.1398
.6	1.4	.9587	8.27	.0996	.0065	.0948
.6	1.5	.9218	11.4	.1454	.0102	.1018
.6	1.6	.8910	13.5	.1816	.0136	.1089
.6	1.7	.8653	16.04	.2130	.0170	.1160
.6	1.8	.8438	16.24	.2415	.0204	.1232
.6	1.9	.8257	17.16	.2679	.0239	.1304
.6	2.0	.8105	17.92	.2928	.0274	.1377
.5	1.2	.9288	10.87	.1112	.0062	.0802
.5	1.3	.8864	13.85	.1510	.0092	.0871
.5	1.4	.8502	15.88	.1843	.0121	.0940
.5	1.5	.8213	17.39	.2139	.0150	.1010
.5	1.6	.7976	18.55	.2413	.0181	.1080
.5	1.7	.7781	19.45	.2669	.0213	.1150
.5	1.8	.7622	20.16	.2913	.0246	.1221
.5	1.9	.7491	20.74	.3147	.0280	.1293
.5	2.0	.7375	21.2	.3371	.0316	.1365
.4	1.0	.8887	13.64	.1146	.0054	.0660
.4	1.1	.8371	16.58	.1504	.0077	.0727
.4	1.2	.7964	18.6	.1814	.0102	.0795
.4	1.3	.7641	20.08	.2096	.0128	.0863
.4	1.4	.7384	21.2	.2360	.0155	.0931
.4	1.5	.7178	22.06	.2611	.0183	.1000
.4	1.6	.7014	22.73	.2851	.0214	.1070
.4	1.7	.6884	23.25	.3082	.0246	.1140
.4	1.8	.6782	23.65	.3307	.0279	.1211
.4	1.9	.6704	23.95	.3524	.0314	.1282
.4	2.0	.6644	24.18	.3737	.0350	.1354
.3	.8	.8309	16.9	.1113	.0042	.2521
.3	.9	.6788	19.87	.1439	.0061	.0587
.3	1.0	.7222	21.88	.1729	.0081	.0653
.3	1.2	.6596	24.38	.2255	.0127	.0767
.3	1.3	.6388	25.15	.2500	.0152	.0855
.3	1.4	.6230	25.73	.2738	.0180	.0923
.3	1.5	.6111	26.16	.2968	.0209	.0991
.3	1.6	.6023	26.49	.3193	.0239	.1060
.3	1.7	.5960	26.7	.3412	.2072	.1130
.3	1.8	.5918	26.86	.3627	.0306	.1200
.3	1.9	.5893	26.95	.3837	.0342	.1271
.3	2.0	.5883	26.98	.4043	.0379	.1842
.2	.5	.8487	15.96	.0661	.0015	.0321
.2	.6	.7382	21.2	.1012	.0028	.0385
.2	.7	.6640	24.2	.1308	.0043	.0450
.2	.8	.6124	26.12	.1581	.0059	.0515
.2	1.0	.5496	28.33	.2088	.0098	.0646

1	2	3	4	5	6	7
.2	1.2	.5180	29.4	.2566	.0144	.0779
.2	1.4	.5037	29.87	.3024	.0198	.0913
.2	1.5	.5007	29.97	.3246	.0228	.0981
.2	1.6	.4999	30.0	.3464	.0260	.1050
.2	1.8	.5027	29.9	.3890	.0328	.1189
.2	2.0	.5098	29.67	.4301	.0403	.1330
.1	.3	.7043	22.6	.0532	.0007	.0190
.1	.4	.5593	28.0	.0829	.0015	.0253
.1	.5	.4793	30.68	.1097	.0026	.0317
.1	.6	.4318	32.2	.1353	.0038	.0381
.1	.8	.3851	33.67	.1846	.0069	.0510
.1	1.0	.3703	34.13	.2322	.0109	.0639
.1	1.2	.3709	34.12	.2786	.0157	.0771
.1	1.4	.3799	33.87	.3237	.0212	.0904
.1	1.6	.3938	33.4	.3677	.0276	.1039
.1	1.8	.4105	32.88	.4103	.0346	.1177
.1	2.0	.4288	32.3	.4517	.0423	.1317
0.0	.1	.0187	44.47	.0250	.0001	.0062
0.0	.2	.0374	43.92	.0500	.0005	.0125
0.0	.3	.0561	43.39	.0749	.0010	.0188
0.0	.4	.0747	42.85	.0997	.0019	.0250
0.0	.5	.0931	42.32	.1244	.0029	.0313
0.0	.6	.1115	41.8	.1491	.0042	.0376
0.0	.8	.1477	40.75	.1978	.0074	.0504
0.0	1.0	.1832	39.72	.2458	.0115	.0632
0.0	1.2	.2178	38.71	.2928	.0165	.0762
0.0	1.4	.2513	37.72	.3388	.0222	.0894
0.0	1.6	.2837	36.71	.3836	.0288	.1028
0.0	1.8	.3150	35.81	.4271	.0360	.1165
0.0	2.0	.3450	34.89	.4693	.0440	.1304
-.8	1.9	-.5607	62.05	.3933	.0350	.1108
-.8	2.0	-.4837	59.47	.4376	.0480	.1174
-.6	1.4	-.6744	66.2	.2584	.0170	.0823
-.6	1.5	-.5825	62.82	.3048	.0214	.0886
-.6	1.6	-.5002	60.01	.3464	.0260	.0950
-.6	1.7	-.4258	57.6	.3845	.0306	.1014
-.6	1.8	-.3582	55.49	.4201	.0354	.1080
-.6	1.9	-.2964	53.62	.4536	.0404	.1146
-.6	2.0	-.2395	51.93	.4854	.0455	.1212
-.5	1.2	-.6772	66.32	.2207	.0124	.0712
-.5	1.3	-.5803	62.73	.2647	.0161	.0774
-.5	1.4	-.4948	59.82	.3041	.0200	.0837
-.5	1.5	-.4184	57.37	.3406	.0239	.0901
-.5	1.6	-.3496	55.23	.3747	.0281	.0965
-.5	1.7	-.2872	53.34	.4071	.0324	.1030
-.5	1.8	-.2301	51.65	.4379	.0369	.1096
-.5	1.9	-.1778	50.12	.4674	.0416	.1162
-.5	2.0	-.1294	48.72	.4958	.0465	.1230
-.4	1.0	-.6684	65.97	.1859	.0087	.0599
-.4	1.1	-.5650	62.2	.2269	.0117	.0661
-.4	1.2	-.4757	59.2	.2639	.0148	.0723

.

1	2	3	4	5	6	7
-.4	1.3	-3974	56.71	.2982	.0182	.0786
-.4	1.4	-.3279	54.57	.3306	.0217	.0850
-.4	1.5	-.2654	52.69	.2615	.0254	.0914
-.4	1.6	-.2089	51.03	.3912	.0293	.0979
-.4	1.8	-.1098	48.15	.4473	.0377	.1111
-.4	2.0	-.0254	45.72	.4998	.0469	.1246
-.3	.8	-.6412	64.94	.1535	.0057	.0484
-.3	.9	-.5295	60.99	.1909	.0080	.0546
-.3	1.0	-.5464	57.94	.2249	.0105	.0608
-.3	1.2	-.2875	53.35	.2873	.0162	.0734
-.3	1.3	-.2262	45.03	.3166	.0193	.0797
-.3	1.4	-.1713	49.93	.3448	.0226	.0862
-.3	1.5	-.1217	48.5	.3722	.0262	.0927
-.3	1.6	-.0763	47.19	.3988	.0299	.0992
-.3	1.7	-.0346	47.99	.4247	.0338	.1058
-.3	1.8	.0040	44.88	.4500	.0380	.1125
-.3	2.0	.0734	42.89	.4986	.0467	.1261
-.2	.5	-.7406	68.89	.0840	.0020	.0305
-.2	.6	-.5794	62.69	.1222	.0034	.0367
-.2	.7	-.4586	58.65	.1555	.0051	.0429
-.2	.8	-.3633	55.65	.1863	.0070	.0491
-.2	1.0	-.2186	51.31	.2439	.0114	.0616
-.2	1.2	-.1103	48.17	.2982	.0168	.0744
-.2	1.4	-.0234	45.67	.3499	.0230	.0873
-.2	1.6	.0493	43.58	.3995	.0300	.1005
-.2	1.8	.1123	41.77	.4471	.0377	.1139
-.2	2.0	.1678	40.17	.4929	.0462	.1276
-.1	.3	-.6251	64.35	.0585	.0008	.0185
-.1	.4	-.4345	57.87	.0901	.0017	.0247
-.1	.5	-.3124	54.1	.1187	.0028	.0309
-.1	.6	-.2247	51.49	.1462	.0041	.0372
-.1	.8	-.1011	47.9	.1990	.0075	.0497
-.1	1.0	-.0126	45.36	.2500	.0117	.0624
-.1	1.2	.0577	43.35	.2995	.9168	.0753
-.1	1.4	.1171	41.63	.3476	.0228	.0884
-.1	1.6	.1691	40.13	.3942	.0296	.1017
-.1	1.8	.2157	38.77	.4394	.0371	.1152
-.1	2.0	.2581	37.52	.4830	.0453	.1290

BIBILIOGRAPHY

1. N.Bloembergen, "Optique Nonlineare" p.1501; Proc.Third International Congress on Quantum Electronics,Paris,1963.

2. A.K.Kamal and M.Subramanian, "Laser Power and Energy Measurement using Nonlinear Polarization in Crystals" Proc. Symposium on Optical Masers, April 1963,Polytechnic Institute of Brooklyn.

3. P.Franken, A.E.Hill, C.W.Peters and G.Weinreich, "Generation of Optical Harmonics" Phys. Rev. Letters,vol 7,pp118-119,1961

4. R.W.Terhune, P.D.Marker and C.M.Savage, "Applied Physics Letters, vol 2, p.54, 1963.

5. R.W.Minck, R.W.Terhune and C.C.Wang "Nonlinear Optics, Proc.I.E.E.E., vol.54,10, pp 1357-1374, Oct.1966

6. M.Bass, "Optical Rectification", Doctoral Thesis, University of Michigan, 1964.

7. P.D.Marker, R.W.Terhune and C.M.Savage, "Optical Third Harmonic Generation", Proc.International Congress on Quantum Electronics, p.1559, Paris, 1963.

8. N.Bloembergen, "Nonlinear Optics", p.8, W.A.Benjamin Inc., New York, 1965.

9. R.W.Terhune, P.D.Marker and C.W.Savage, Phys.Rev.Letters, vol.8, p.404, 1962.

10. J.A.Armstrong, N.Bloembergen, J.Ducuing and P.S.Pershan "Interaction between Light Waves in a Nonlinear Dielectric" Phys.Rev. vol.127, p.1918-1939, 1962.

11 P.A.Franken and J.F.Ward, "Optical Harmonics and Nonlinear Phenomen", Rev.Mod.Phys.,vol.35,1,p.23, January 1963.

12 P.D.Marker, R.W.Terhune, M.Nissenoff and C.W.Savage, "Effects of dispersion and focusing on the production of Optical Harmonics", Phys.Rev.Letters,vol.8,p.21,Jan.1962.

13 D.A.Kleinman, "Theory of Second Harmonic Generation of Light" Phys.Rev., vol.128,4, p.1761, 1962.

14. C.C.Wang and G.W.Rachette, "Second Harmonic Generation and Parametric Amplification using Intense Unfocused Laser Beams", Physics of Quantum Electronics, Conference Proceedings, Puerto Rico, June 1965. Edited P.L.Kelley, B.Lax and P.E.Tunnenwald.

15. S.A.Akhmanov, V.G.Dmitriev, R.V.Khokhlov and A.I.Kovrygin, "Nonlinear Effects at Multiples of Laser Frequencies,Ibid.

16. S.A.Akhmanov, A.I.Kovrygin, V.A.Kolosov, A.S.Piskarskas, V.V.Fadeev, and R.V.Khokhlov, "Tunable Parametric Light Generator with KDP crystal", JETP Letters, vol.3, pp 241-245, May 1966.

17. J.A.Giordmaine and R.C.Miller, "Tunable Coherent Parametric Oscillations in $LiNbO_3$ at optical frequencies", Phys.Rev. Letters, vol.14,24, pp 973-976, June 1965.

18. S.A.Akhmanov, A.I.Kovrigin, A.S.Piskarskas, V.V.Fadeev, and R.V.Khakhlov, "Observation of Parametric amplification in the optical range", JETP Letters, vol.2, pp 191-193, Oct.1965.

19. L.B.Kreuzer, "Ruby-Laser-Pumped Optical Parametric Oscillator with Electro-Optic Tuning", App.Phys.Letters, vol.10,12,p.336, June 1967.

20 E.J.Woodbury, "Raman Laser Action in Organic Liquids" Third Int.Conf.on Quantum Electronics, Paris,1963.

21 R.C.Miller and W.A.Nordland, "Tunable $LiNbO_3$ Optical Oscillator with External Mirrors", App.Phys.Letters, vol.10, No.2,15 Jan.1967.

22. S.A.Akhmanov and R.V.Khokhlov, "Parametric Amplifiers and Generators of Light", Soviet Phys.USPEKHI,vol.9, No.2,pp 210-222, Sept.-Oct.,1966

23 W.H.Louisell, A.Yariv and A.E.Siegman, "Quantum Fluctuations and Noise in Parametric Processes I",Phys.Rev. 124,pp 1646-1654, Dec.1961.

24. W.H.Louisell, Coupled Mode Theory and Parametric Electronics, John Wiley and Sons Inc., New York, N.Y. 1960.

25. Chihiro Hayashi, Nonlinear Oscillations in Physical Systems, McGraw Hill (New York) 1964.

26. G.D.Boyd, R.C.Miller, K.Nassau, M.L.Bond and A.Savage, "$LiNbO_3$: an Efficient Phase Matchable Nonlinear Optical Material", App.Phys.Letters, vol.5,11, December 1964.

27 G.D.Boyd, W.L.Bond and H.L.Carter, "Refractive Index as a Function of Temperature in $LiNbO_3$", Jour.App.Phys., vol.38, pp 1941 (March) 1967.

28 F.Zernike, "Calculation of Refractive Index of Uniaxial Crystals", Jour.Opt.Soc.Am., vol.54, pp 1215, 1964 and vol.55,pp 210 (Appendix) 1965.

29 S.A.Akhmanov and R.V.Khokhlov, "Concerning the Possibility of Amplification of Light Waves", JETP Letters, vol.16, p.252, 1963.

30 J.A.Giordmaine and R.C.Miller, "Optical Parametric Oscillation in $LiNbO_3$", Physics of Quantum Electronics (Puerto Rico Conf. Proc., June 1965)

31 A.G.Fox and T.Li, "Resonant Modes in a Maser Interferometer" Bell Sys.Tech.J., vol.40, pp 453-488, March 1961.

32 G.D.Boyd and J.P.Gordon, "Confocal Multimode Resonator for Millimeter through Optical Wavelength Masers", Bell Sys. Tech.J., vol.40, pp 489-508, March 1961.

33 H.Kogelnik and T.Li, "Laser beams and Resonators", Proc.IEEE, vol.54,10, pp 1312-1329, Oct.1966.

34 R.H.Kingston and A.L.McWhorter, "Electromagnetic Mode Mixing in Nonlinear Media", Proc.IEEE, vol.53,1,pp 4-12 Jan.1965.

35 G.D.Boyd and A.Ashkin, "Theory of Parametric Oscillator Threshold with Single Mode Optical Masers and Observation of Amplification in $LiNbO_3$", Phy.Rev.,vol.146,1,pp 187-198, June 1966.

36 A.Yariv, "Parametric Interactions of Normal Modes", IEEE Jour.of Quantum Electronics,vol.QE-2,2, Feb. 1966.

LIST OF ILLUSTRATIONS

14.1 Matching angle for Parametric process in

a) KDP at λ_p = 3164 Å

b) ADP at λ_p = 3164 Å

14.2 Matching angle for Parametric process in

a) KDP at λ_p = 3472 Å

b) ADP at λ_p = 3472 Å

14.3 Matching angle for Parametric process in

a) KDP at λ_p = 4332 Å

b) ADP at λ_p = 4332 Å

14.4 Matching angle for Parametric process in

a) KDP at λ_p = 5300 Å

b) ADP at λ_p = 5300 Å

c) $LiNbO_3$ at λ_p = 5300 Å

14.5 Matching angle for Parametric process in

a) KDP at λ_p = 5761 Å

b) ADP at λ_p = 5761 Å

c) $LiNbO_3$ at λ_p = 5761 Å

14.6 Matching angle for Parametric process in

$LiNbO_3$ at λ_p = 6943 Å

14.7 Matching angle for Parametric process in

$LiNbO_3$ at λ_p = 11,523 Å

15.1 Tuning curve of

a) KDP for λ_p = 3164 Å

b) ADP for λ_p = 3164 Å

15.2 Tuning curve of

a) KDP for λ_p = 3472 Å

b) ADP for λ_p = 3472 Å

15.3 Tuning curve of

a) KDP for λ_p = 4332 Å

b) ADP for λ_p = 4332 Å

15.4 Tuning curve of

a) KDP for λ_p = 5300 Å
b) ADP for λ_p = 5300 Å
c) $LiNbO_3$ for λ_p = 5300 Å

15.5 Tuning curve of

a) KDP for λ_p = 5761 Å
b) ADP for λ_p = 5761 A
c) $LiNbO_3$ for λ_p = 5761 A

15.6 Tuning curve of

$LiNbO_3$ for λ_p = 6943 A

15.7 Tuning curve of

$LiNbO_3$ for λ_p = 11,523 A

15.8 Frequency Deviation with crystal rotation $\Delta\theta$ in

a) KDP
b) ADP
c) $LiNbO_3$

15.9 Wavelength deviation with crystal rotation $\Delta\theta$ in

a) KDP
b) ADP
c) $LiNbO_3$

16.1 Mismatch gradient ($dn^e/d\theta$) for $LiNbO_3$ at different pump frequencies.

17.1 Cavity resonator with plane parallel mirrors.

19.1 Gain constant g as a function of the pump intensity I_p

19.1(a) Multiplying factor F for different crystals as a function of the deviation ratio $\gamma = \Delta w/w_o$ for KDP, ADP and $LiNbO_3$

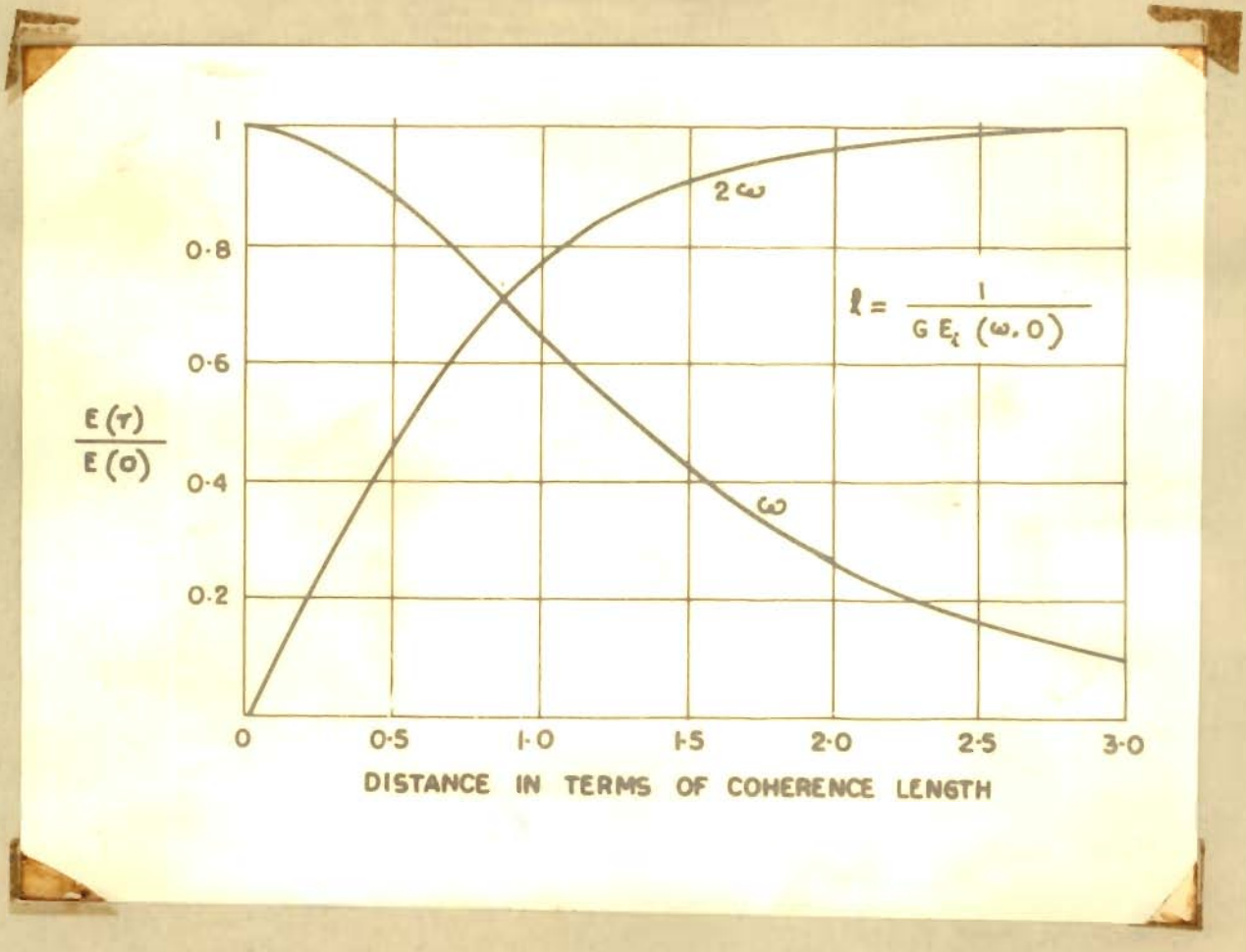
1
0·8
0·6
0·4
0·2
E(r)
E(0)
2ω
ω
ℓ = 1 / G E_t (ω, 0)
0
0·5
1·0
1·5
2·0
2·5
3·0
DISTANCE IN TERMS OF COHERENCE LENGTH

Fig. 6.1

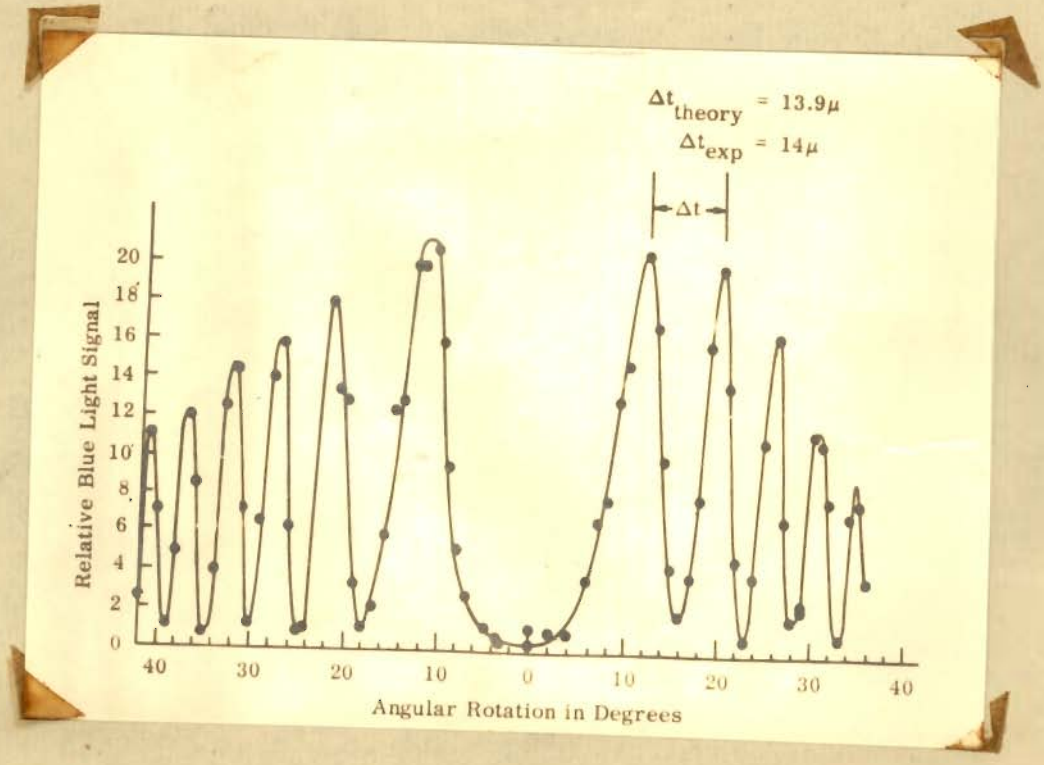
Δt_{theory} = 13.9μ
Δt_{exp} = 14μ
Δt
Relative Blue Light Signal
0
2
4
6
8
10
12
14
16
18
20
40
30
20
10
0
10
20
30
40
Angular Rotation in Degrees

Fig. 6.2

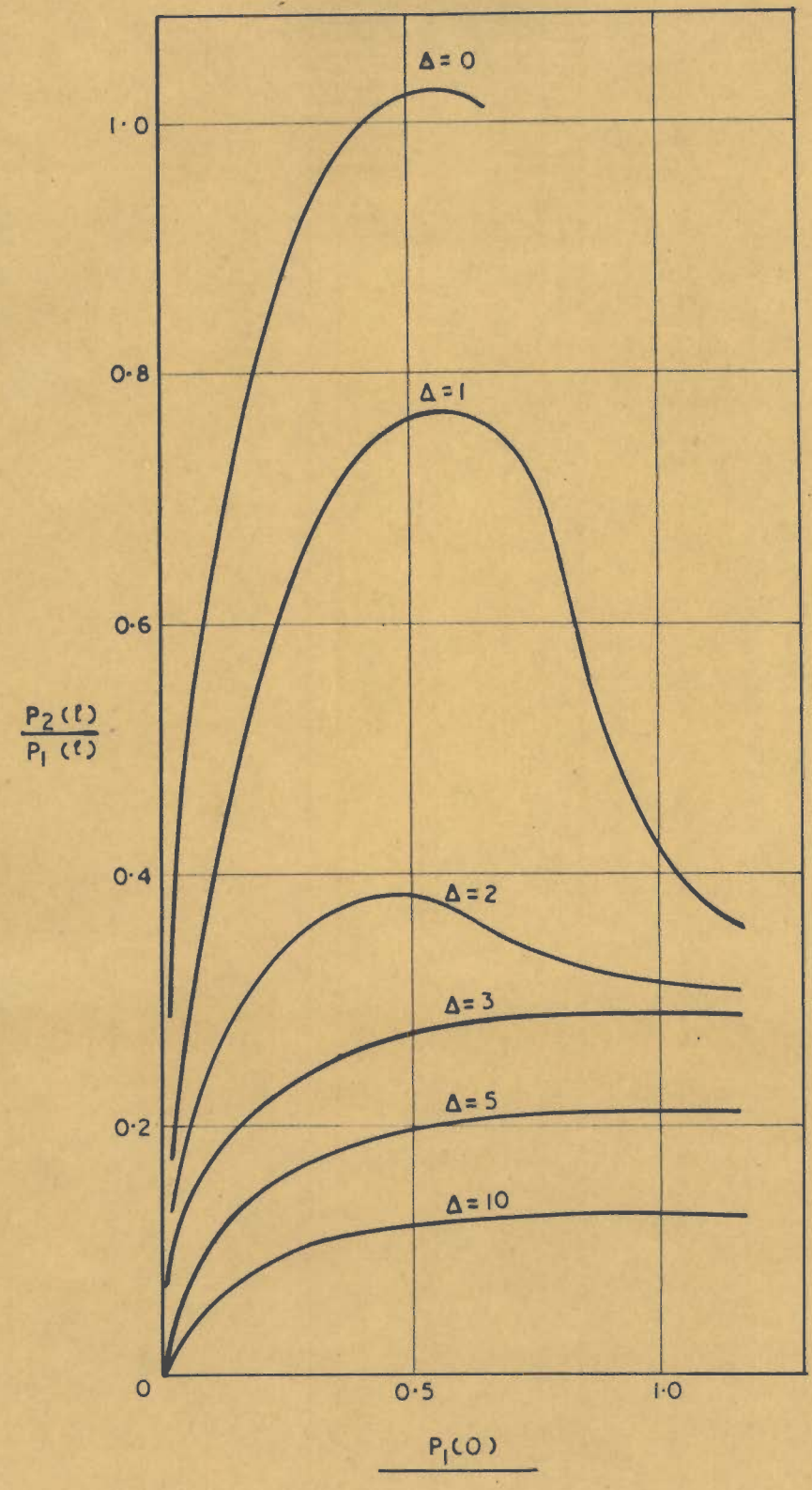

FIG. 6.3

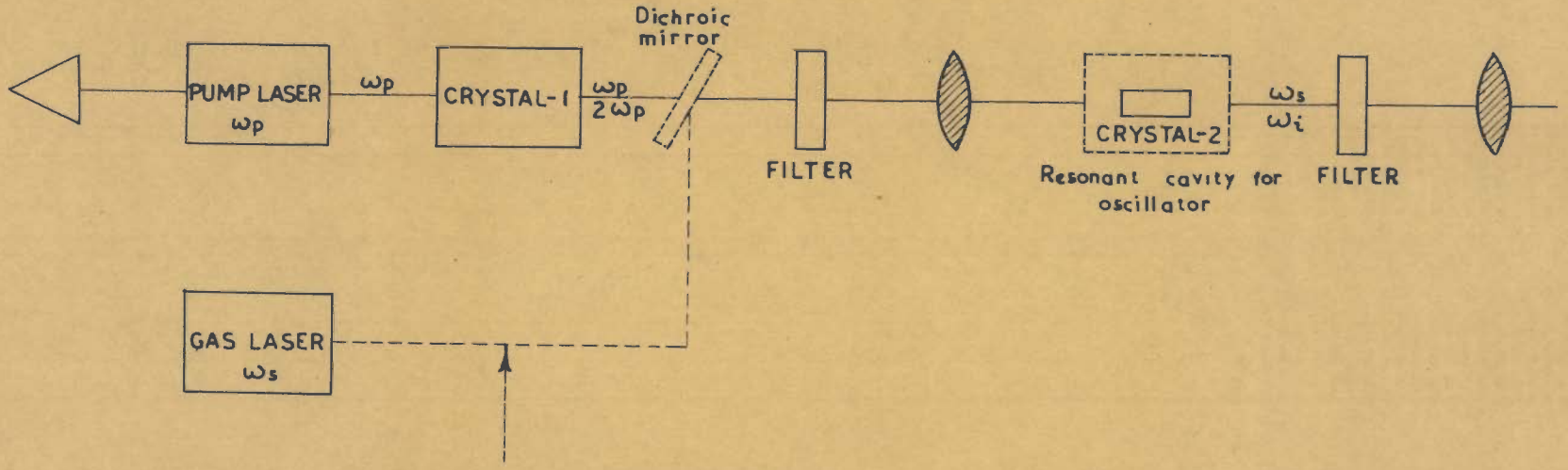
Dichroic mirror
PUMP LASER
ωp
ωp
CRYSTAL-1
ωp
2ωp
FILTER
CRYSTAL-2
ωs
ωi
FILTER
Resonant cavity for oscillator
GAS LASER
ωs
Signal when the system is to be used for parametric amplification
CRYSTAL :— KDP
ADP
LiNbO3

FIG. 7.1

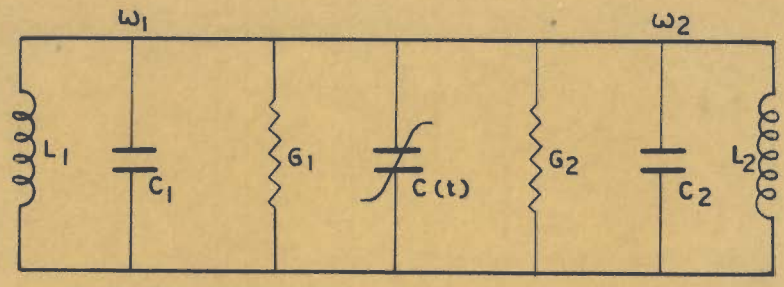

DOUBLE CAVITY

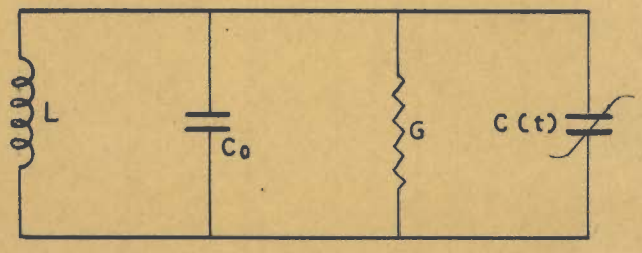

FIG. 9.1

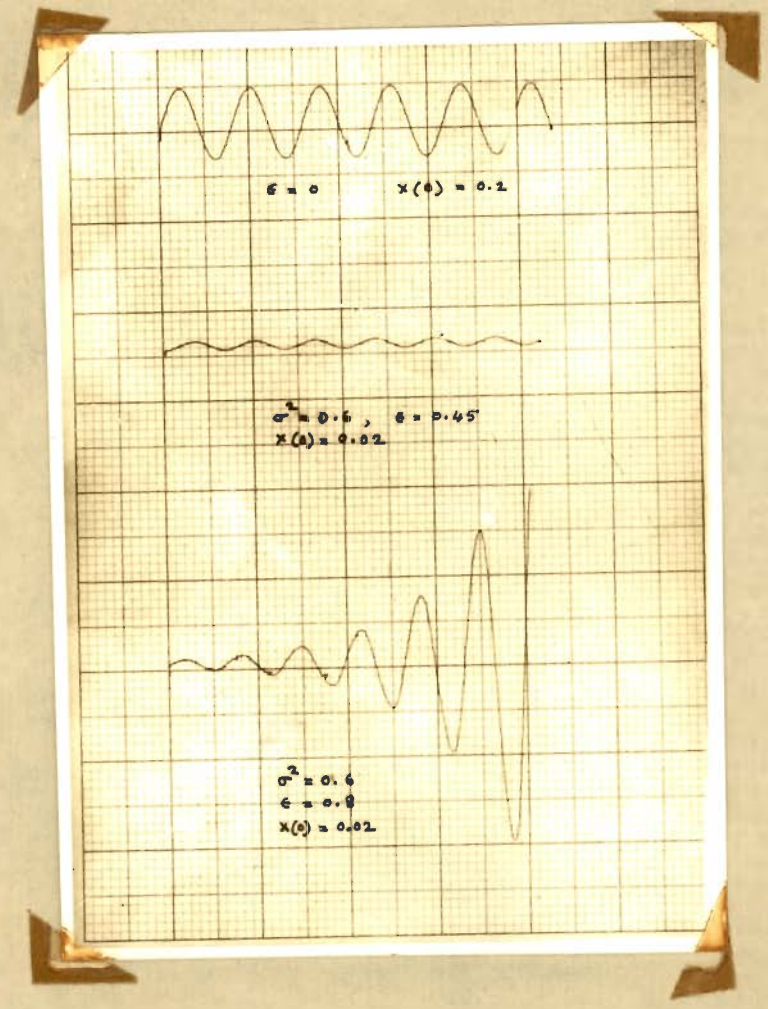

Fig. 10.1

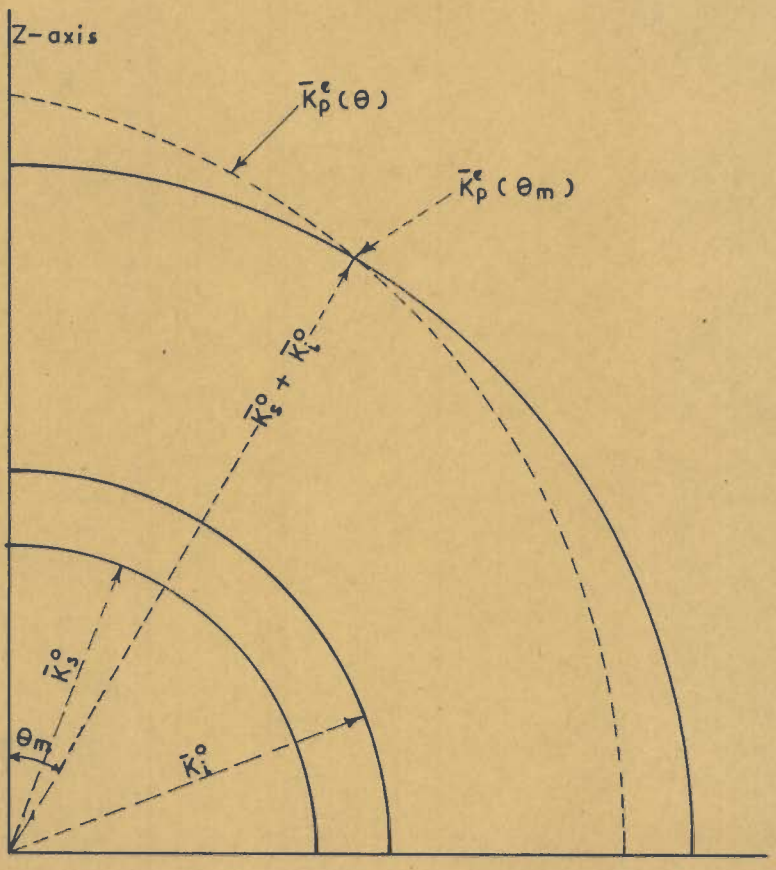
Z-axis
$\bar{K}_p^e(\theta)$
$\bar{K}_p^e(\theta_m)$
$\bar{K}_s^o + \bar{K}_i^o$
$\bar{K}_2^o$
θ_m
$\bar{K}_1^o$

FIG 11.1

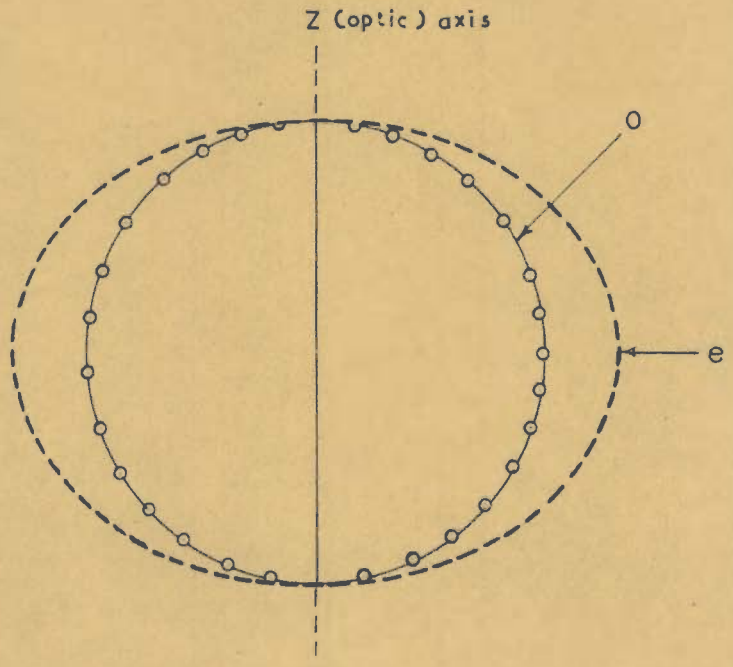

FIG. 12.1

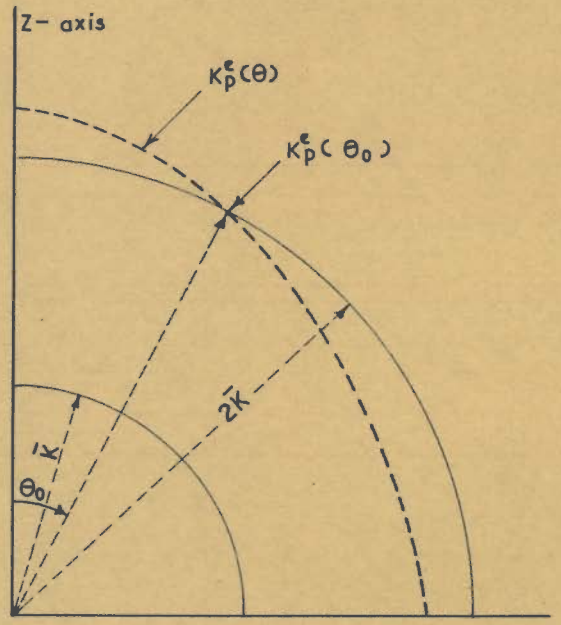
Z- axis
$K_p^e(\theta)$
$K_p^e(\theta_0)$
$2\bar{K}$
$|\bar{K}|$
θ_0

(a)

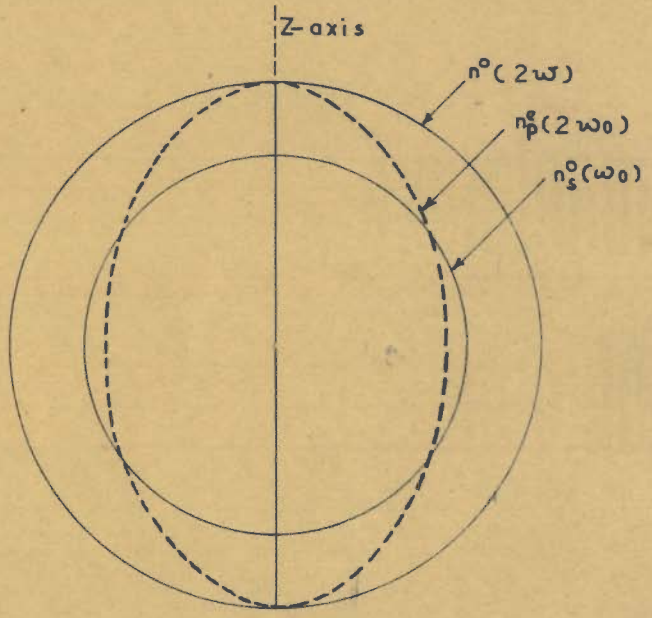
Z-axis
$n^o(2\omega)$
$n_p^e(2\omega_0)$
$n_s^o(\omega_0)$

(b)

FIG. 13·1

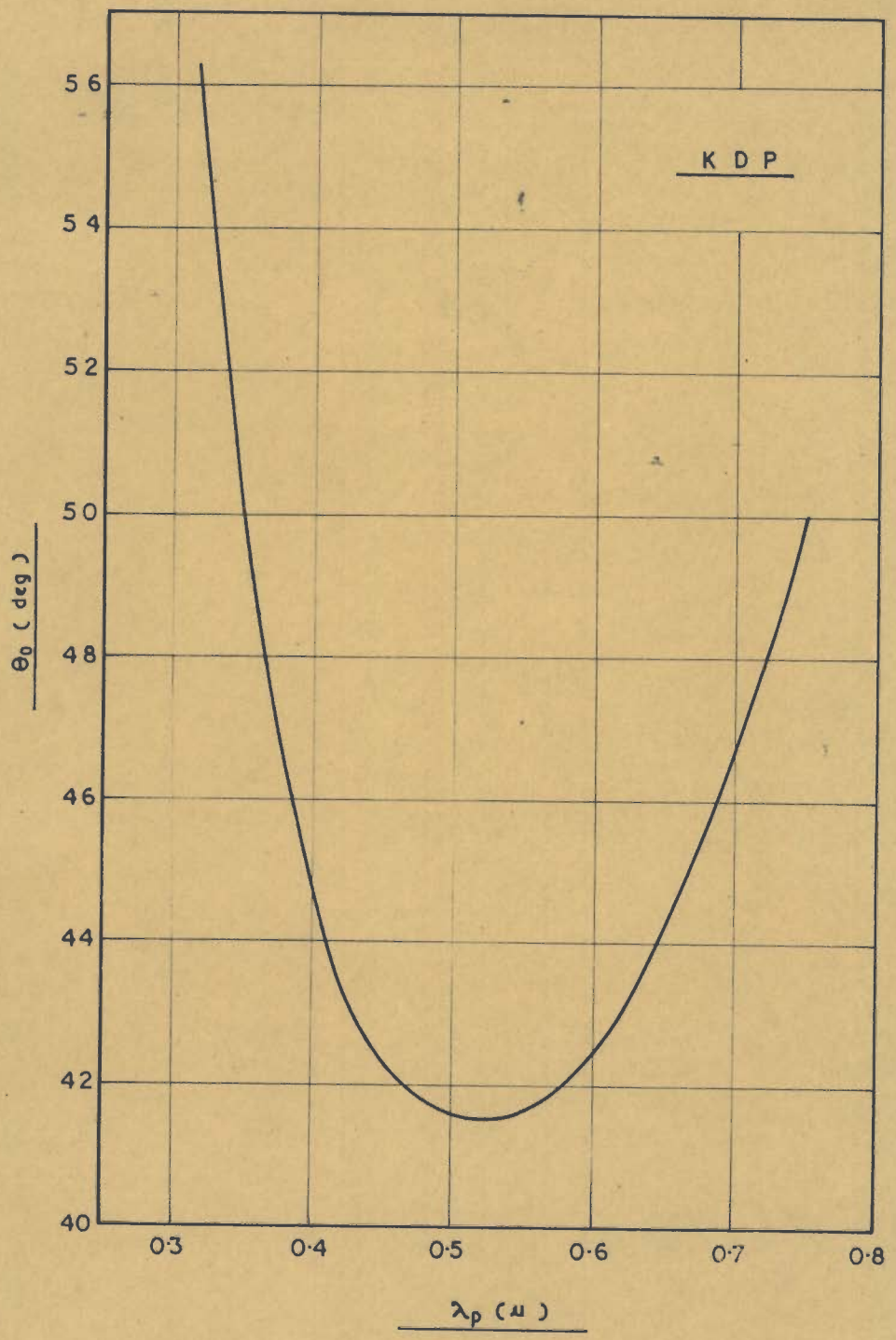

FIG. 13.2 a

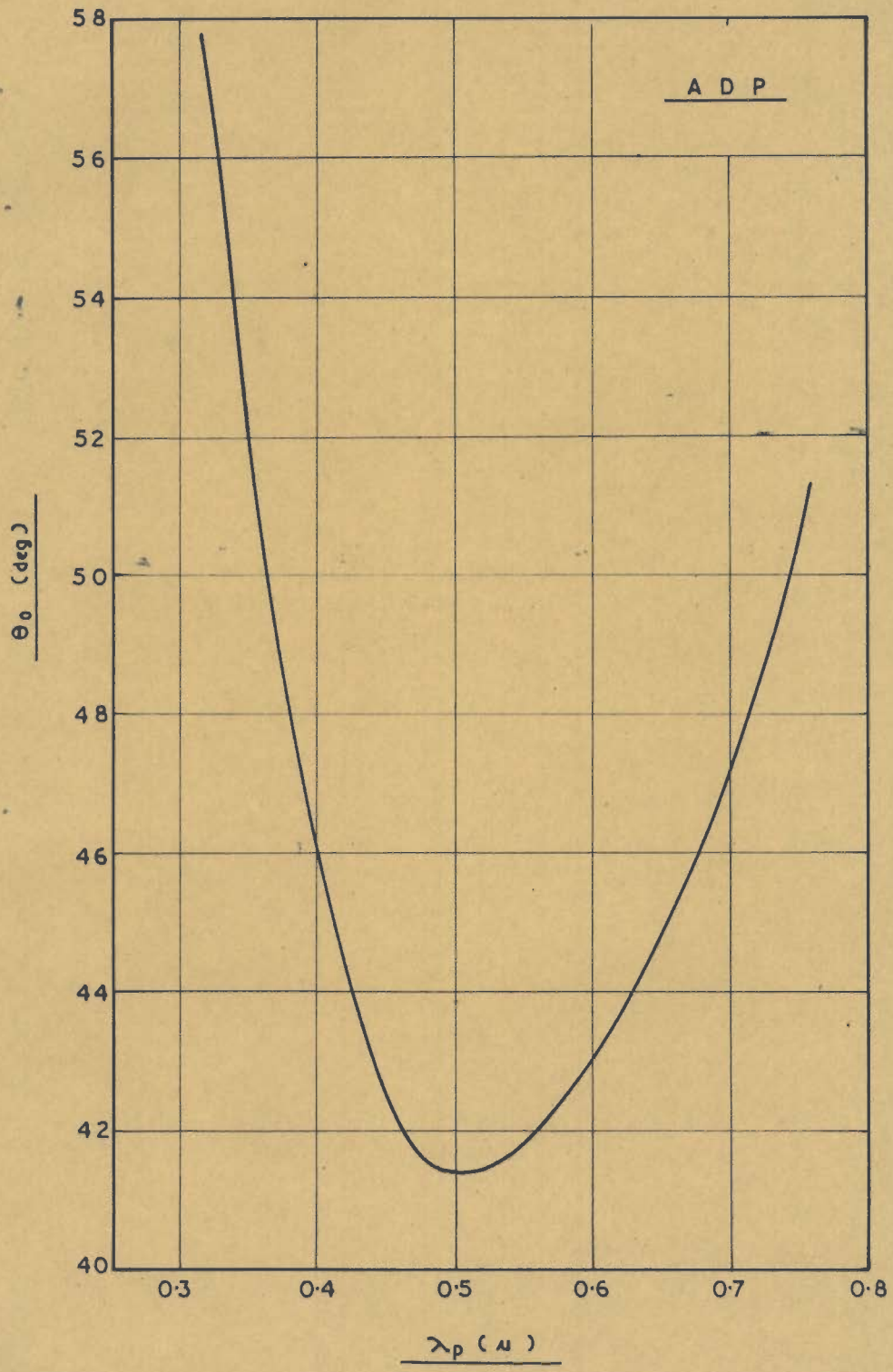

FIG. 13.2 b

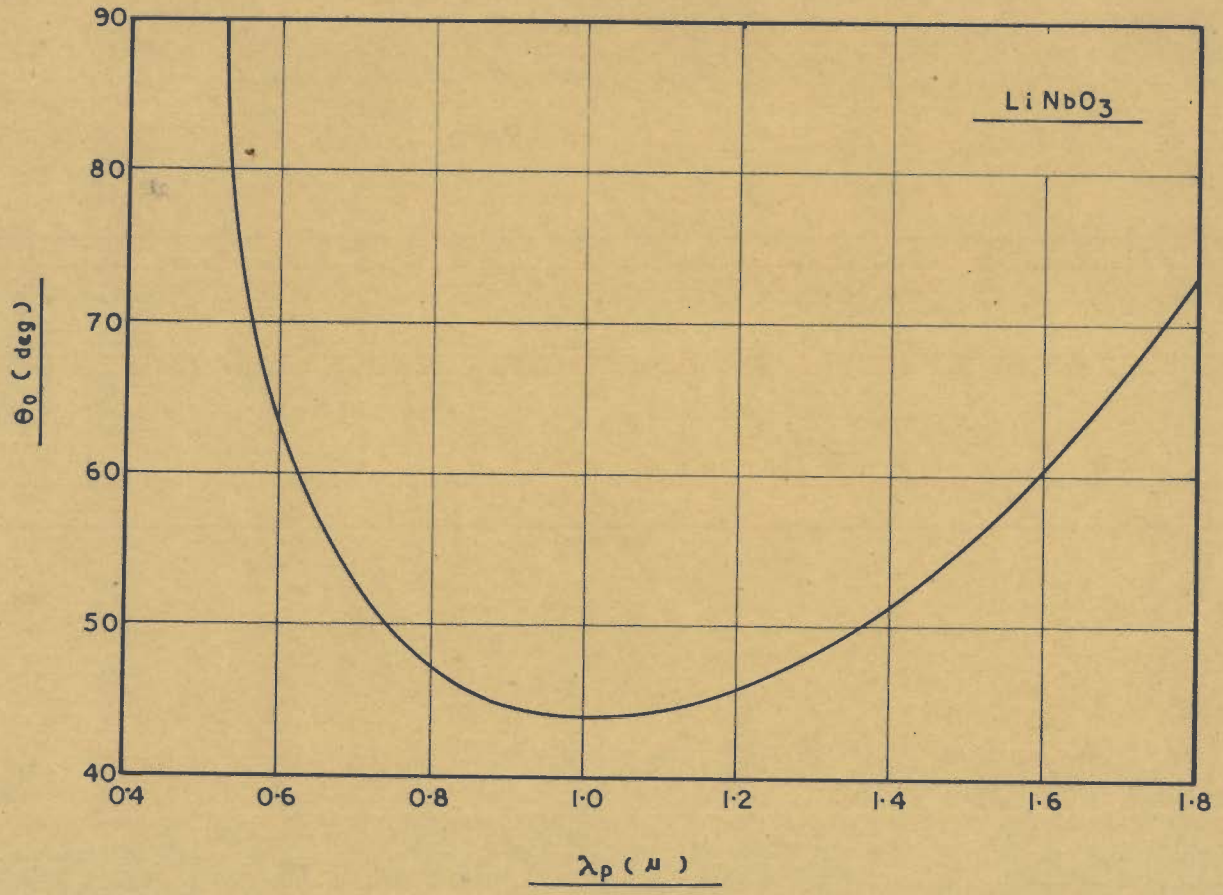

FIG. 13.2 c

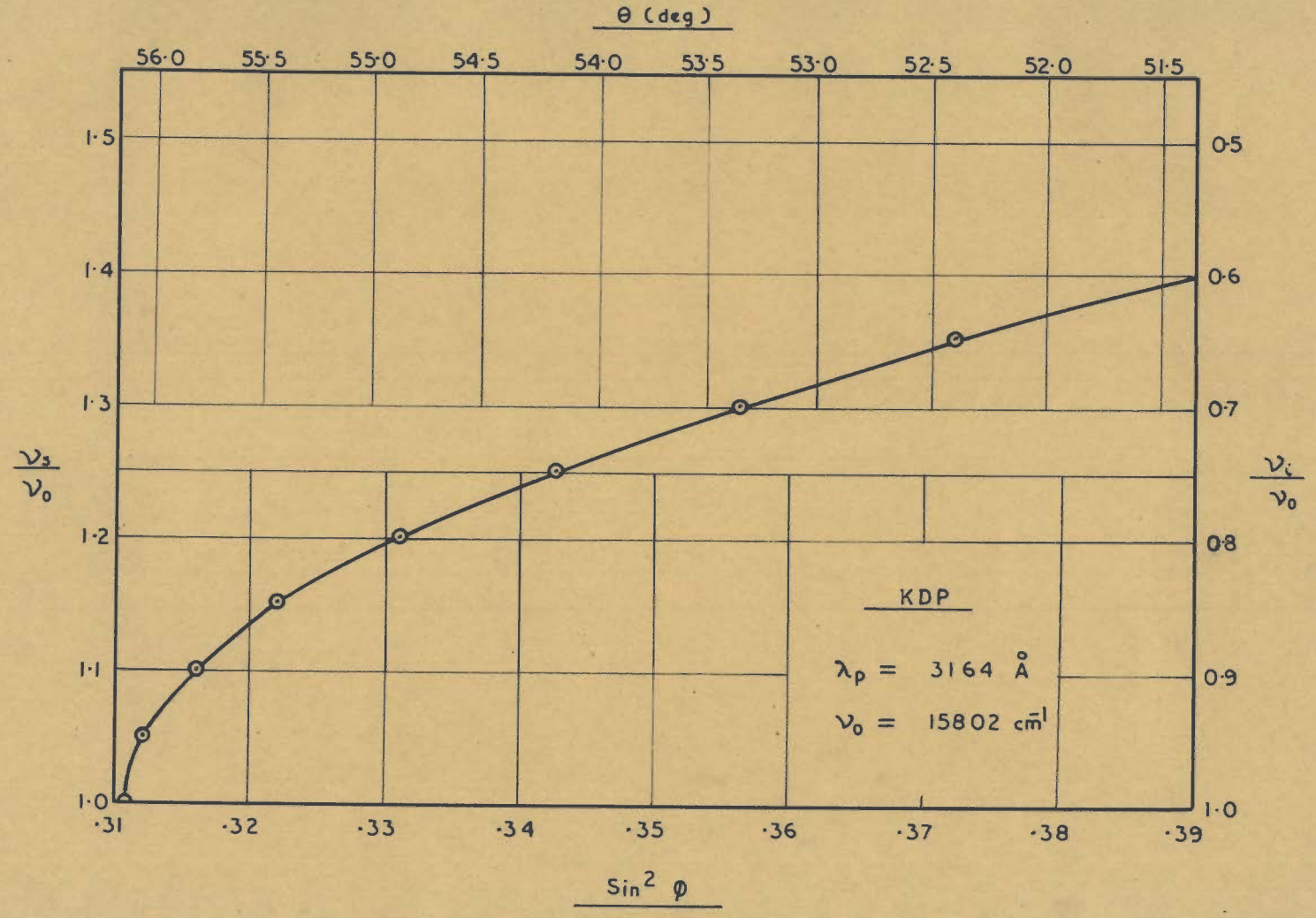
θ (deg)
56·0
55·5
55·0
54·5
54·0
53·5
53·0
52·5
52·0
51·5
1·5
1·4
1·3
1·2
1·1
1·0
0·5
0·6
0·7
0·8
0·9
1·0
$\frac{\nu_s}{\nu_0}$
$\frac{\nu_i}{\nu_0}$
KDP
λ_p = 3164 Å
ν_0 = 15802 cm^{-1}
·31
·32
·33
·34
·35
·36
·37
·38
·39
Sin^2 φ

FIG. 14.1 a

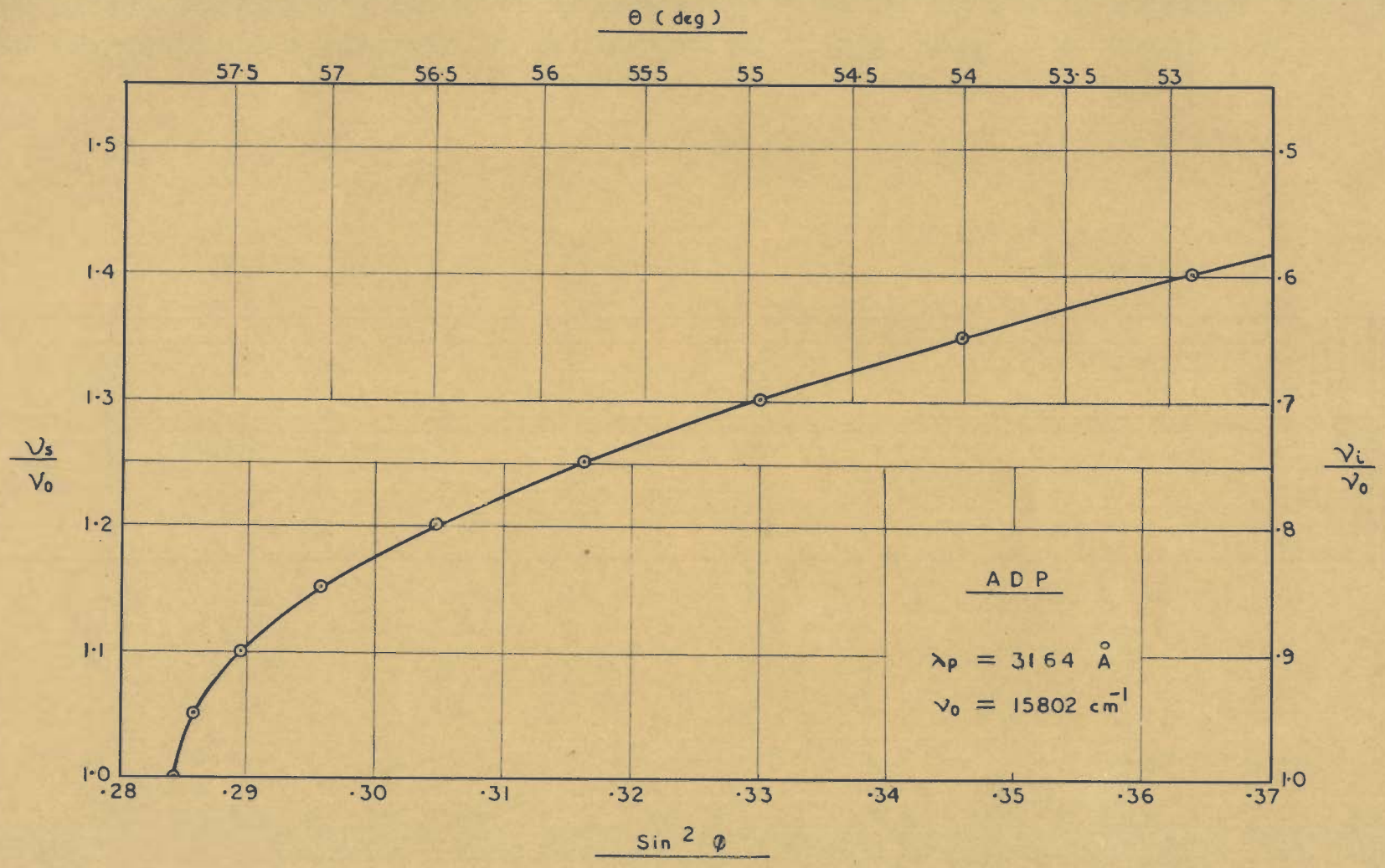
θ (deg)
57·5
57
56·5
56
55·5
55
54·5
54
53·5
53
1·5
1·4
1·3
1·2
1·1
1·0
·5
·6
·7
·8
·9
1·0
Vs/V0
Vi/V0
·28
·29
·30
·31
·32
·33
·34
·35
·36
·37
Sin² φ
ADP
λp = 3164 Å
ν0 = 15802 cm⁻¹

FIG. 14·1 b

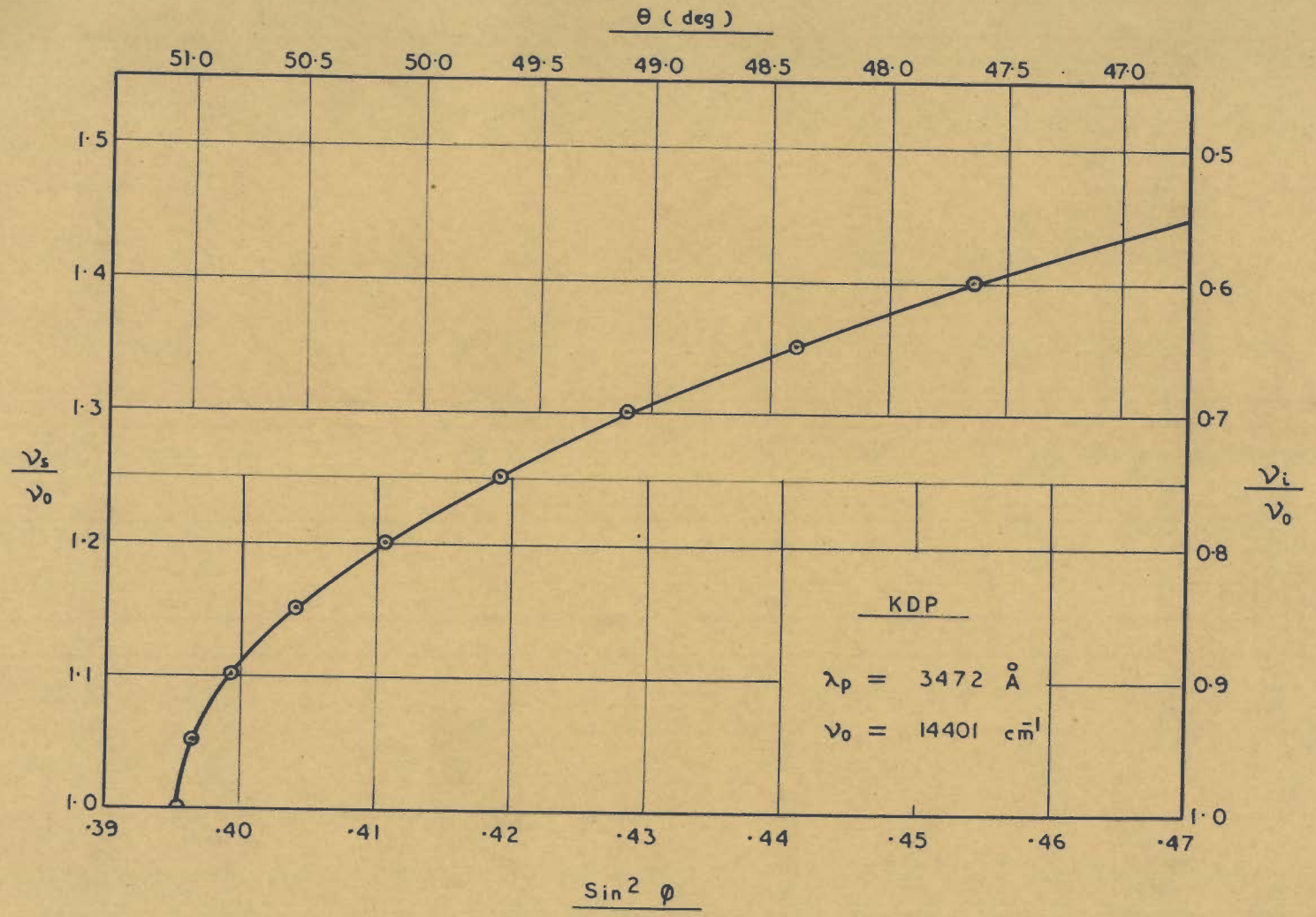
θ (deg)
51·0
50·5
50·0
49·5
49·0
48·5
48·0
47·5
47·0
1·5
1·4
1·3
1·2
1·1
1·0
νs/ν0
0·5
0·6
0·7
0·8
0·9
1·0
νi/ν0
KDP
λp = 3472 Å
ν0 = 14401 cm⁻¹
·39
·40
·41
·42
·43
·44
·45
·46
·47
Sin² φ

FIG. 14.2a

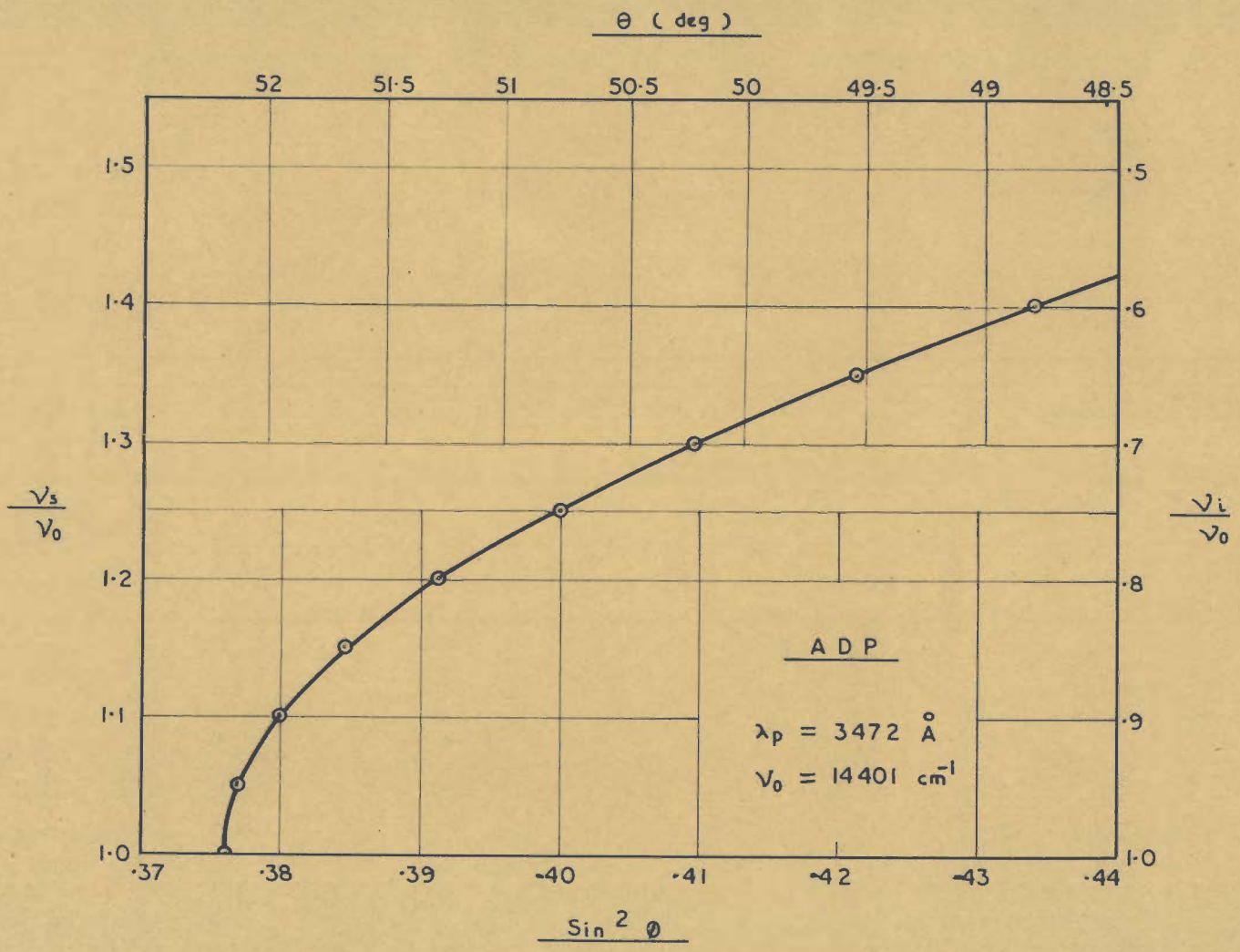
θ (deg)
52
51·5
51
50·5
50
49·5
49
48·5
1·5
1·4
1·3
1·2
1·1
1·0
·5
·6
·7
·8
·9
1·0
$\frac{\nu_s}{\nu_0}$
$\frac{\nu_i}{\nu_0}$
·37
·38
·39
·40
·41
·42
·43
·44
$\sin^2 \phi$
A D P
λ_p = 3472 Å
ν_0 = 14401 cm^{-1}

FIG. 14.2 b

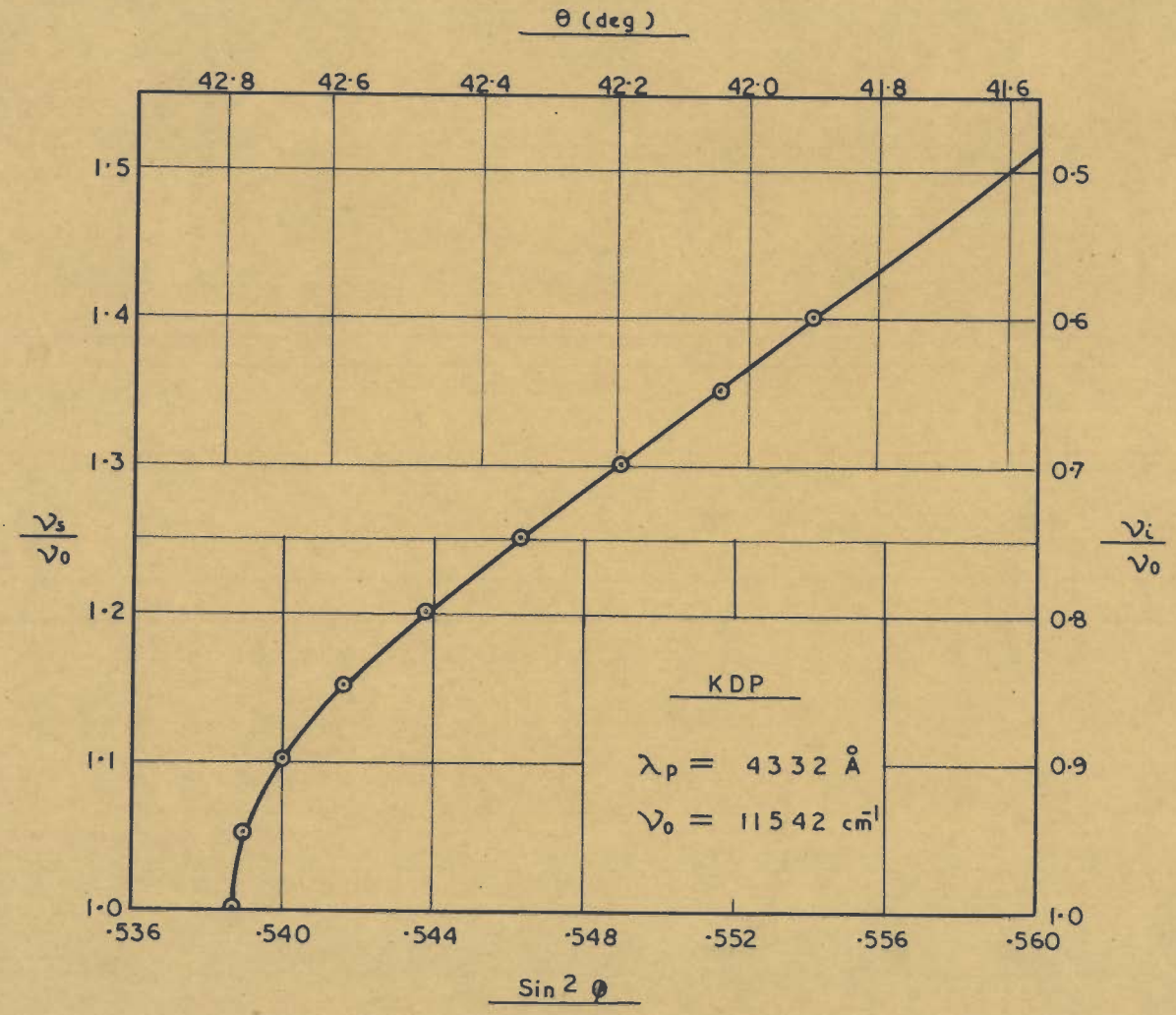
θ (deg)
42·8
42·6
42·4
42·2
42·0
41·8
41·6
1·5
1·4
1·3
1·2
1·1
1·0
νs/ν0
0·5
0·6
0·7
0·8
0·9
1·0
νi/ν0
KDP
λp = 4332 Å
ν0 = 11542 cm⁻¹
·536
·540
·544
·548
·552
·556
·560
Sin² θ

FIG. 14.3 a

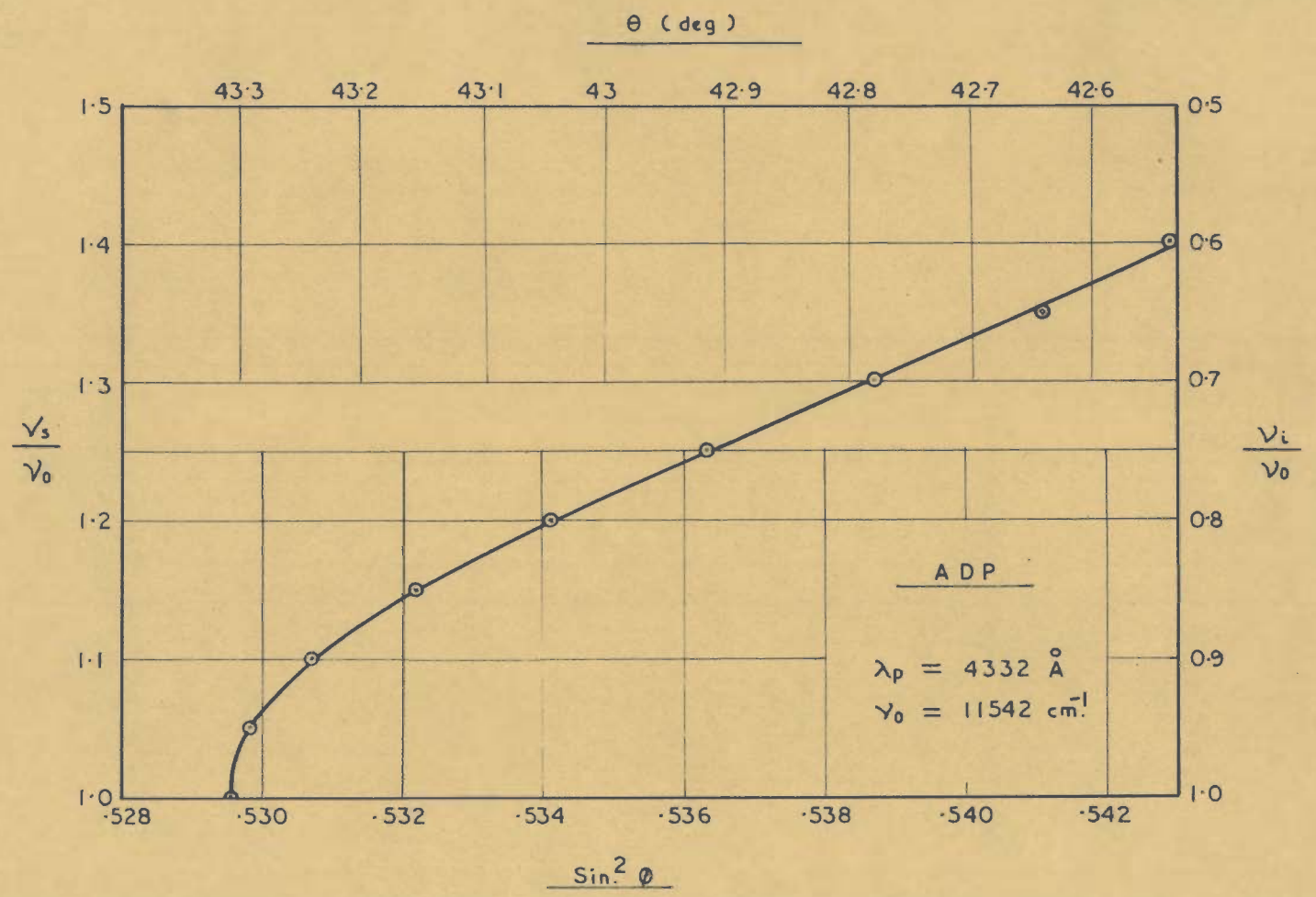
θ (deg)
43·3
43·2
43·1
43
42·9
42·8
42·7
42·6
1·5
1·4
1·3
1·2
1·1
1·0
0·5
0·6
0·7
0·8
0·9
1·0
νs/ν0
νi/ν0
ADP
λp = 4332 Å
ν0 = 11542 cm⁻¹
·528
·530
·532
·534
·536
·538
·540
·542
Sin.² ∅

Fig. 14·3 b

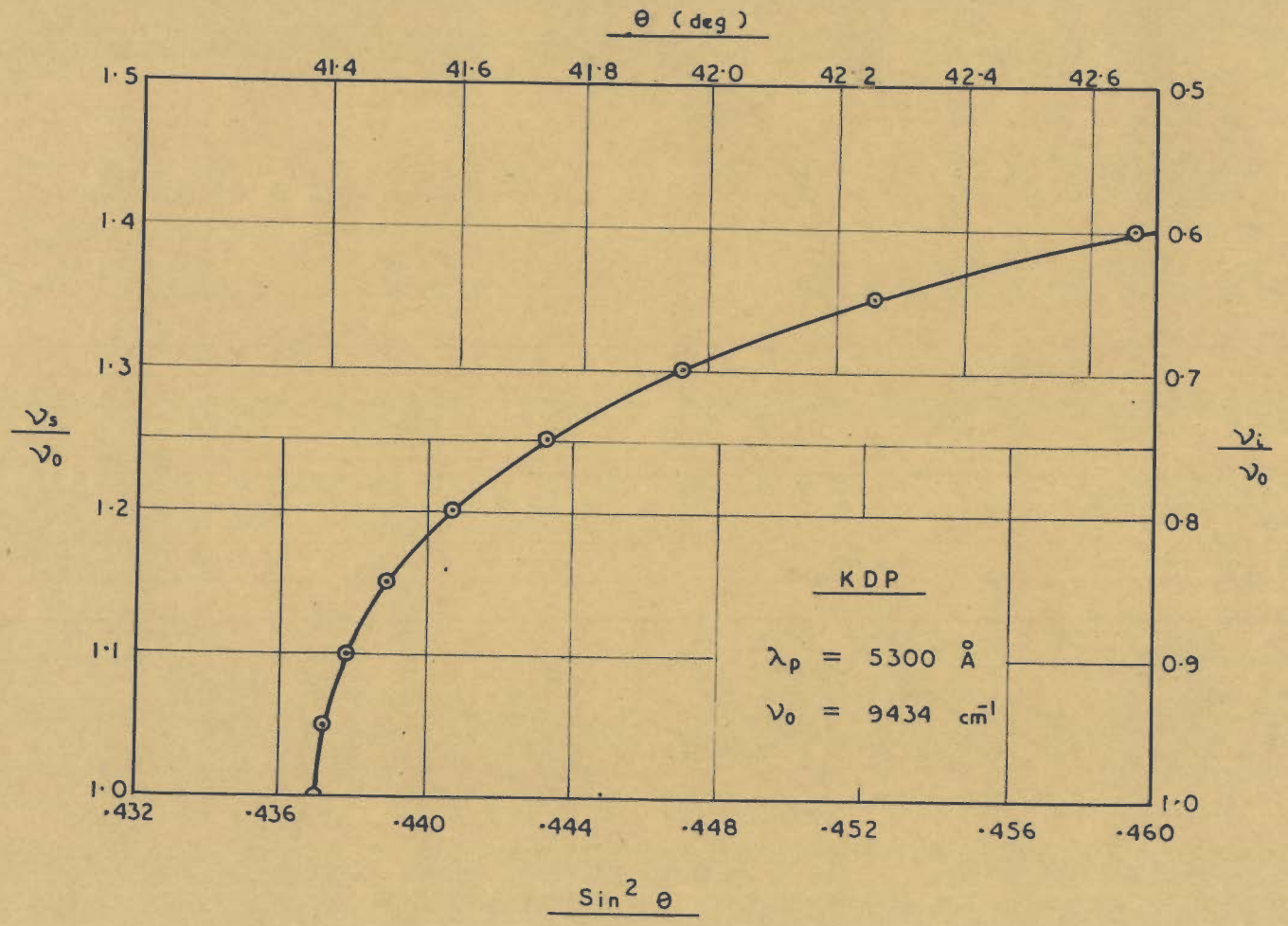
θ (deg)
41·4
41·6
41·8
42·0
42·2
42·4
42·6
1·5
1·4
1·3
1·2
1·1
1·0
0·5
0·6
0·7
0·8
0·9
1·0
νs/ν0
νi/ν0
KDP
λp = 5300 Å
ν0 = 9434 cm⁻¹
·432
·436
·440
·444
·448
·452
·456
·460
Sin² θ

FIG. 14.4 a

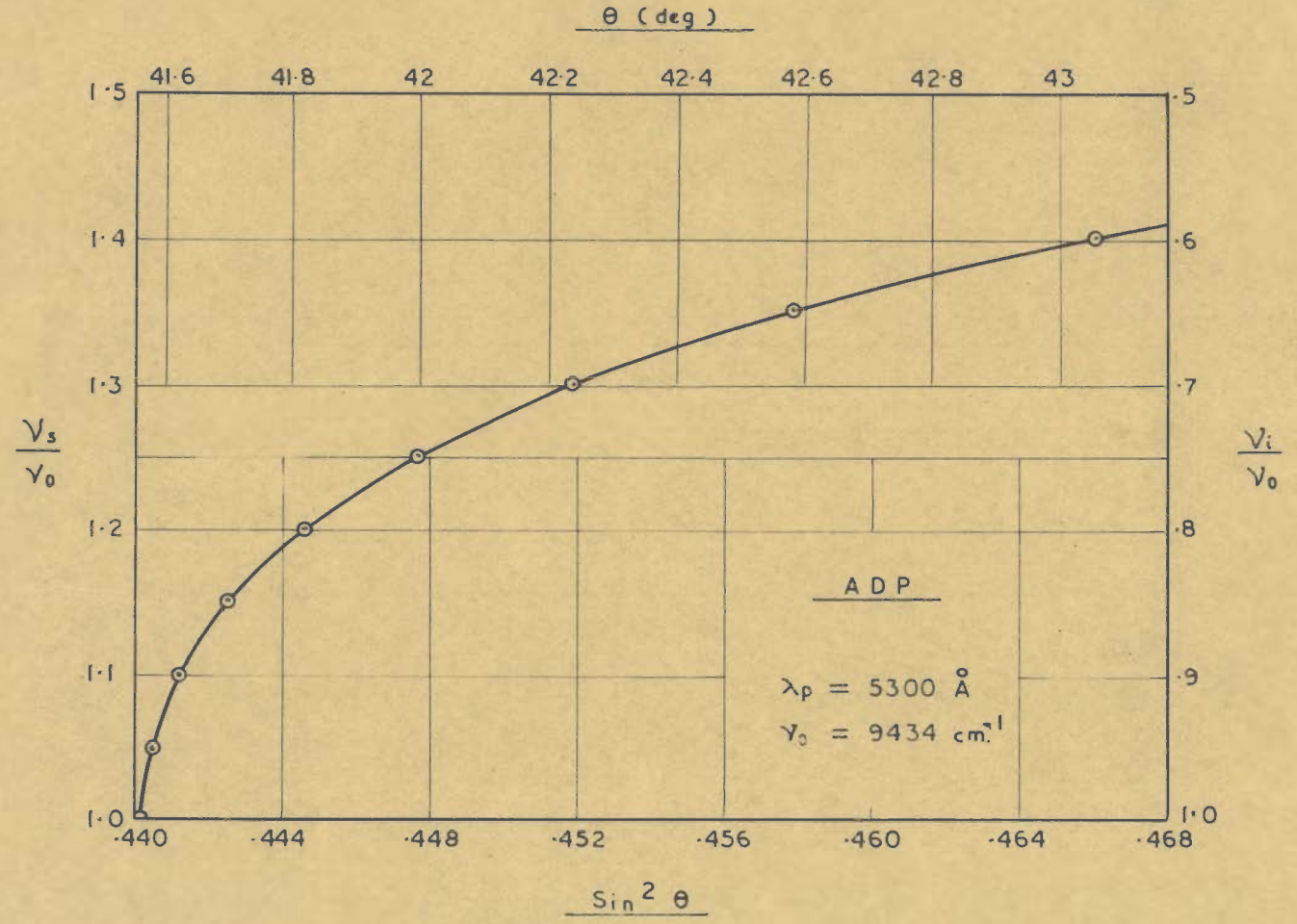
θ (deg)
41·6
41·8
42
42·2
42·4
42·6
42·8
43
1·5
1·4
1·3
1·2
1·1
1·0
·5
·6
·7
·8
·9
1·0
Vs/V0
Vi/V0
ADP
λp = 5300 Å
V0 = 9434 cm.-1
·440
·444
·448
·452
·456
·460
·464
·468
Sin2 θ

FIG. 14.4 b

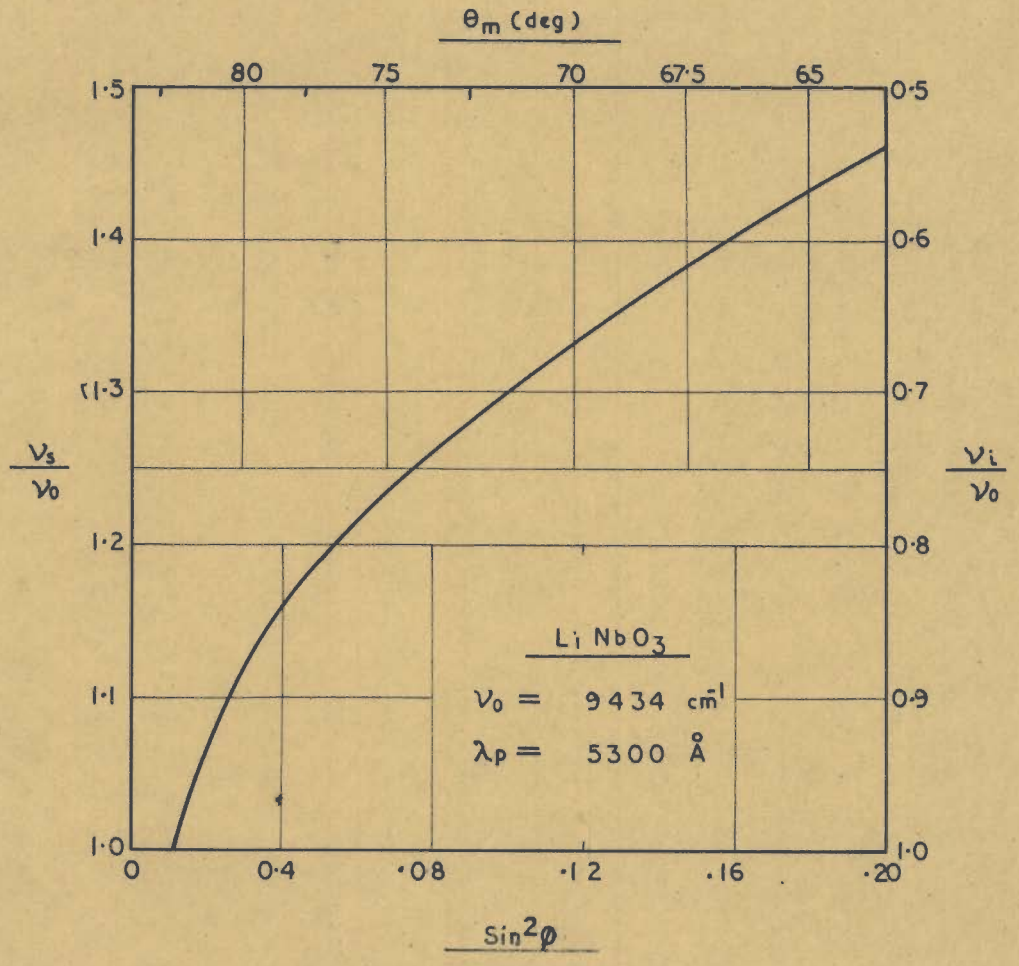
θm (deg)
80
75
70
67·5
65
1·5
1·4
1·3
1·2
1·1
1·0
0·5
0·6
0·7
0·8
0·9
1·0
νs/ν0
νi/ν0
Li NbO3
ν0 = 9434 cm⁻¹
λp = 5300 Å
0
0·4
·08
·12
·16
·20
Sin²φ

FIG. 14.4 c

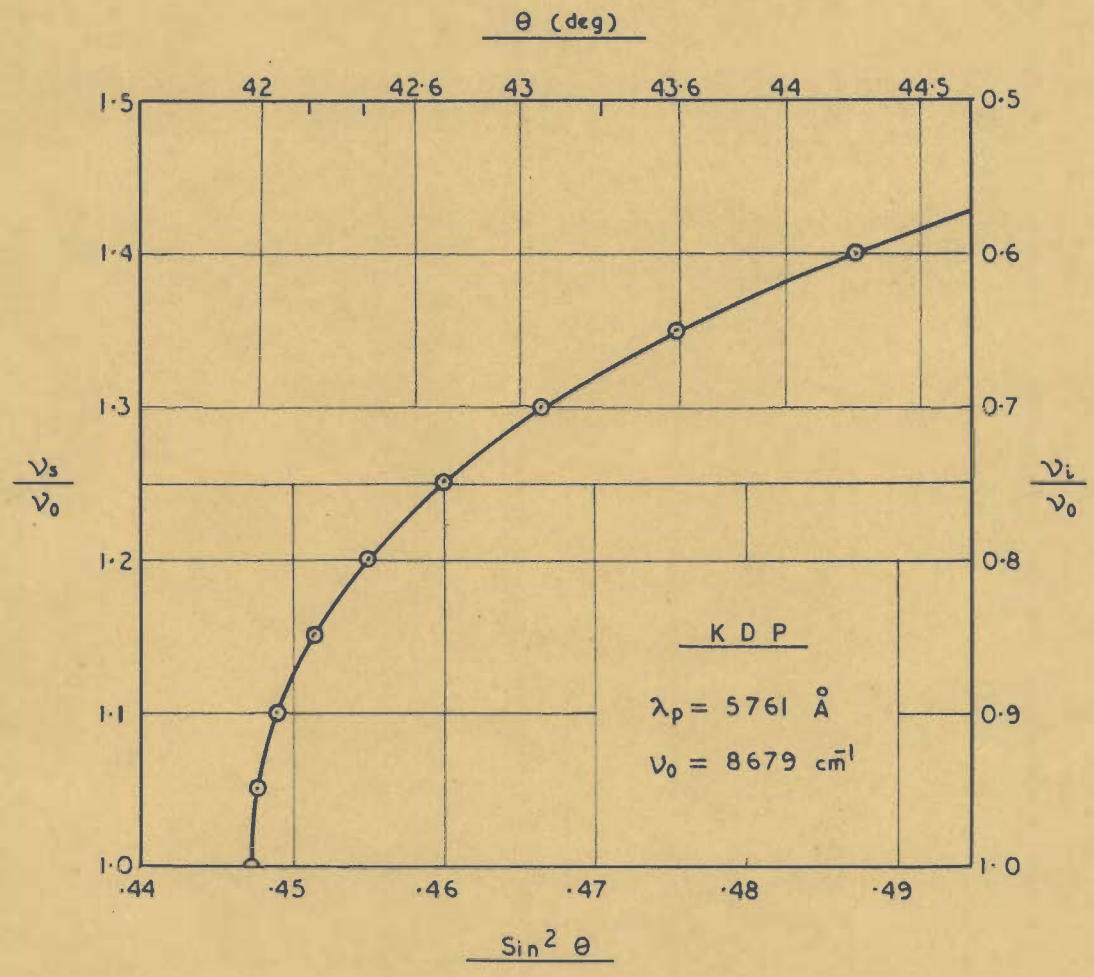
θ (deg)
42
42·6
43
43·6
44
44·5
1·5
1·4
1·3
1·2
1·1
1·0
0·5
0·6
0·7
0·8
0·9
1·0
νs/ν0
νi/ν0
K D P
λp = 5761 Å
ν0 = 8679 cm⁻¹
·44
·45
·46
·47
·48
·49
Sin² θ

FIG. 14.5a

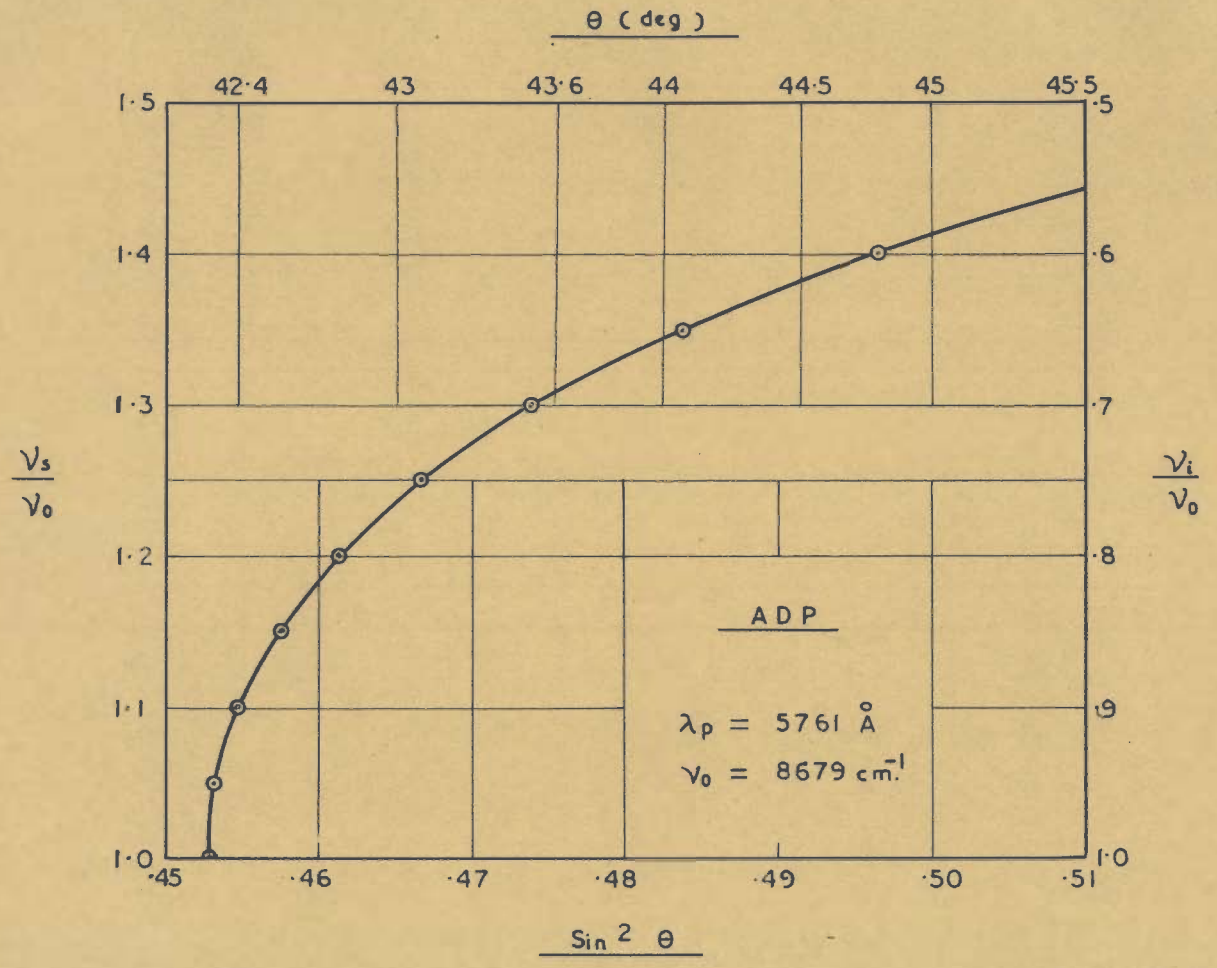
θ (deg)
42·4
43
43·6
44
44·5
45
45·5
1·5
1·4
1·3
1·2
1·1
1·0
·5
·6
·7
·8
·9
1·0
$\frac{\nu_s}{\nu_0}$
$\frac{\nu_i}{\nu_0}$
ADP
λ_p = 5761 Å
ν_0 = 8679 cm^{-1}
·45
·46
·47
·48
·49
·50
·51
Sin^2 θ

FIG. 14.5 b

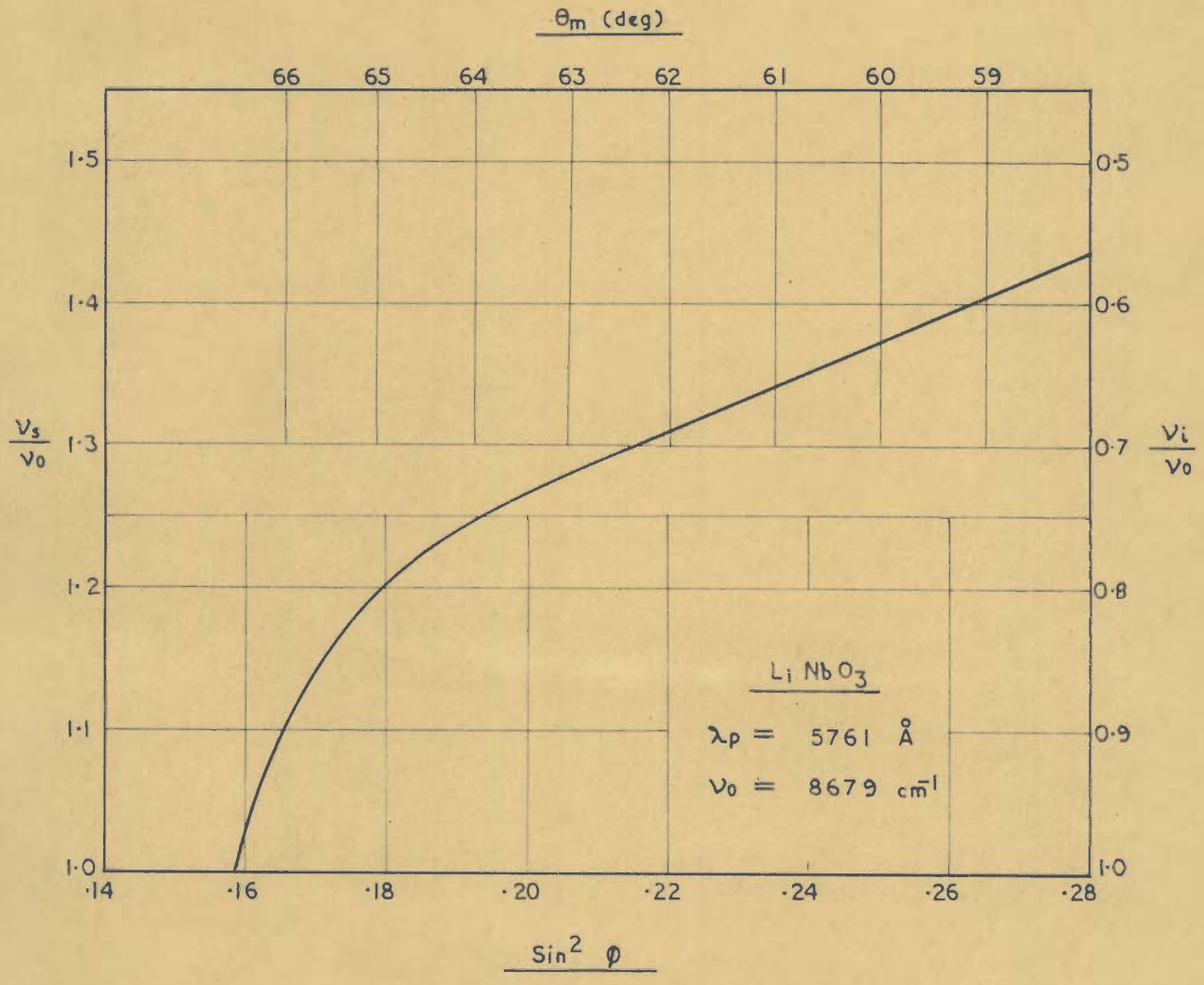
θm (deg)
66
65
64
63
62
61
60
59
1·5
1·4
1·3
1·2
1·1
1·0
0·5
0·6
0·7
0·8
0·9
1·0
νs/ν0
νi/ν0
·14
·16
·18
·20
·22
·24
·26
·28
Sin² φ
Li Nb O3
λp = 5761 Å
ν0 = 8679 cm⁻¹

FIG. 14·5 c

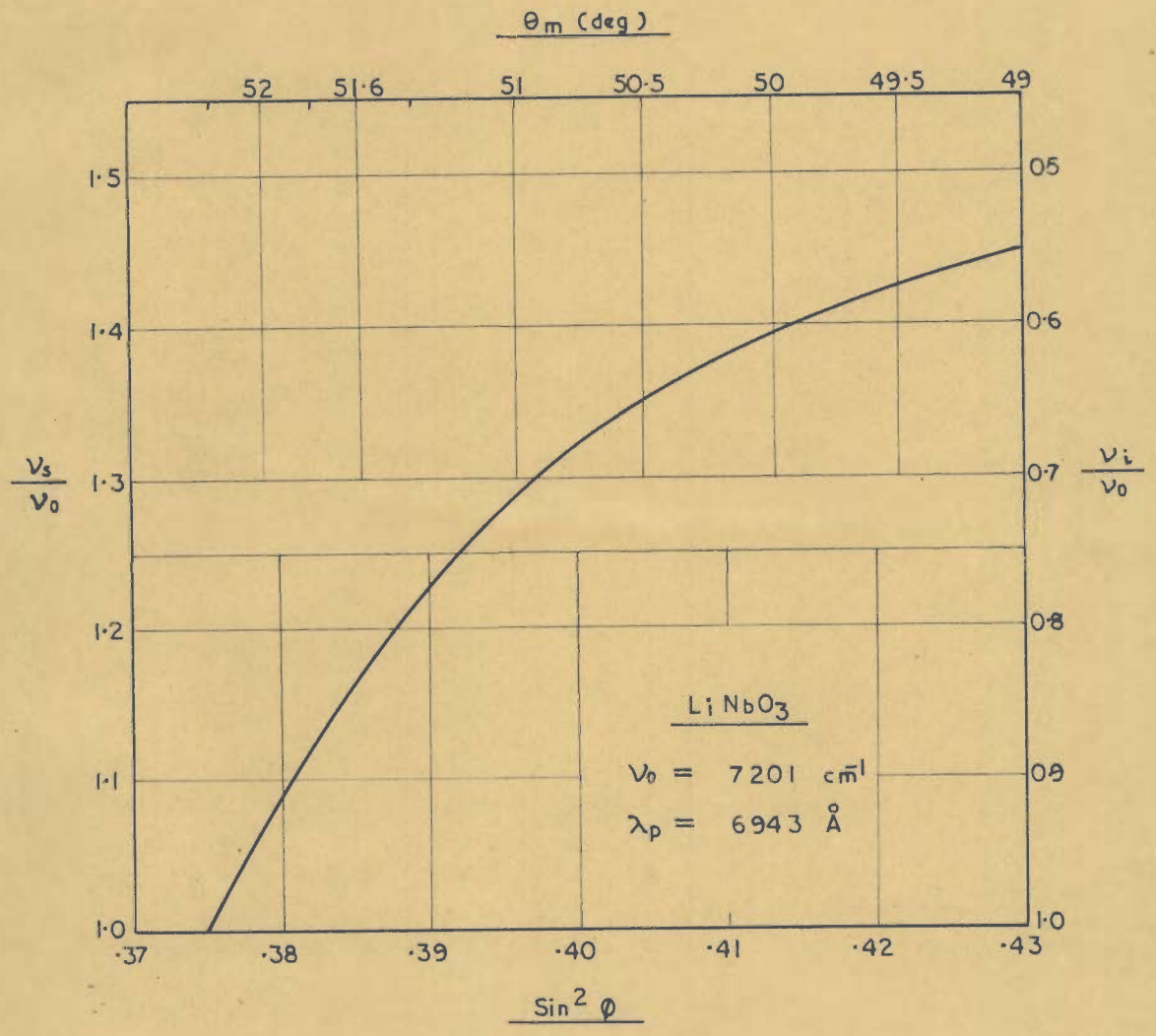
θm (deg)
52
51·6
51
50·5
50
49·5
49
1·5
1·4
1·3
1·2
1·1
1·0
·37
·38
·39
·40
·41
·42
·43
Sin² ϕ
νs/ν0
νi/ν0
05
0·6
0·7
0·8
0·9
1·0
LiNbO3
ν0 = 7201 cm⁻¹
λp = 6943 Å

FIG. 14.6

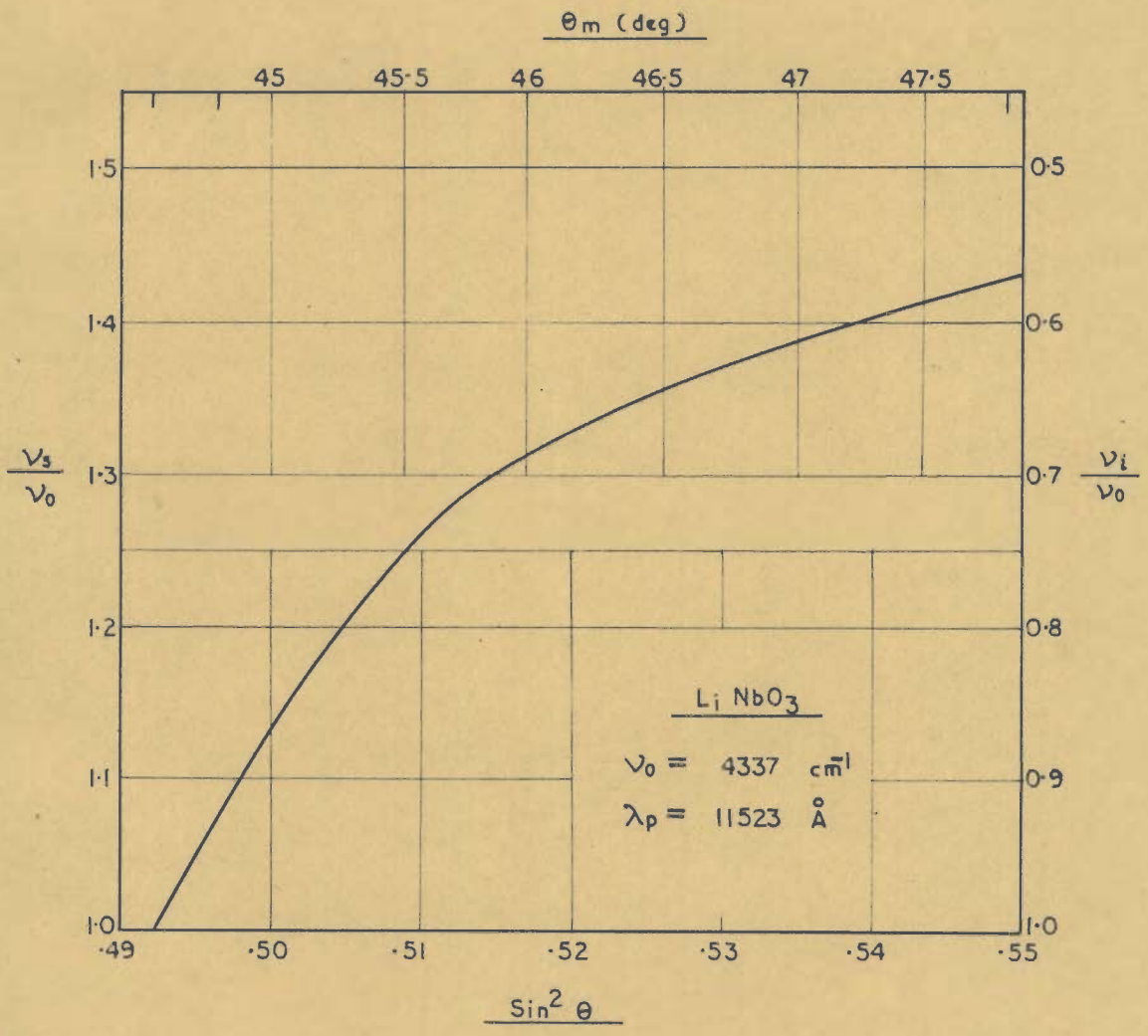
θm (deg)
45
45·5
46
46·5
47
47·5
1·5
1·4
1·3
1·2
1·1
1·0
0·5
0·6
0·7
0·8
0·9
1·0
νs/ν0
νi/ν0
Li NbO3
ν0 = 4337 cm⁻¹
λp = 11523 Å
·49
·50
·51
·52
·53
·54
·55
Sin² θ

FIG. 14.7

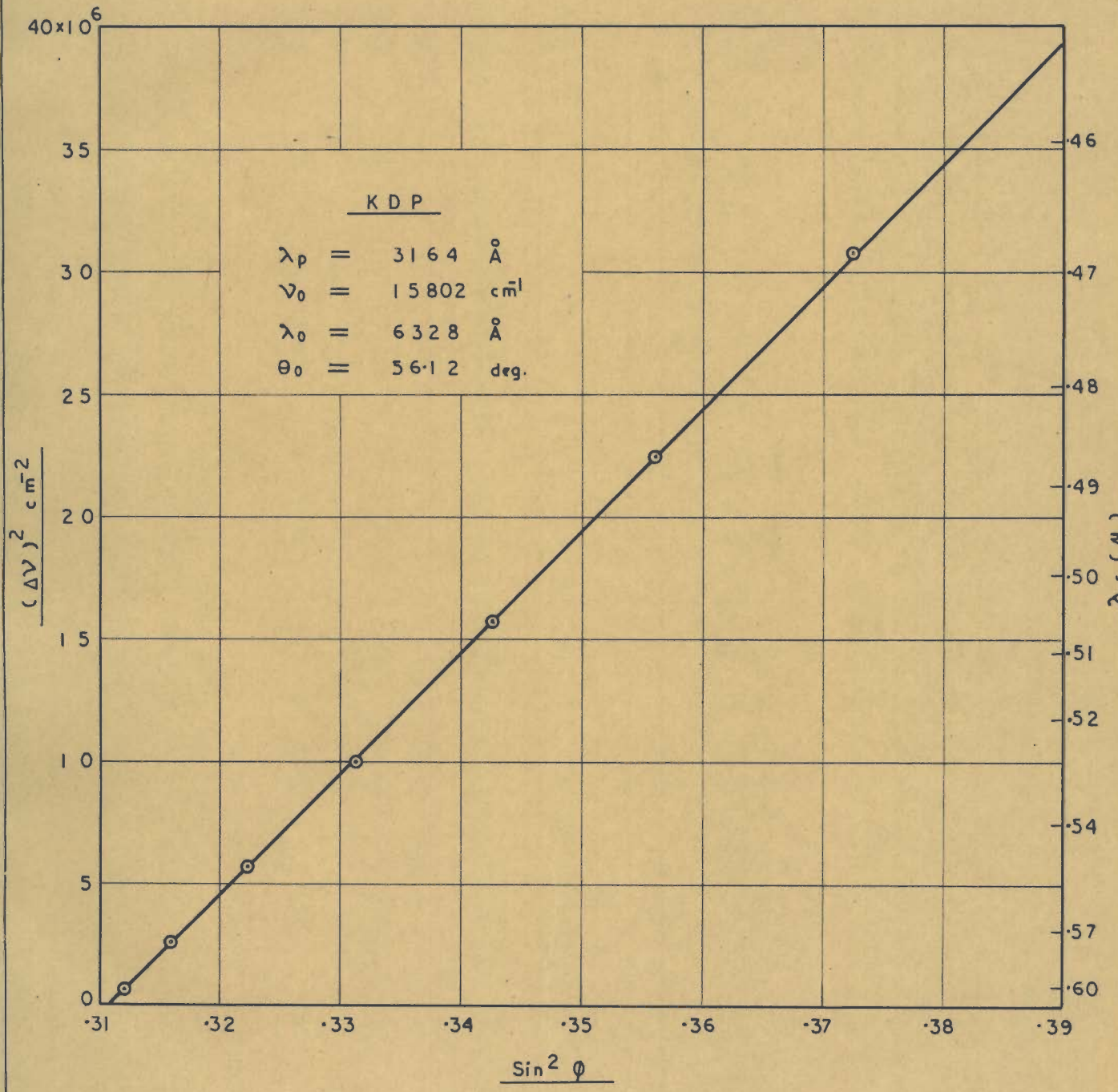
KDP
λp = 3164 Å
ν0 = 15802 cm⁻¹
λ0 = 6328 Å
θ0 = 56·12 deg.
40×10⁶
35
30
25
20
15
10
5
0
(Δν)² cm⁻²
·31
·32
·33
·34
·35
·36
·37
·38
·39
Sin² φ
·46
·47
·48
·49
·50
·51
·52
·54
·57
·60

FIG. 15·1 a

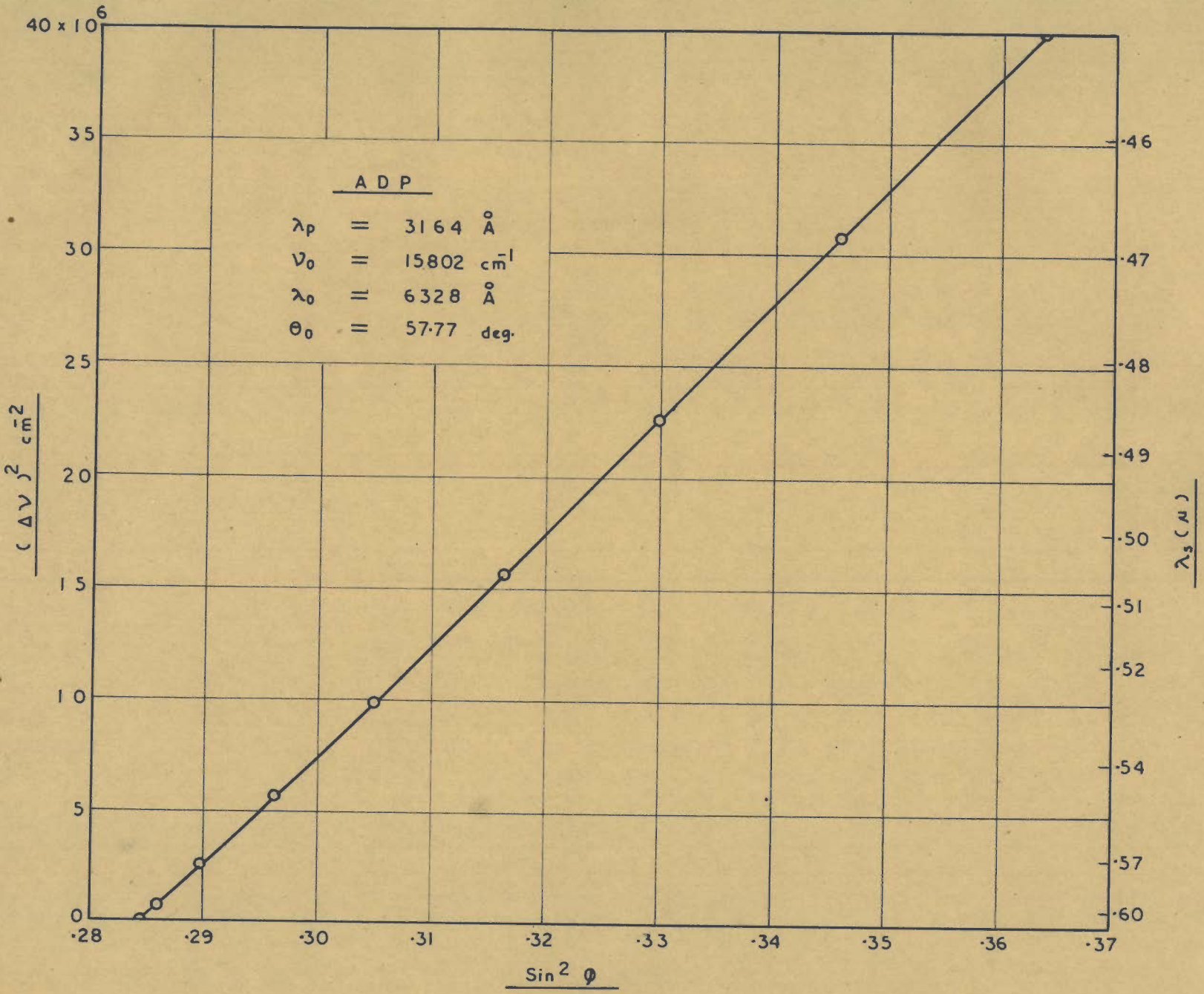
ADP
λp = 3164 Å
ν0 = 15802 cm⁻¹
λ0 = 6328 Å
θ0 = 57·77 deg.
40 x 10⁶
35
30
25
20
15
10
5
0
(Δν)² cm⁻²
·28
·29
·30
·31
·32
·33
·34
·35
·36
·37
Sin² φ
·46
·47
·48
·49
·50
·51
·52
·54
·57
·60
λs (μ)

FIG. 15.1 b

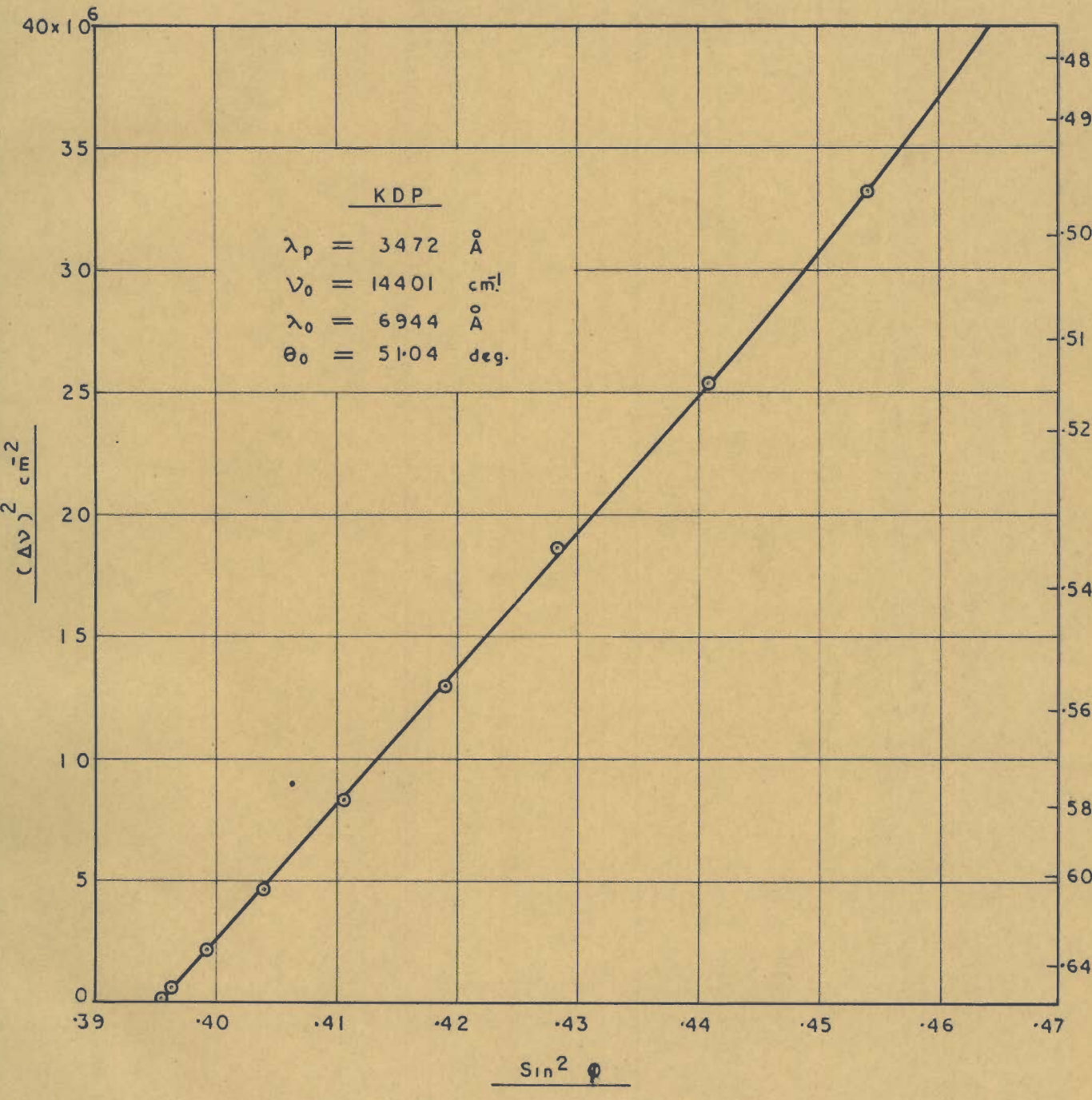
KDP
λ_p = 3472 Å
ν_0 = 14401 cm⁻¹
λ_0 = 6944 Å
θ_0 = 51·04 deg.
40x10⁶
35
30
25
20
15
10
5
0
$(\Delta\nu)^2$ cm⁻²
·39
·40
·41
·42
·43
·44
·45
·46
·47
Sin² φ
·48
·49
·50
·51
·52
·54
·56
·58
·60
·64

FIG. 15.2 a

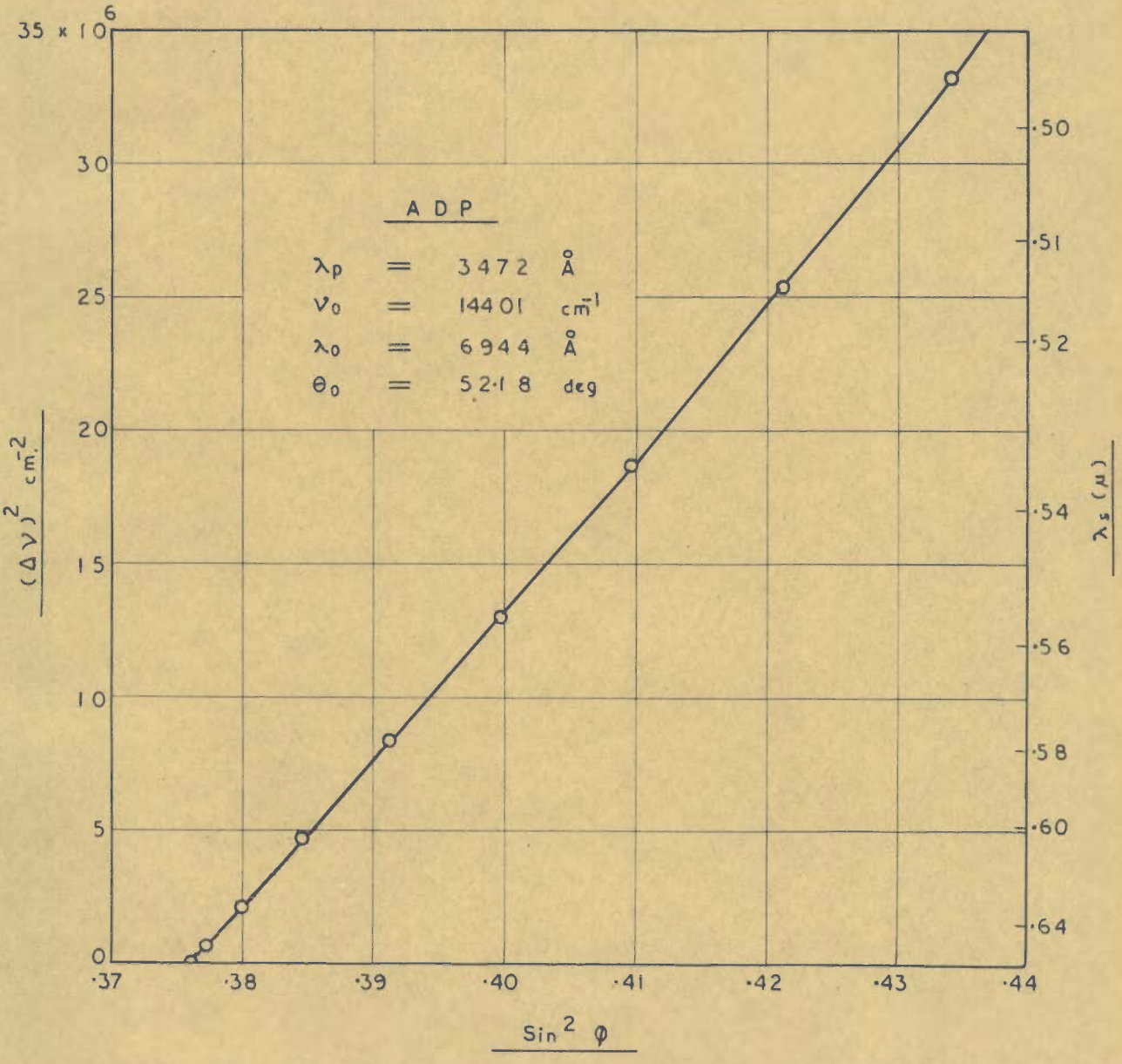
35 x 10^6
30
25
20
15
10
5
0
·37
·38
·39
·40
·41
·42
·43
·44
·50
·51
·52
·54
·56
·58
·60
·64
ADP
λp = 3472 Å
ν0 = 14401 cm⁻¹
λ0 = 6944 Å
θ0 = 52·18 deg
(Δν)² cm.⁻²
λs (μ)
Sin² φ

FIG. 15.2 b

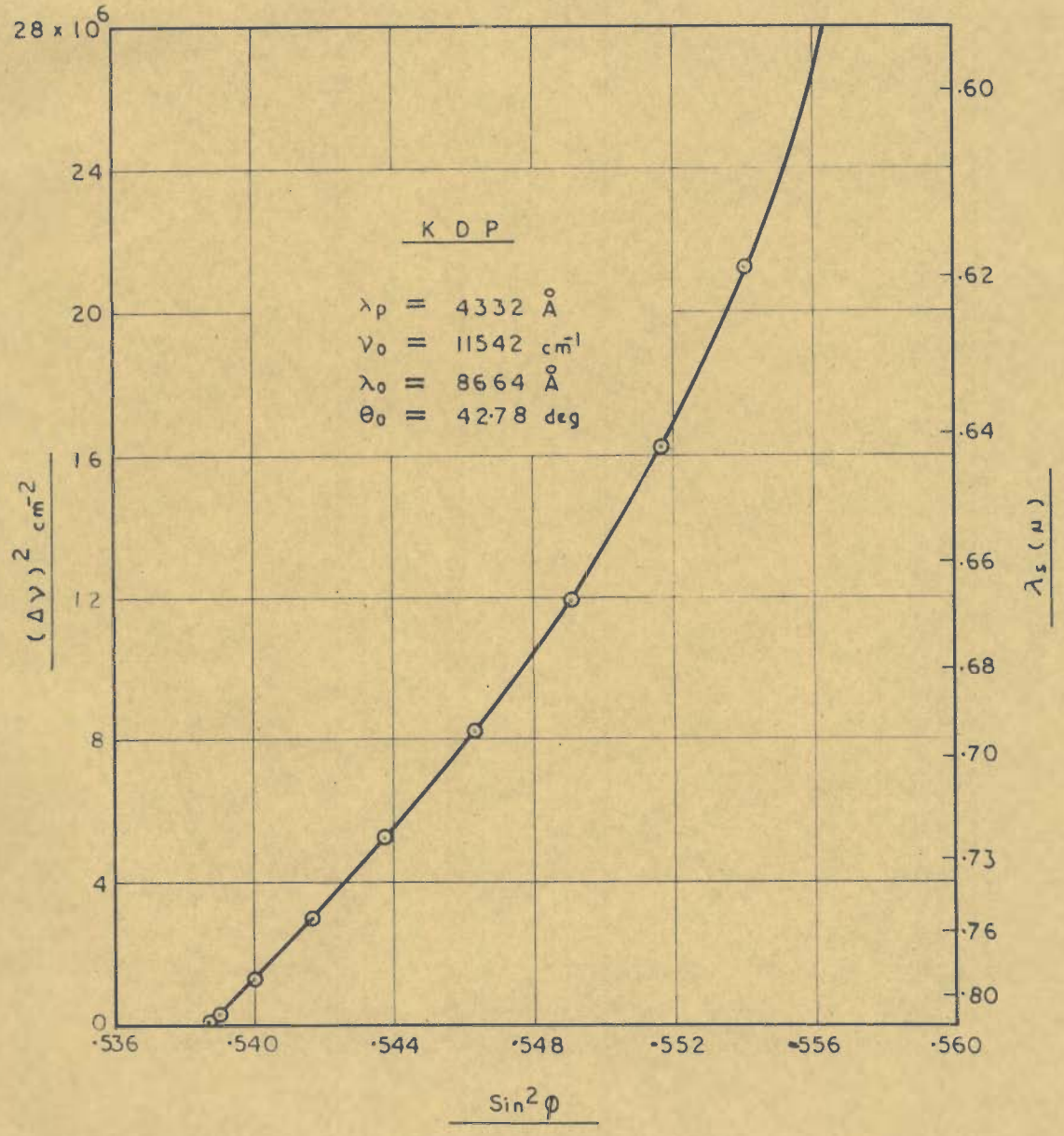
28 x 10^6
24
20
16
12
8
4
0
(Δν)² cm⁻²
·536
·540
·544
·548
·552
·556
·560
Sin²φ
·60
·62
·64
·66
·68
·70
·73
·76
·80
λs (μ)
K D P
λp = 4332 Å
ν0 = 11542 cm⁻¹
λ0 = 8664 Å
θ0 = 42·78 deg

FIG. 15·3 a

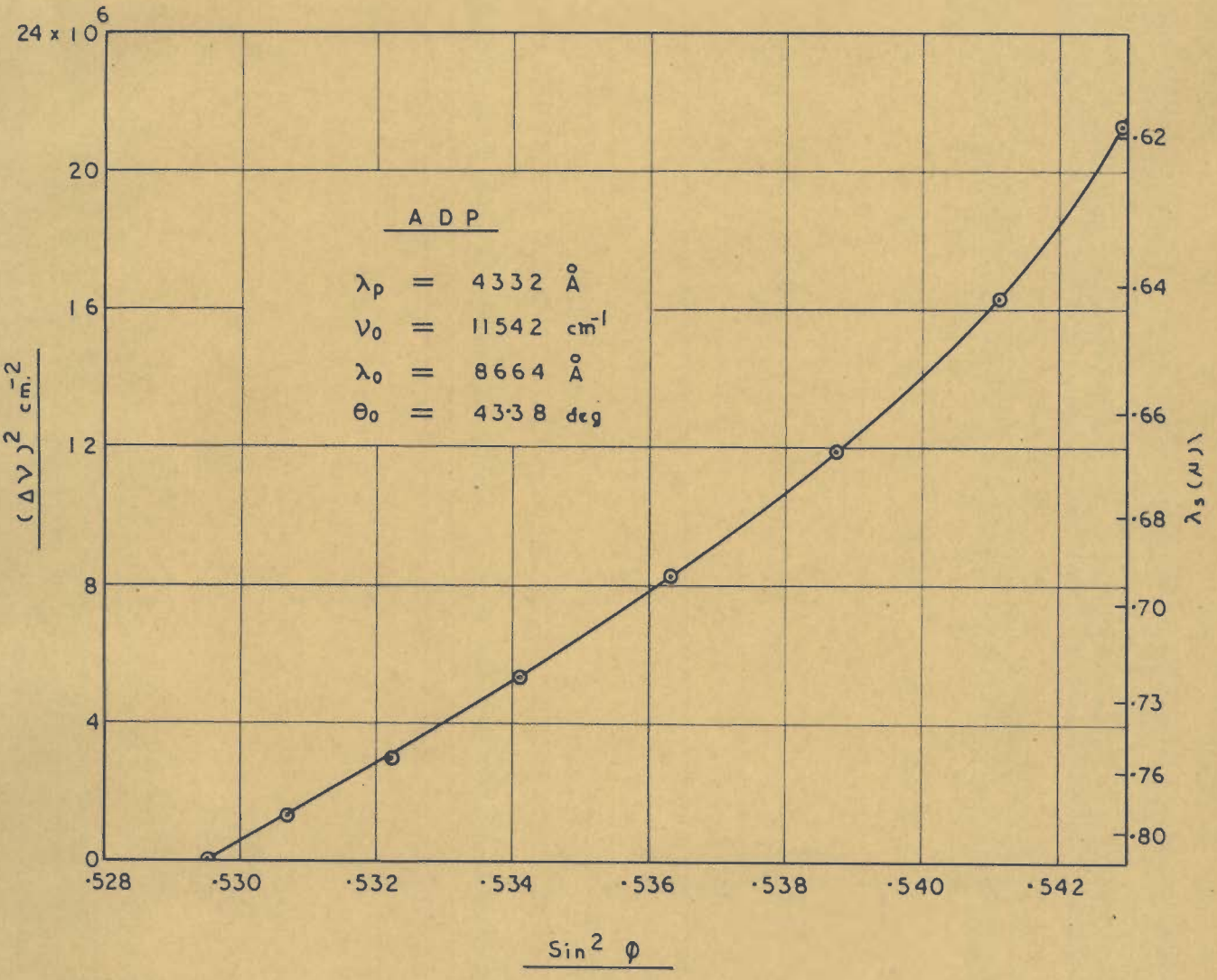
24 x 10^6
20
16
12
8
4
0
(Δν)^2 cm.^-2
ADP
λp = 4332 Å
ν0 = 11542 cm^-1
λ0 = 8664 Å
θ0 = 43·38 deg
·528
·530
·532
·534
·536
·538
·540
·542
Sin^2 φ
·62
·64
·66
·68
·70
·73
·76
·80
λs (M)

FIG. 15.3 b

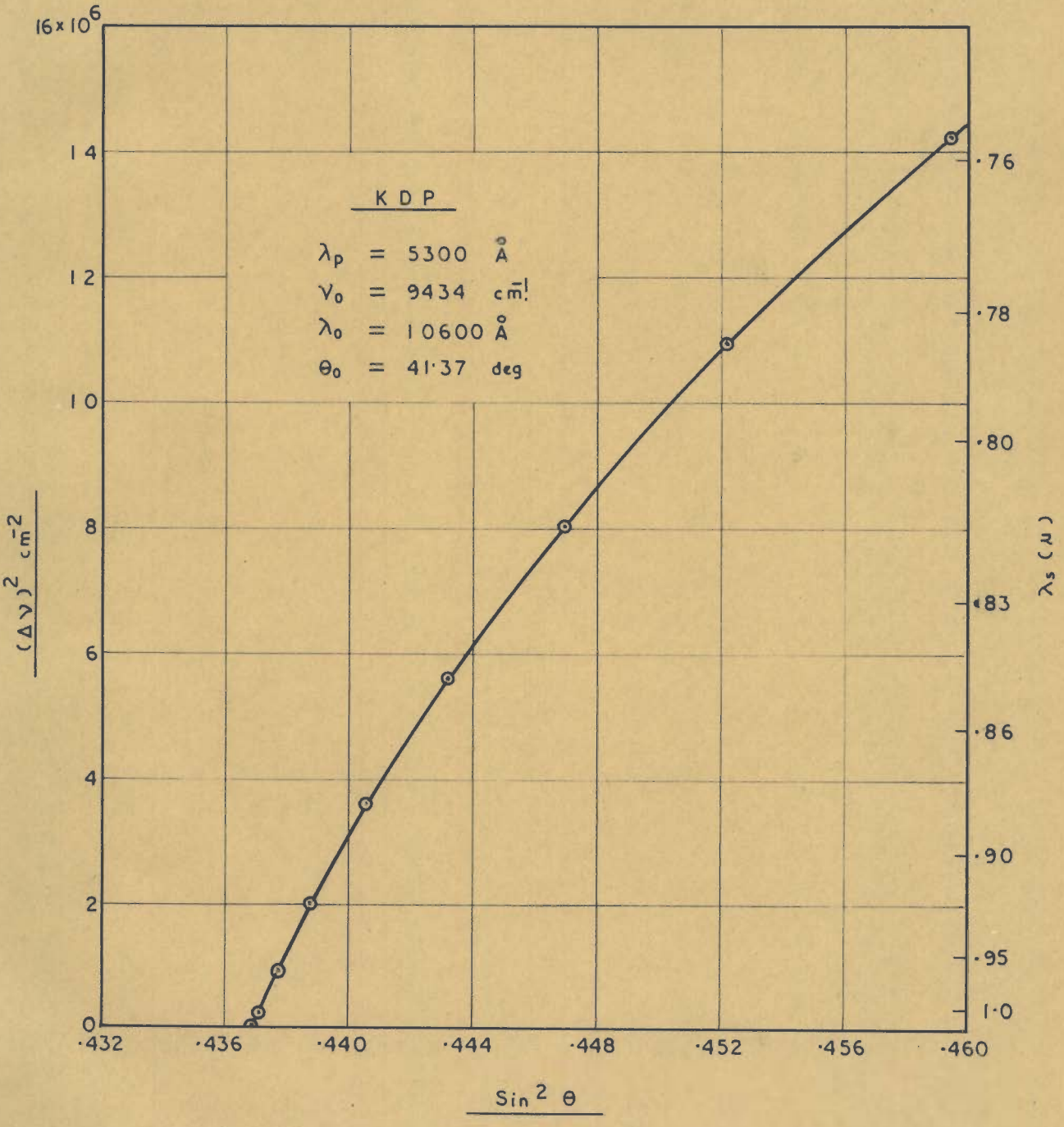
16 x 10^6
14
12
10
8
6
4
2
0
(Δν)² cm⁻²
KDP
λp = 5300 Å
ν0 = 9434 cm⁻¹
λ0 = 10600 Å
θ0 = 41·37 deg
·432
·436
·440
·444
·448
·452
·456
·460
Sin² θ
·76
·78
·80
·83
·86
·90
·95
1·0
λs (μ)

FIG. 15.4 a

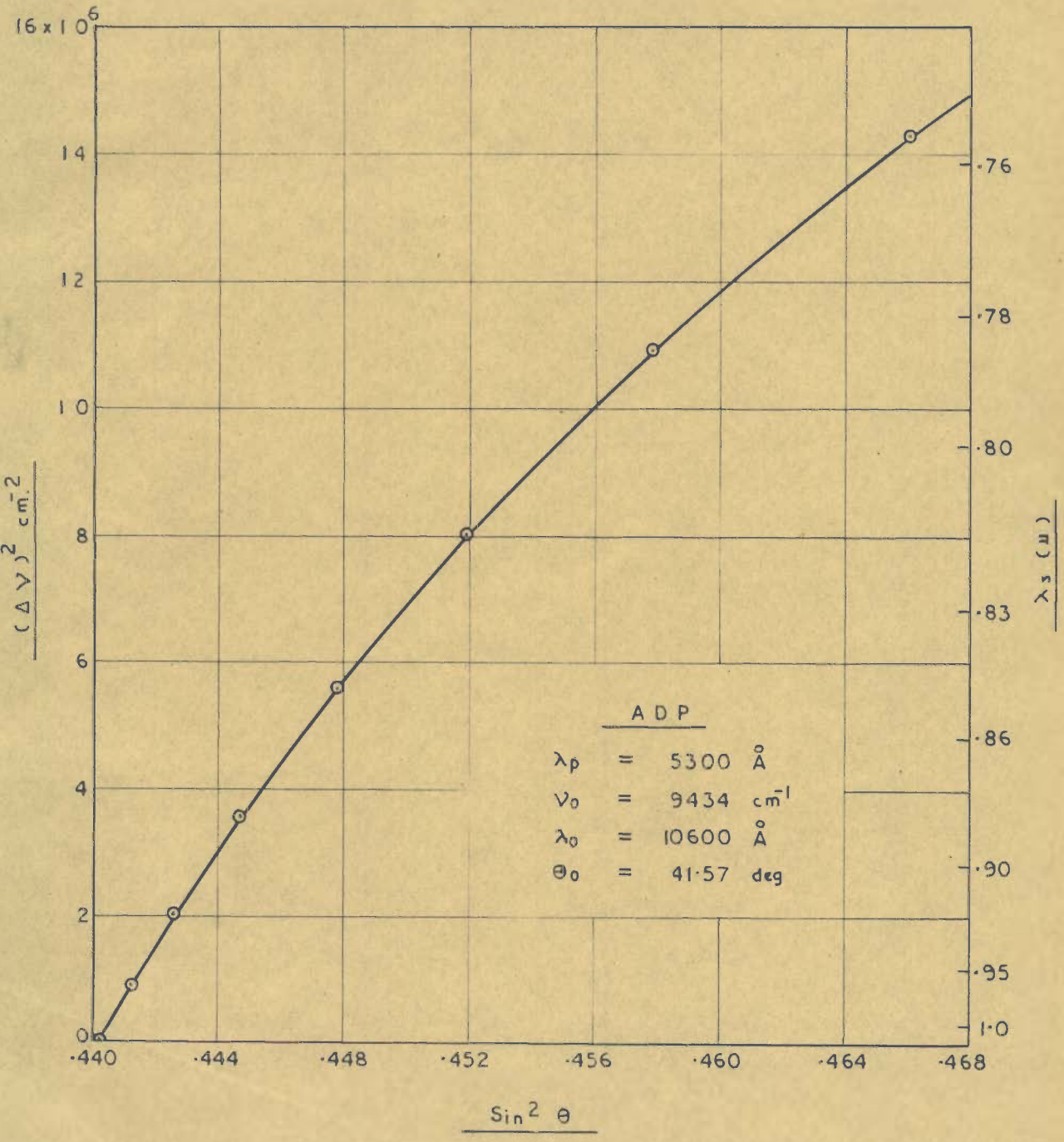
16 x 10^6
14
12
10
8
6
4
2
0
(Δν)² cm⁻²
·76
·78
·80
·83
·86
·90
·95
1·0
λs (μ)
·440
·444
·448
·452
·456
·460
·464
·468
Sin² θ
ADP
λp = 5300 Å
ν0 = 9434 cm⁻¹
λ0 = 10600 Å
θ0 = 41·57 deg

FIG. 15.4 b

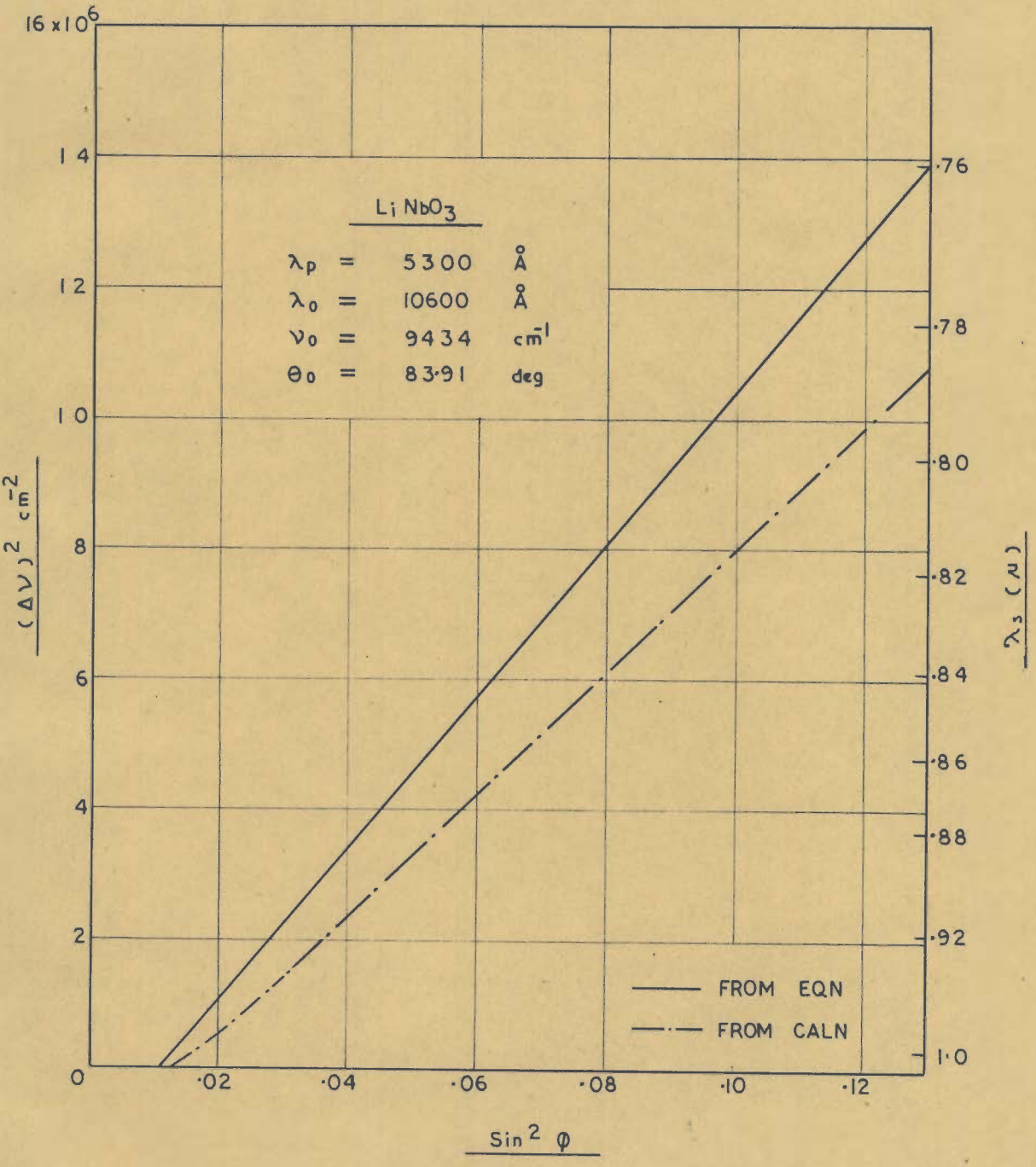
16 x 10^6
14
12
10
8
6
4
2
0
(Δν)^2 cm^-2
·02
·04
·06
·08
·10
·12
Sin^2 φ
·76
·78
·80
·82
·84
·86
·88
·92
1·0
λs (μ)
LiNbO3
λp = 5300 Å
λ0 = 10600 Å
ν0 = 9434 cm^-1
θ0 = 83·91 deg
FROM EQN
FROM CALN

FIG. 15.4 c

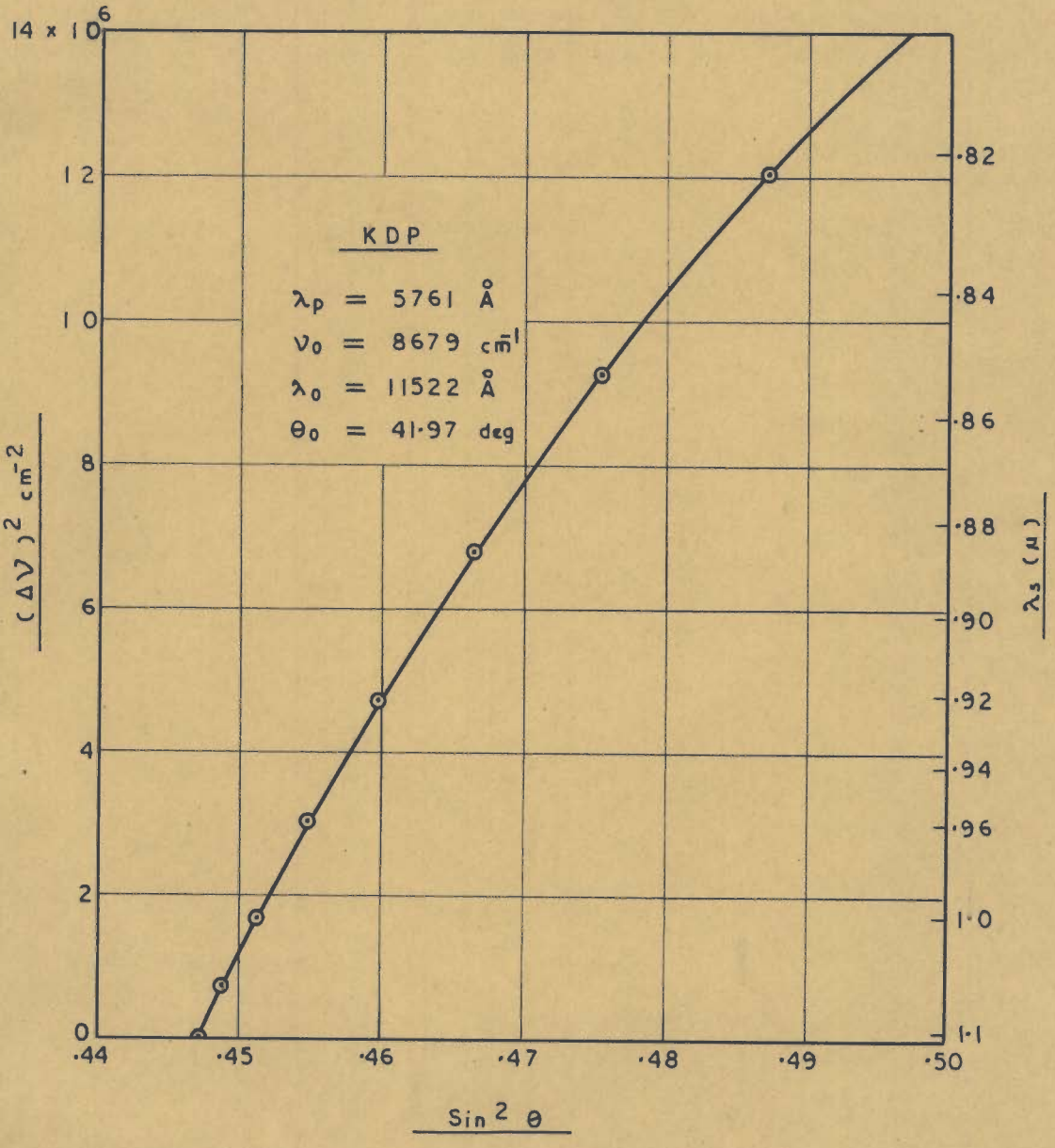
KDP
λ_p = 5761 Å
ν_0 = 8679 cm^{-1}
λ_0 = 11522 Å
θ_0 = 41·97 deg
$(\Delta\nu)^2\ cm^{-2}$
$\lambda_s\ (\mu)$
$Sin^2\ \theta$
14 x 10^6
12
10
8
6
4
2
0
·82
·84
·86
·88
·90
·92
·94
·96
1·0
1·1
·44
·45
·46
·47
·48
·49
·50

FIG. 15.5 a

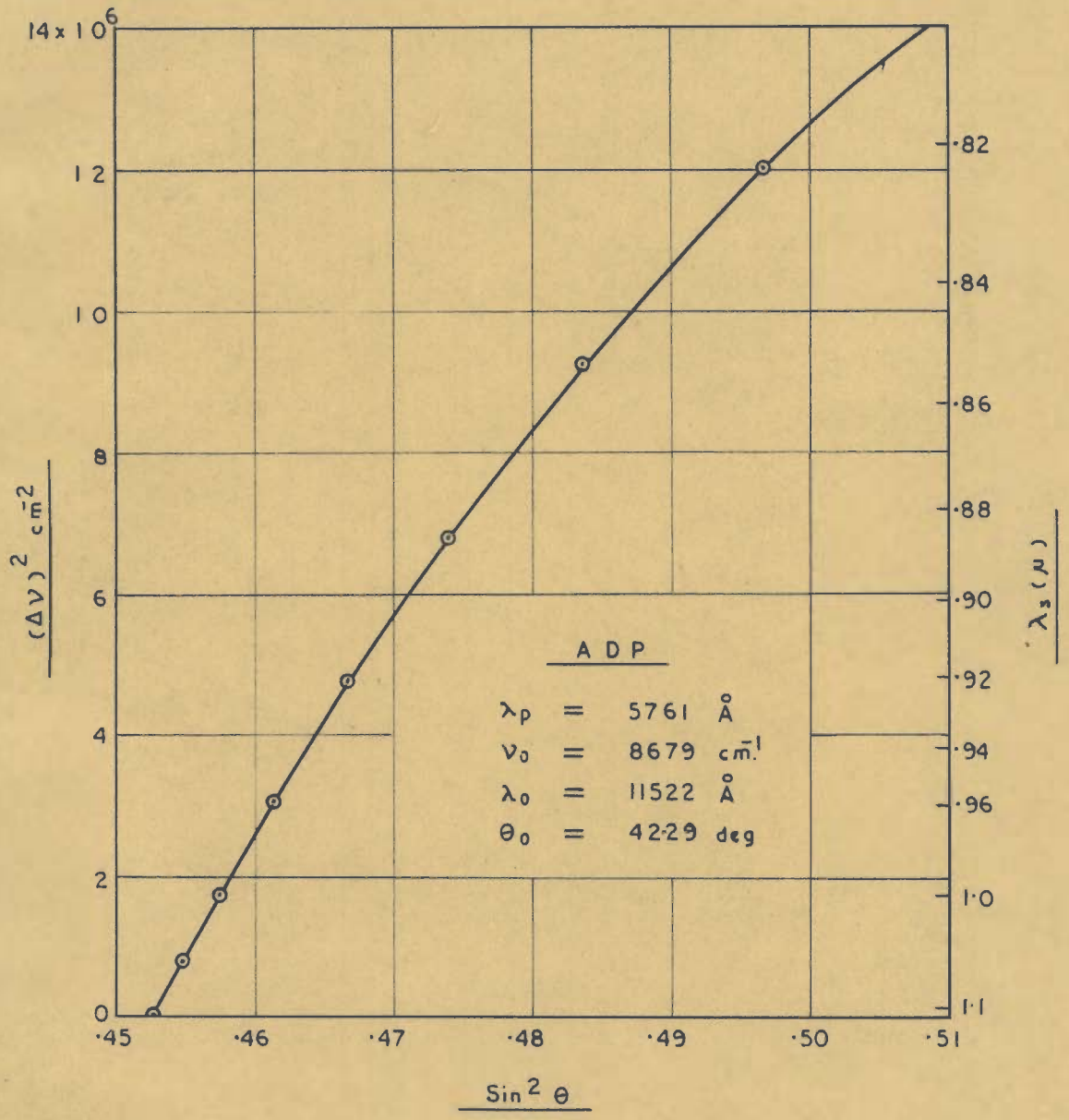
14 x 10^6
12
10
8
6
4
2
0
(Δν)² cm⁻²
·82
·84
·86
·88
·90
·92
·94
·96
1·0
1·1
λ₃ (μ)
·45
·46
·47
·48
·49
·50
·51
Sin² θ
ADP
λp = 5761 Å
ν0 = 8679 cm⁻¹
λ0 = 11522 Å
θ0 = 42·29 deg

FIG. 15.5 b

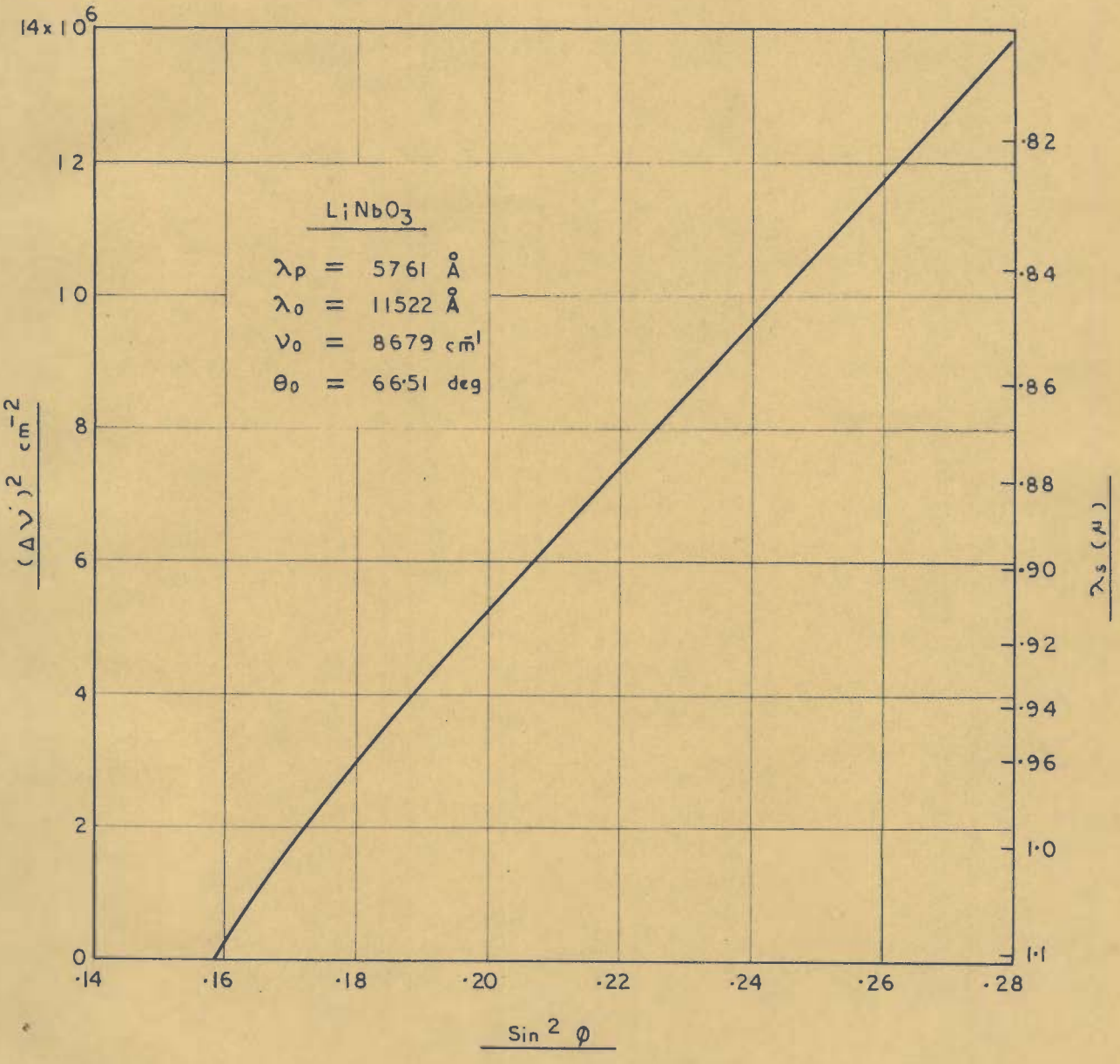
14x10^6
12
10
8
6
4
2
0
(Δν)² cm⁻²
·14
·16
·18
·20
·22
·24
·26
·28
Sin² φ
·82
·84
·86
·88
·90
·92
·94
·96
1·0
1·1
λs (Å)
LiNbO3
λp = 5761 Å
λ0 = 11522 Å
ν0 = 8679 cm⁻¹
θ0 = 66·51 deg

FIG. 15.5 c

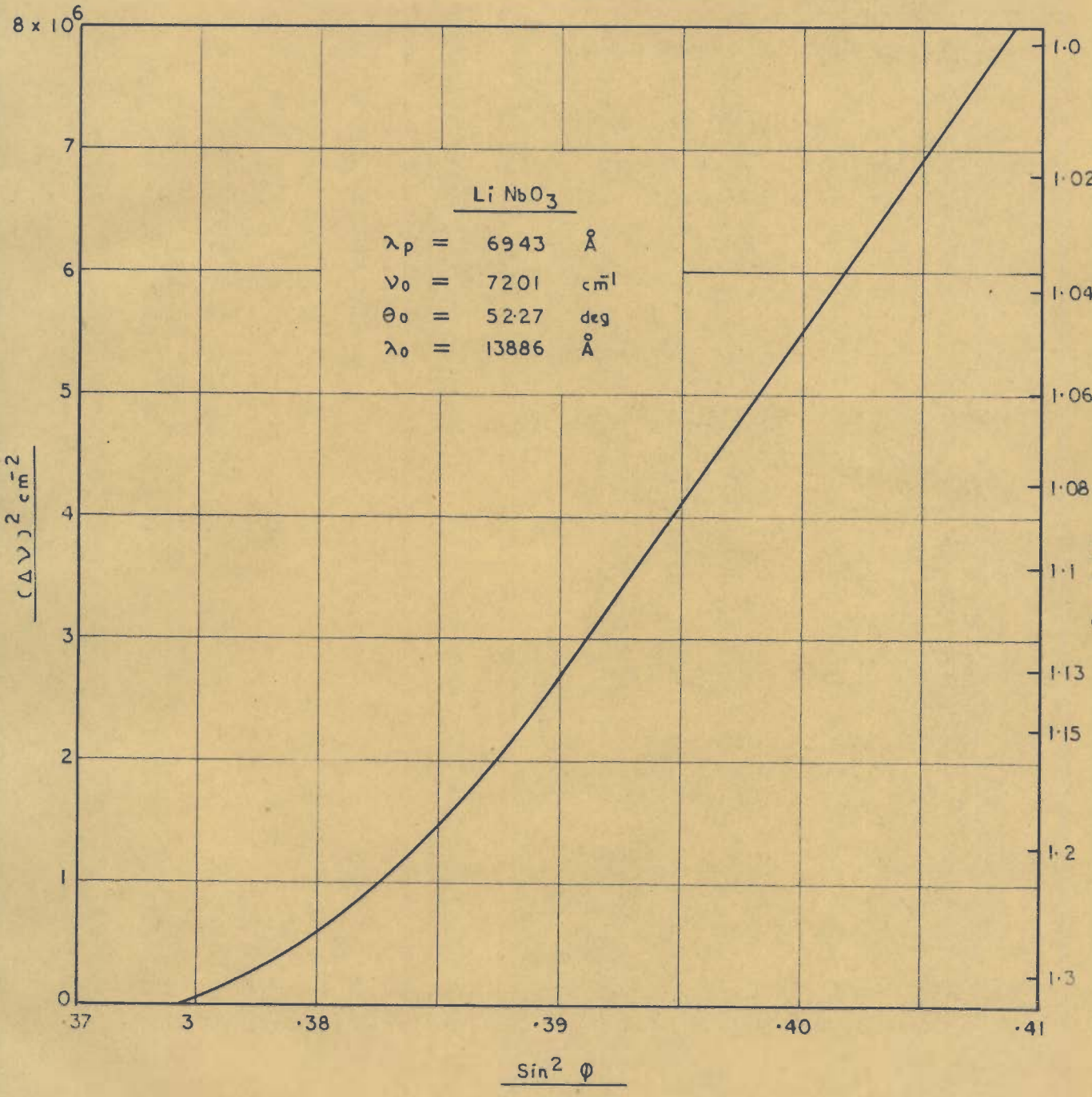
Li NbO3
λp = 6943 Å
ν0 = 7201 cm⁻¹
θ0 = 52·27 deg
λ0 = 13886 Å
8 x 10^6
7
6
5
4
3
2
1
0
(Δν)² cm⁻²
·37
3
·38
·39
·40
·41
Sin² φ
1·0
1·02
1·04
1·06
1·08
1·1
1·13
1·15
1·2
1·3

FIG. 15.6

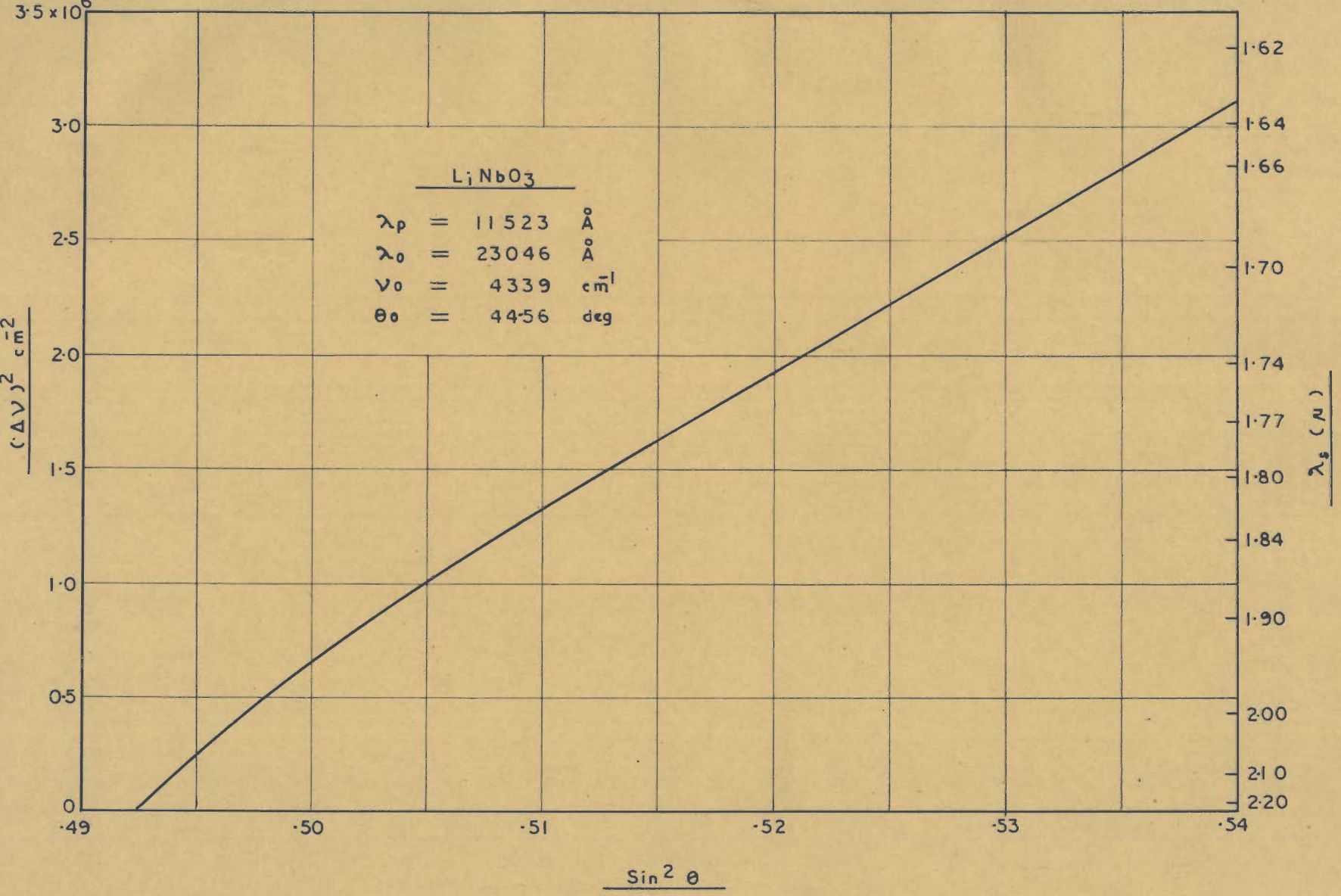
LiNbO3
λp = 11523 Å
λ0 = 23046 Å
ν0 = 4339 cm⁻¹
θ0 = 44·56 deg
(Δν)² cm⁻²
3·5 x 10⁶
3·0
2·5
2·0
1·5
1·0
0·5
0
·49
·50
·51
·52
·53
·54
Sin² θ
1·62
1·64
1·66
1·70
1·74
1·77
1·80
1·84
1·90
2·00
2·10
2·20
λs (μ)

FIG. 15·7

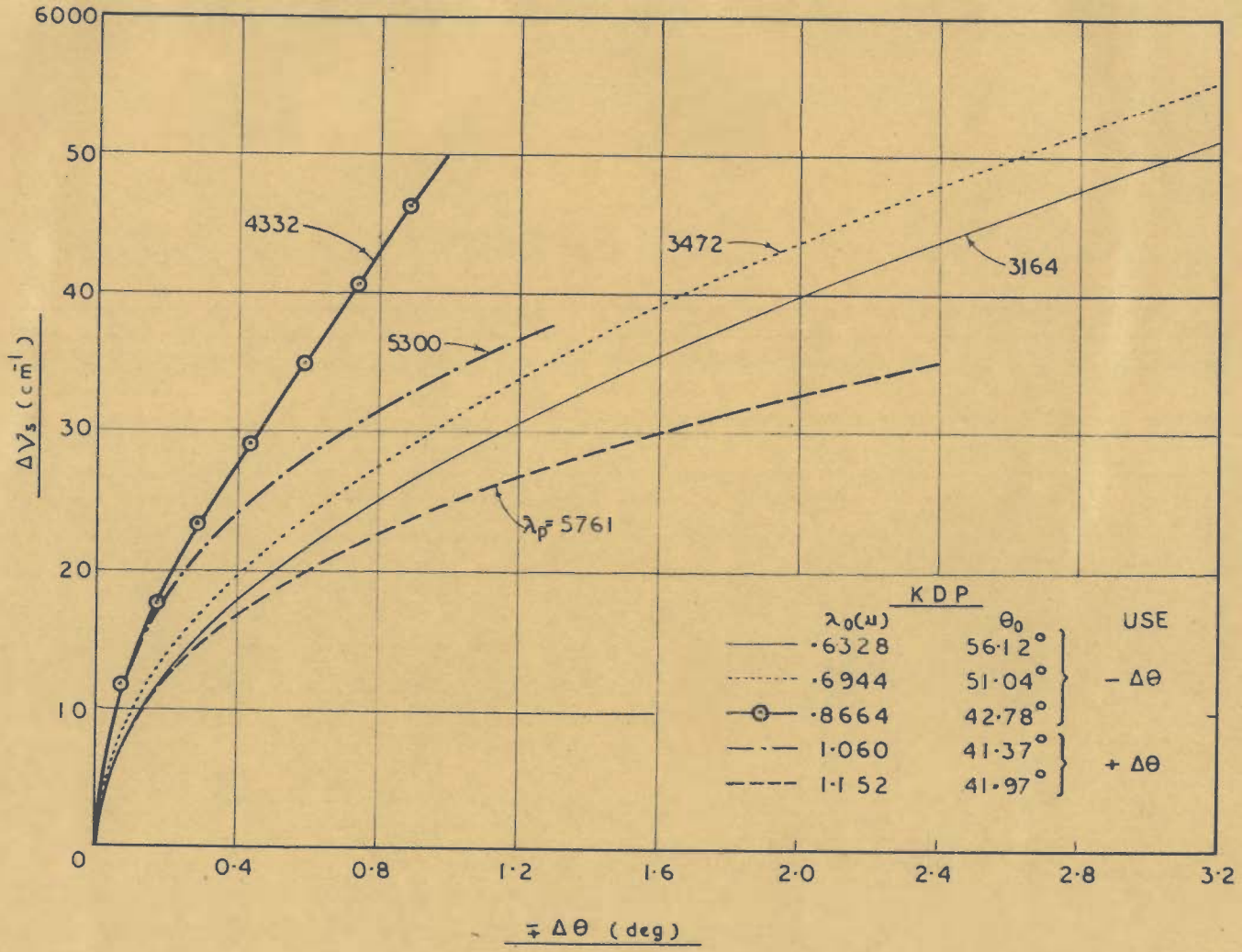
6000
50
40
30
20
10
0
ΔVs (cm⁻¹)
4332
3472
3164
5300
λp = 5761
KDP
λ0(μ)
θ0
USE
·6328
56·12°
·6944
51·04°
− Δθ
·8664
42·78°
1·060
41·37°
+ Δθ
1·152
41·97°
0·4
0·8
1·2
1·6
2·0
2·4
2·8
3·2
∓ Δθ (deg)

FIG. 15.8 a

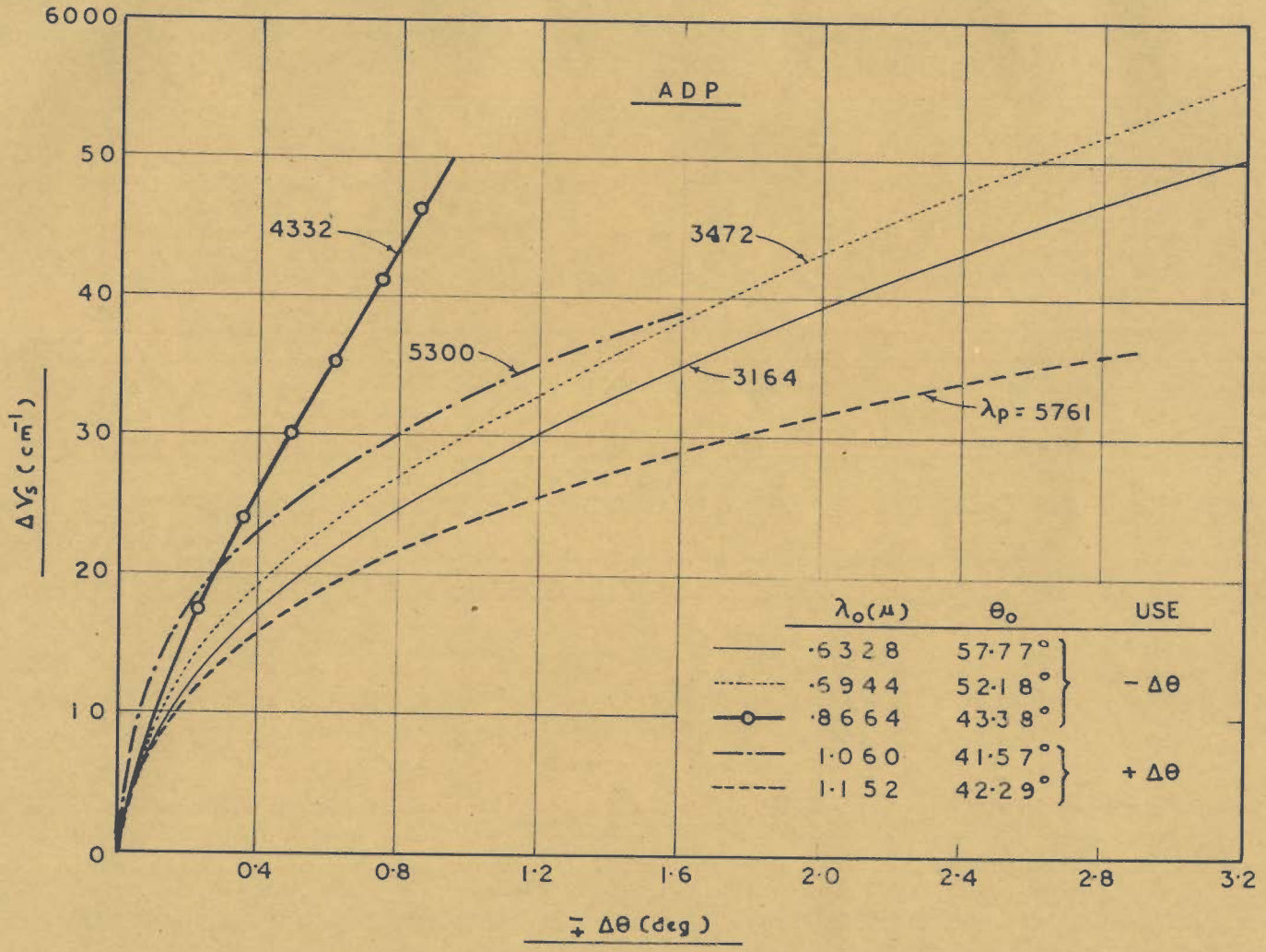
ADP
4332
3472
5300
3164
λ_p = 5761
$\lambda_o(\mu)$ θ_o USE
·6328 57·77°
·6944 52·18° − Δθ
·8664 43·38°
1·060 41·57°
1·152 42·29° + Δθ
ΔV_s (cm^{-1})
∓ Δθ (deg)
6000
50
40
30
20
10
0
0·4
0·8
1·2
1·6
2·0
2·4
2·8
3·2

FIG. 15.8 b

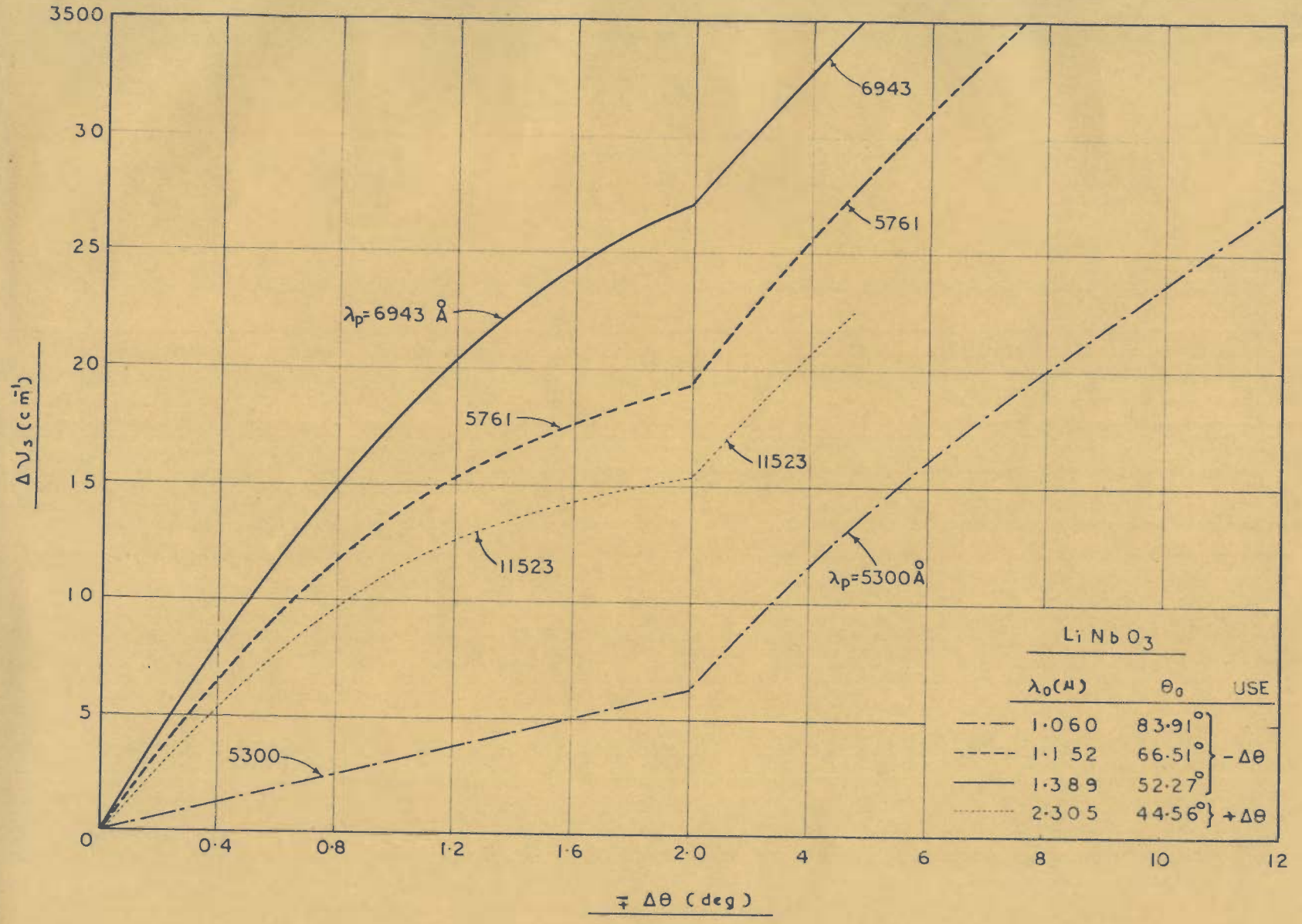
3500
30
25
20
15
10
5
0
Δν_s (cm⁻¹)
0·4
0·8
1·2
1·6
2·0
4
6
8
10
12
∓ Δθ (deg)
6943
5761
λp=6943 Å
5761
11523
11523
λp=5300Å
5300
Li Nb O3
λ0(Å)
θ0
USE
1·060
83·91°
1·152
66·51°
-Δθ
1·389
52·27°
2·305
44·56°
+Δθ

FIG. 15.8 C

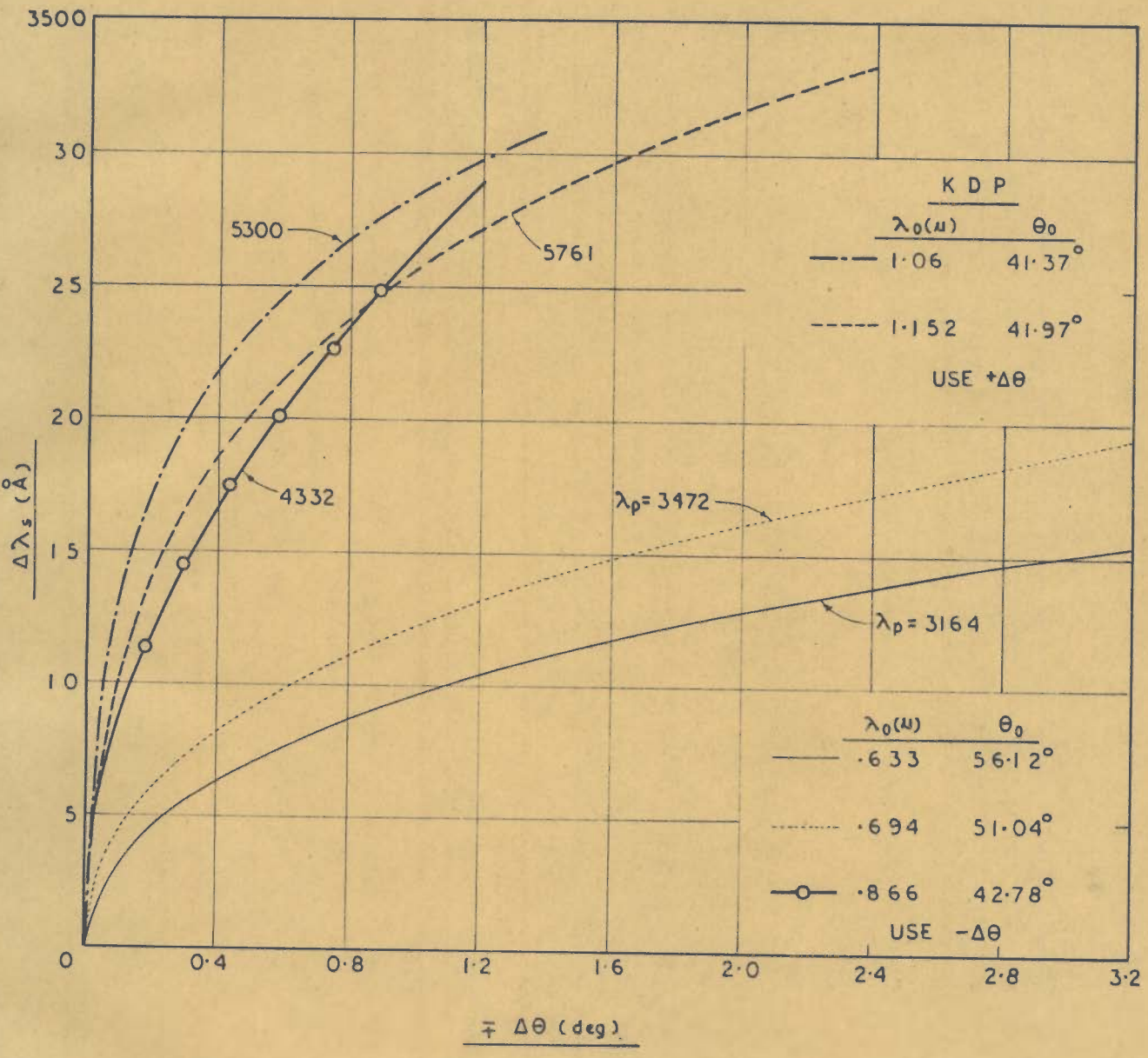
3500
30
25
20
15
10
5
0
0·4
0·8
1·2
1·6
2·0
2·4
2·8
3·2
Δλs (Å)
∓ Δθ (deg)
KDP
λ0(μ) θ0
1·06 41·37°
1·152 41·97°
USE +Δθ
5300
5761
4332
λp= 3472
λp= 3164
λ0(μ) θ0
·633 56·12°
·694 51·04°
·866 42·78°
USE −Δθ

FIG. 15.9 a

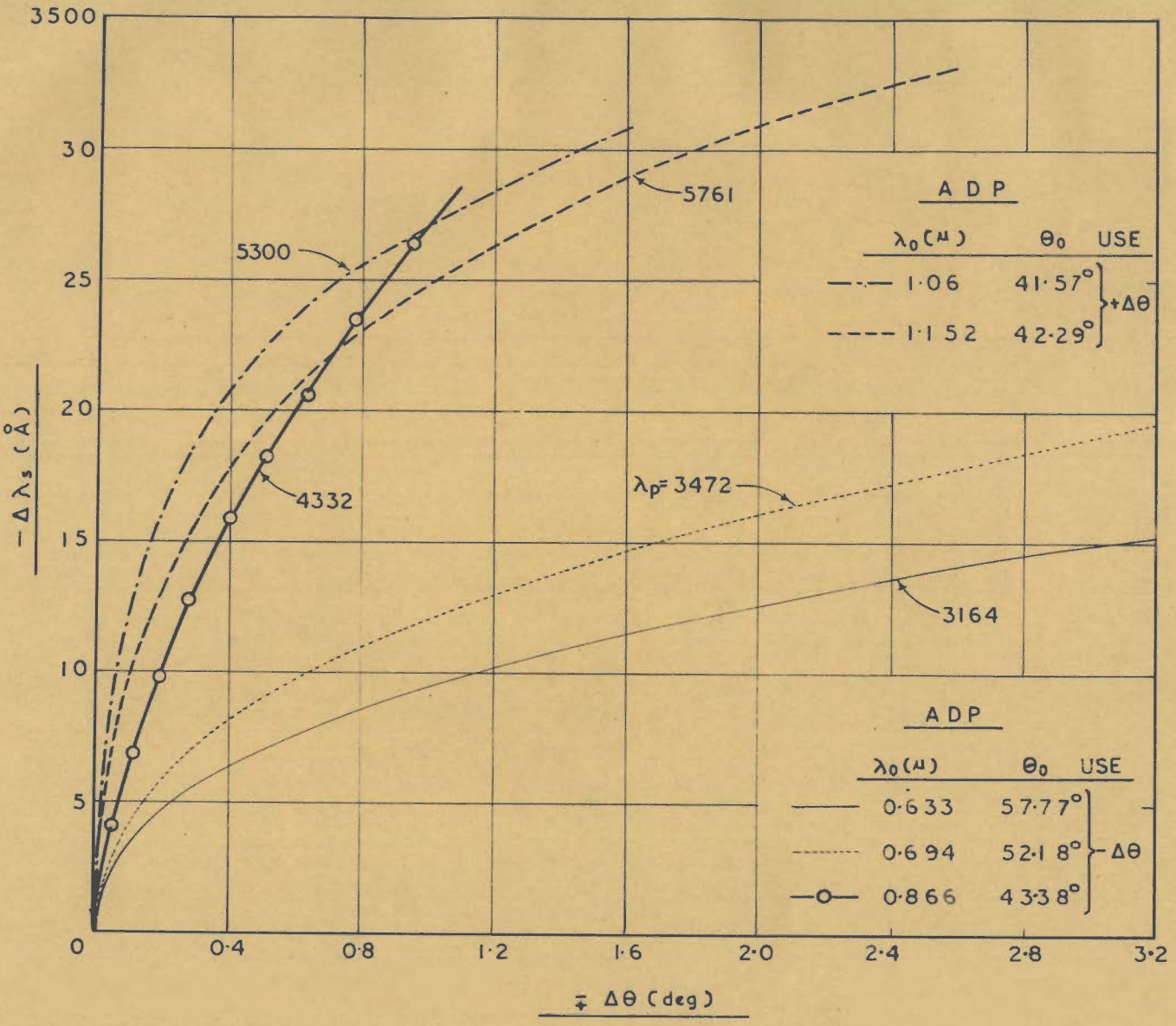
3500
30
25
20
15
10
5
0
0·4
0·8
1·2
1·6
2·0
2·4
2·8
3·2
$-\Delta\lambda_s$ (Å)
$\mp\Delta\theta$ (deg)
5761
5300
4332
λ_p= 3472
3164
ADP
λ_0(μ) θ_0 USE
1·06 41·57° +Δθ
1·152 42·29°
ADP
λ_0(μ) θ_0 USE
0·633 57·77°
0·694 52·18° -Δθ
0·866 43·38°

Fig. 15.9 b

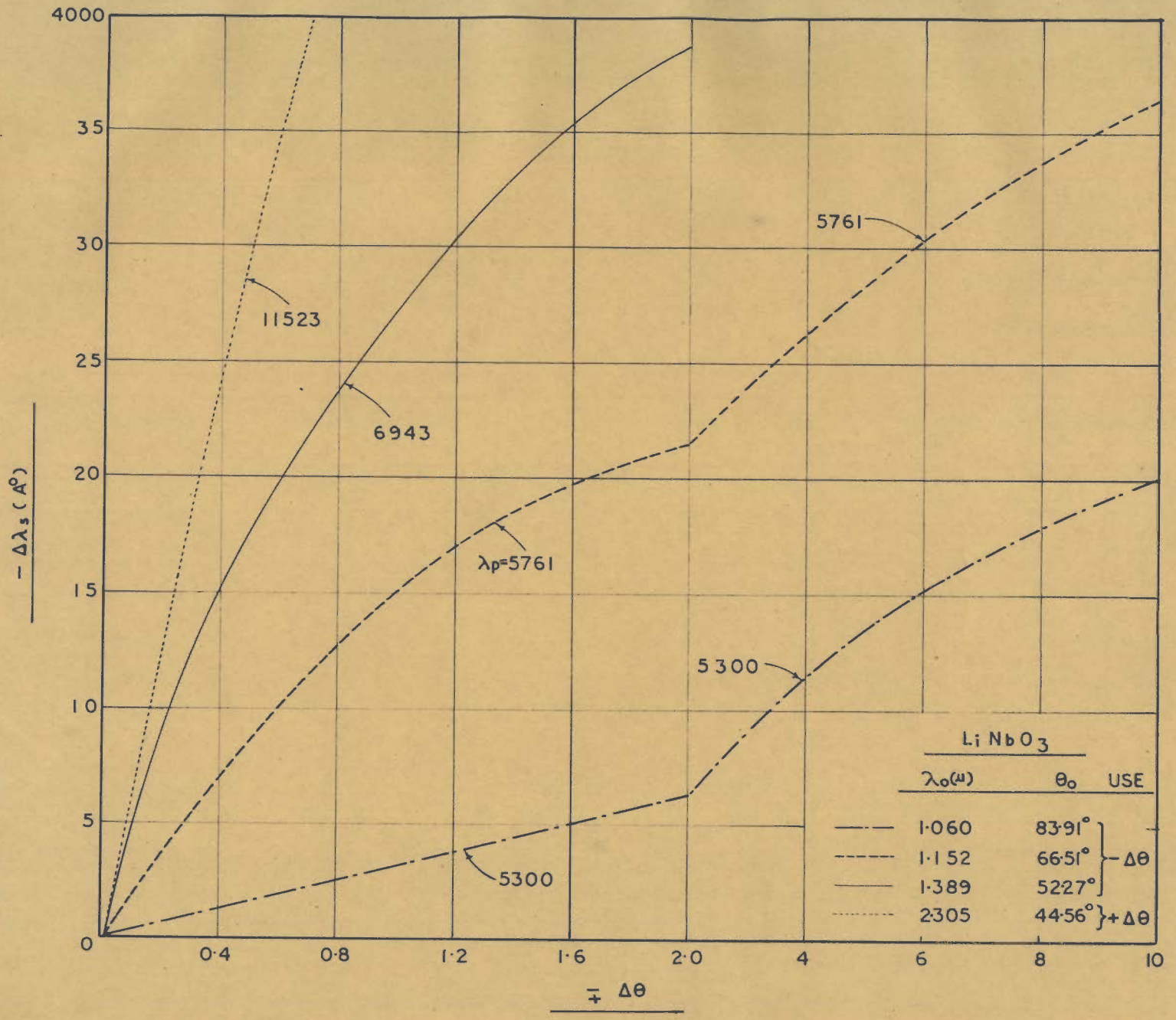
4000
35
30
25
20
15
10
5
0
$-\Delta\lambda_s$ (A°)
0·4
0·8
1·2
1·6
2·0
4
6
8
10
$\mp\Delta\theta$
11523
6943
5761
λ_p=5761
5300
5300
LiNbO3
λo(ω)
θo
USE
1·060
83·91°
1·152
66·51°
−Δθ
1·389
52·27°
2·305
44·56°
+Δθ

FIG. 15.9 c

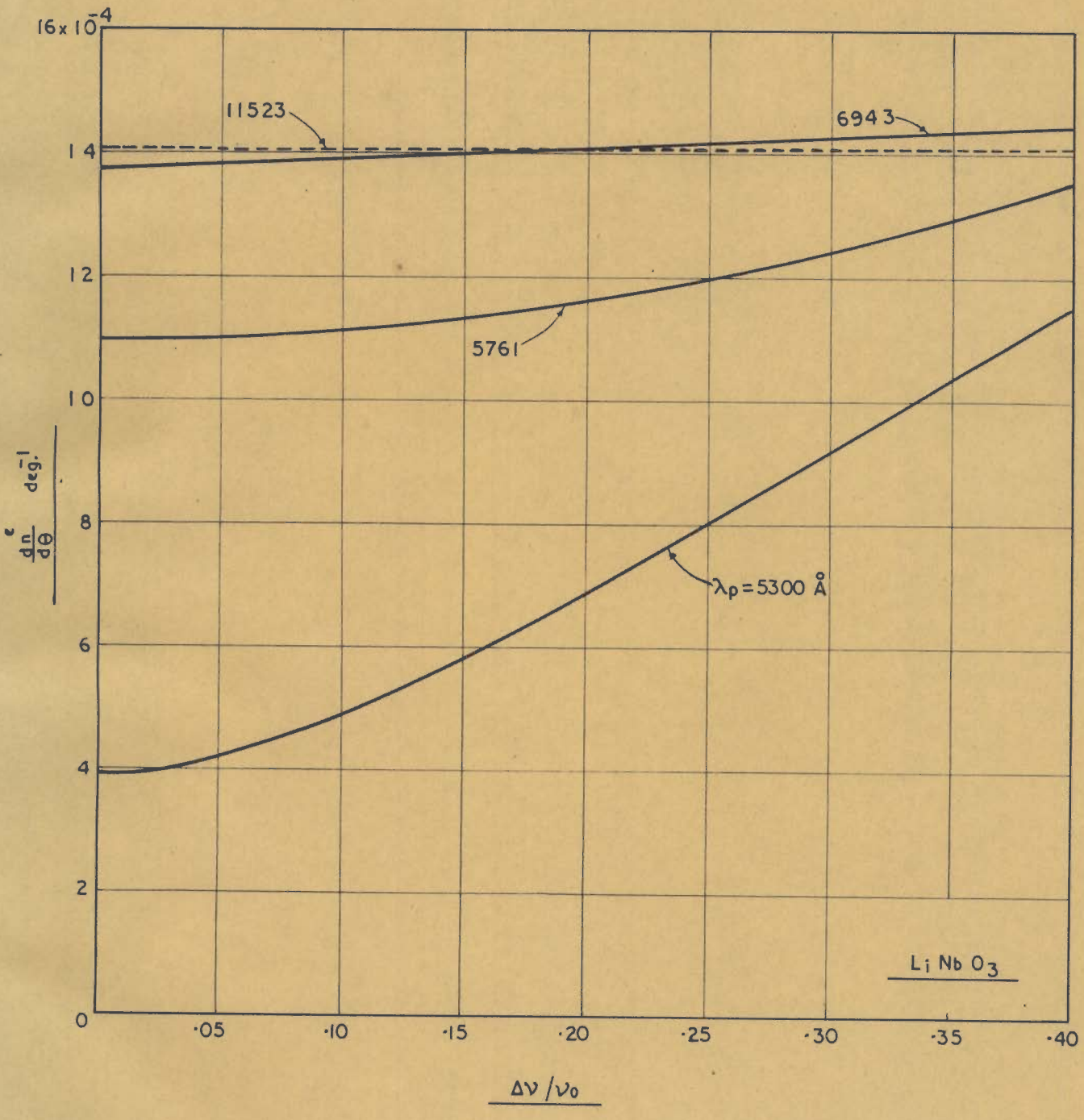
16 x 10⁻⁴
14
12
10
8
6
4
2
0
11523
6943
5761
λp = 5300 Å
Li Nb O3
ε dn/dθ deg.⁻¹
·05
·10
·15
·20
·25
·30
·35
·40
Δν/ν0

FIG. 16.1

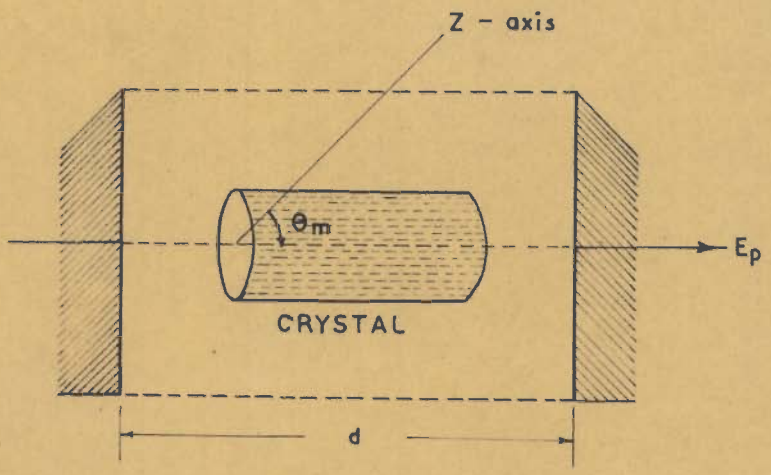

FIG. 17.1

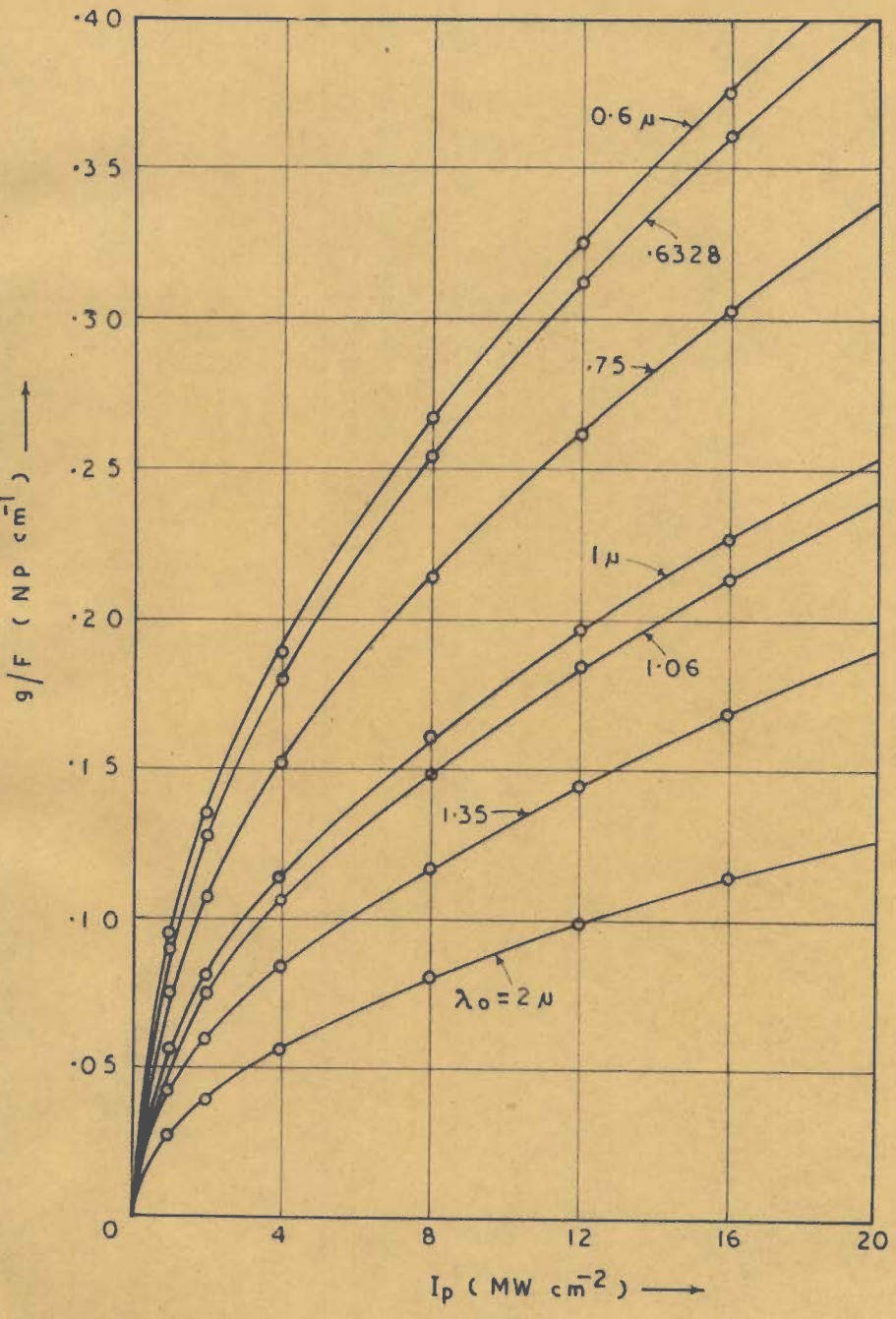
·40
·35
·30
·25
·20
·15
·10
·05
0
4
8
12
16
20
g/F (Np cm⁻¹) ⟶
Ip (MW cm⁻²) ⟶
0·6 μ
·6328
·75
1 μ
1·06
1·35
λo = 2 μ

FIG. 19.1

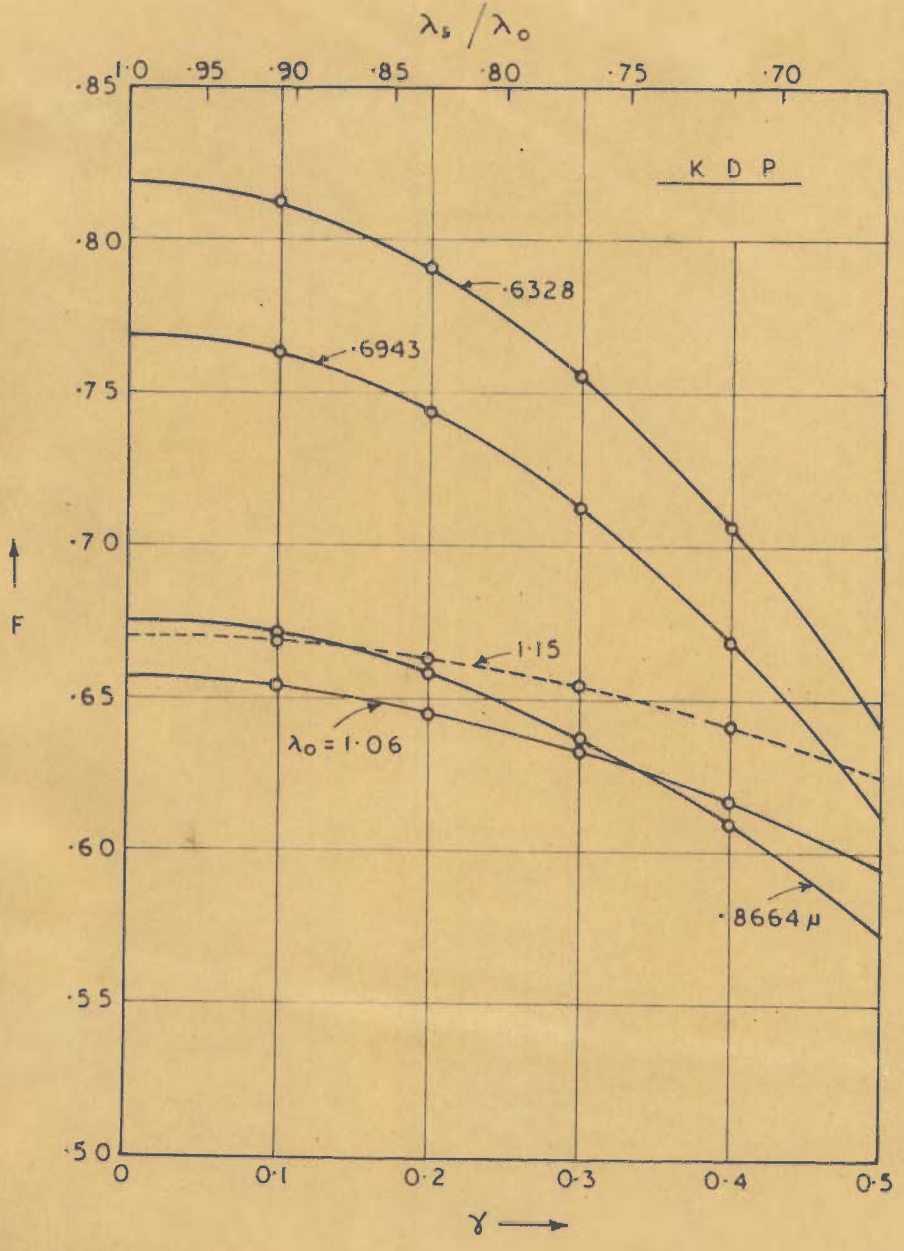
λs / λo
1·0
·95
·90
·85
·80
·75
·70
·85
·80
·75
·70
·65
·60
·55
·50
F
K D P
·6328
·6943
1·15
λo = 1·06
·8664 μ
0
0·1
0·2
0·3
0·4
0·5
γ

Fig. 19·1 a

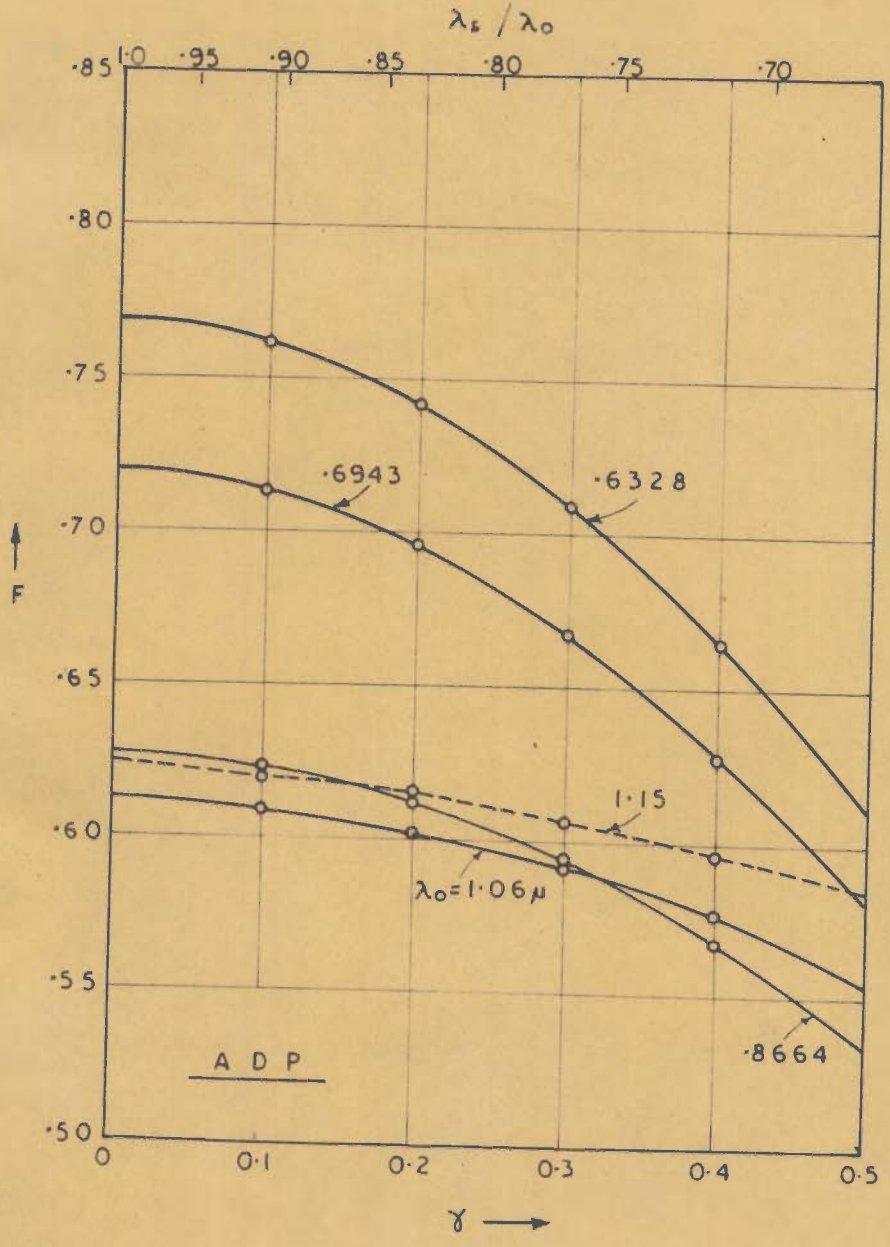
λε / λo
1·0
·95
·90
·85
·80
·75
·70
·85
·80
·75
·70
·65
·60
·55
·50
F
·6943
·6328
1·15
λo=1·06μ
·8664
A D P
0
0·1
0·2
0·3
0·4
0·5
γ

FIG. 19.1 a

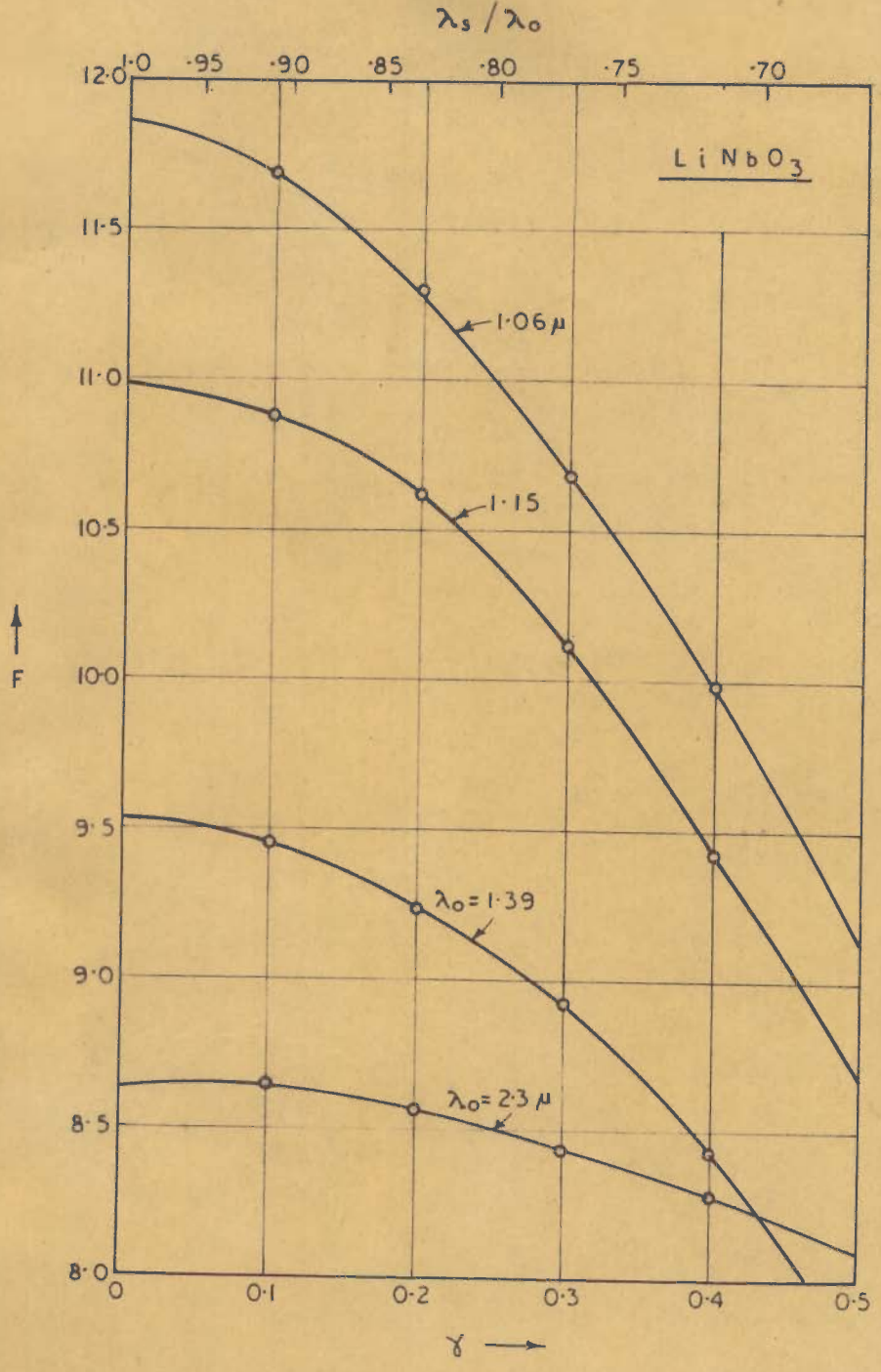

FIG. 19.1 a